Aus der Kinderchirurgischen Klinik und Poliklinik

im Dr. von Haunerschen Kinderspital

der Ludwig-Maximilians-Universität München

Direktor: Prof. Dr. Oliver Muensterer

The Neurokinin-1 receptor as a target in pediatric rhabdoid tumors and pancreatic cancer

Dissertation

zum Erwerb des Doktorgrades der Medizin

an der Medizinischen Fakultät der

Ludwig-Maximilians-Universität München

vorgelegt von

Julian Frederik Kolorz

aus

Berlin

Jahr

2024

Mit Genehmigung der Medizinischen Fakultät der

Ludwig-Maximilians-Universität zu München

Erster Gutachter:	Prof. Dr. Michael Berger
Zweiter Gutachter:	Prof. Dr. Sebastian Kobold
Dritter Gutachter:	Priv. Doz. Dr. Ujjwal Mahajan
Mitbetreuung durch den promovierten Mitarbeiter:	Prof. Dr. Roland Kappler
Dekan:	Prof. Dr. med. Thomas Gudermann
Tag der mündlichen Prüfung:	12.12.2024

In Widmung an meine Familie

Affidavit

Eidesstattliche Versicherung

Kolorz, Julian Frederik

Name, Vorname

Ich erkläre hiermit an Eides statt, dass ich die vorliegende Dissertation mit dem Titel:

„The Neurokinin-1 receptor as a target in pediatric rhabdoid tumors and pancreatic cancer"

selbständig verfasst, mich außer der angegebenen keiner weiteren Hilfsmittel bedient und alle Erkenntnisse, die aus dem Schrifttum ganz oder annähernd übernommen sind, als solche kenntlich gemacht und nach ihrer Herkunft unter Bezeichnung der Fundstelle einzeln nachgewiesen habe.

Ich erkläre des Weiteren, dass die hier vorgelegte Dissertation nicht in gleicher oder in ähnlicher Form bei einer anderen Stelle zur Erlangung eines akademischen Grades eingereicht wurde.

Essen, 22.12.2024
Ort, Datum

Julian Kolorz
Unterschrift Doktorandin bzw. Doktorand

Table of contents

Affidavit ..... **IV**

Table of contents ..... **V**

Abbreviations ..... **VI**

List of publications ..... **VII**

1. Contributions **1**

1.1 Contribution to Paper I 1

1.2 Contribution to Paper II 1

2. Introduction **2**

2.1 Neurokinin-1 receptor 2

2.1.1 Neurokinin-1 receptor/ substance P-complex 2

2.1.2 Splice variants of NK1R 4

2.1.3 NK1R-antagonist Aprepitant 4

2.2 Rhabdoid Tumor 6

2.2.1 Epidemiology 6

2.2.2 Treatment 6

2.2.3 SMARCB1 Mutation 7

2.3 Pancreatic Ductal Adenocarcinoma 8

2.3.1 Epidemiology 8

2.3.2 Treatment 8

2.4 Goal and scope of this study 10

2.4.1 The Neurokinin-1 Receptor is a Target in Pediatric Rhabdoid Tumors 10

2.4.2 Identification of the Neurokinin-1 Receptor as Targetable Stratification Factor for Drug Repurposing in Pancreatic Cancer 11

3. Zusammenfassung **13**

4. Abstract **14**

5. Paper I **15**

6. Paper II **32**

7. References **51**

Acknowledgement **55**

Curriculum vitae **56**

Abbreviations

AT/RT	-	atypical teratoid/ rhabdoid tumor
CSCs	-	cancer stem cell-like cells
CINV	-	chemotherapy-induced nausea and vomiting
ELISA	-	enzyme-linked immunosorbent assay
FDA	-	Food and Drug Administration
fl-NK1R	-	full length neurokinin-1 receptor
GPCRs	-	G-protein-coupled receptors
HB	-	hepatoblastoma
IBS	-	irritable bowel syndrome
INI1	-	integrase inhibitor 1
MTT	-	3-(4,5-dimethylthiazol-2-yl)-2,5-diphenyltetrazolium bromide)
MRT	-	malignant rhabdoid tumor
NK1R	-	neurokinin-1 receptor
NK2R	-	neurokinin-2 receptor
NK3R	-	neurokinin-3 receptor
PDAC	-	pancreatic ductal adenocarcinoma
PI	-	propidium iodide
qPCR	-	quantitative polymerase chain reaction
RT	-	rhabdoid tumor
RTK	-	rhabdoid tumor of the kidney
RT-qPCR	-	real-time quantitative polymerase chain reaction
SMARCB1	-	SWI/SNF-related matrix-associated actin-dependent regulator of chromatin subfamily B member 1
SP	-	substance P
SWI/SNF	-	SWItch/Sucrose non-fermentable
tr-NK1R	-	truncated neurokinin-1 receptor
PONV	-	postoperative nausea and vomiting

List of publications

Paper I:

Kolorz, J., Demir, S., Gottschlich, A., Beirith, I., Ilmer, M., Lüthy, D, Walz C, Dorostkar MM, Magg T, Hauck F, von Schweinitz D, Kobold S, Kappler R, Berger M. (2021). The Neurokinin-1 Receptor Is a Target in Pediatric Rhabdoid Tumors. *Current Oncology, 29(1), 94–110.* https://doi.org/10.3390/curroncol29010008

Paper II:

Beirith, I., Renz, B. W., Mudusetti, S., Ring, N. S., **Kolorz, J.,** Koch, D., Bazhin, A. V., Berger, M., Wang, J., Angele, M. K., D'Haese, J. G., Guba, M. O., Niess, H., Andrassy, J., Werner, J., & Ilmer, M. (2021). Identification of the Neurokinin-1 Receptor as Targetable Stratification Factor for Drug Repurposing in Pancreatic Cancer. *Cancers, 13(11), 2703.* https://doi.org/10.3390/cancers13112703

Further publications:

Ritz, A., **Kolorz, J.,** Hubertus, J., Ley-Zaporozhan, J., von Schweinitz, D., Koletzko, S., Häberle, B., Schmid, I., Kappler, R., Berger, M., Lurz, E. (2020). Sarcopenia is a prognostic outcome marker in children with high-risk hepatoblastoma. *Pediatric Blood & Cancer.* https://doi.org/10.1002/pbc.28862

Ritz, A., Froeba-Pohl, A., **Kolorz, J.,** Vigodski, V., Hubertus, J., Ley-Zaporozhan, J., von Schweinitz, D., Häberle, B., Schmid, I., Kappler, R., Lurz, E. and Berger, M. (2021). Total Psoas Muscle Area as a Marker for Sarcopenia Is Related to Outcome in Children With Neuroblastoma. *Frontiers in Surgery.* https://doi.org/10.3389/fsurg.2021.718184

1. Contributions

1.1 Contribution to Paper I

The doctoral candidate Julian Kolorz contributed to the paper “The Neurokinin-1 Receptor Is a Target in Pediatric Rhabdoid Tumors” by data curation, experimental investigation, formal analysis and validation of results, visualization and writing the original draft for the manuscript. More specifically, he performed data base analysis with data sets from the cBio Cancer Genomics Portal, in which he analyzed five different pediatric cancer studies and compared mRNA expression of 2 genes. Furthermore, he showed that there was no significant correlation between TACR1 and TAC1 expression levels and tumor stage, gender, age of diagnosis and overall survival (Paper I, Figure 1a-l, Table 3). As a next step, the doctoral candidate cultivated fibroblasts, hepatoblastoma (HB) and rhabdoid tumor (RT) cell lines and performed RNA extraction, complementary DNA synthesis and quantitative polymerase chain reaction (qPCR) analysis on cell lines and tumor samples obtained from pediatric patients (Paper I, Figure 2a-d, Table 1, Table 2). He performed MTT (3-(4,5-dimethylthiazol-2-yl)-2,5-diphenyltetrazolium bromide))-proliferation assays, Western blot analysis and in vitro analysis of apoptosis using flow cytometry with different drugs and cell lines (Paper I, Figure 3, Figure 4). Finally, he carried out the statistical analysis of clinical data and wrote and reviewed the manuscript.

1.2 Contribution to Paper II

For the paper “Identification of the Neurokinin-1 Receptor as Targetable Stratification Factor for Drug Repurposing in Pancreatic Cancer“ the doctoral candidate was responsible for data curation, formal analysis of results and methodology of experiments. He contributed by cell cultivation of HB cell line HepG2, isolation of RNA, complementary DNA synthesis and qPCR analysis of several cell lines (Paper II, Figure 1a, Figure 3a). Furthermore, he tested primer functionality in HepG2 for TACR1-tr, TACR1-fl, TAC1 and contributed to the writing and reviewing of the manuscript.

2. Introduction

2.1 Neurokinin-1 receptor

2.1.1 Neurokinin-1 receptor/ substance P-complex

The neurokinin-1 receptor (NK1R)/ substance P (SP)-complex plays a critical role in the development of cancer. The neurokinin receptor is a tachykinin-receptor of the neuropeptide G-protein-coupled receptors (GPCRs) that is known for a variety of physiological functions ranging from inflammation to nociception to cancer progression (Munoz and Rosso, 2010, Yin et al., 2018). There are three forms of the tachykinin receptor: the neurokinin-1 receptor (NK1R), the neurokinin-2 receptor (NK2R) and the neurokinin-3 receptor (NK3R), which are encoded by the genes *TACR1*, *TACR2* and *TACR3*, respectively. The NK1R and the NK2R are expressed in the central nervous system, in the peripheral nervous system, in the gastrointestinal system and in immune cells. The expression of the NK3R is mostly restricted to the nervous system. The mentioned receptors play diverse physiological roles and are currently being investigated in several clinical trials, by using antagonists of tachykinin receptors for the treatment of depression, chemotherapy-induced nausea and vomiting (CINV), schizophrenia, irritable bowel syndrome (IBS) and cancer (Yin et al., 2018, Munoz and Covenas, 2020).

The undecapeptide Substance P, an 11-amino acid long neuropeptide encoded by the gene *TAC1*, is part of the tachykinin family of peptides, including hemokinin-1, kassinin, ranakinin, eledoisin, neurokinin A, neurokinin B, neuropeptide K and neuropeptide Gamma, and is widely distributed in the central and peripheral nervous system, where it acts a as neurotransmitter and neuromodulator (Munoz and Covenas, 2014). After binding to the NK1R, to which it has the highest affinity, SP mediates several functions such as migration of tumor cells, mitogenesis, favors angiogenesis and anti-apoptotic effects (seen in Figure 1a) (Munoz and Covenas, 2020).

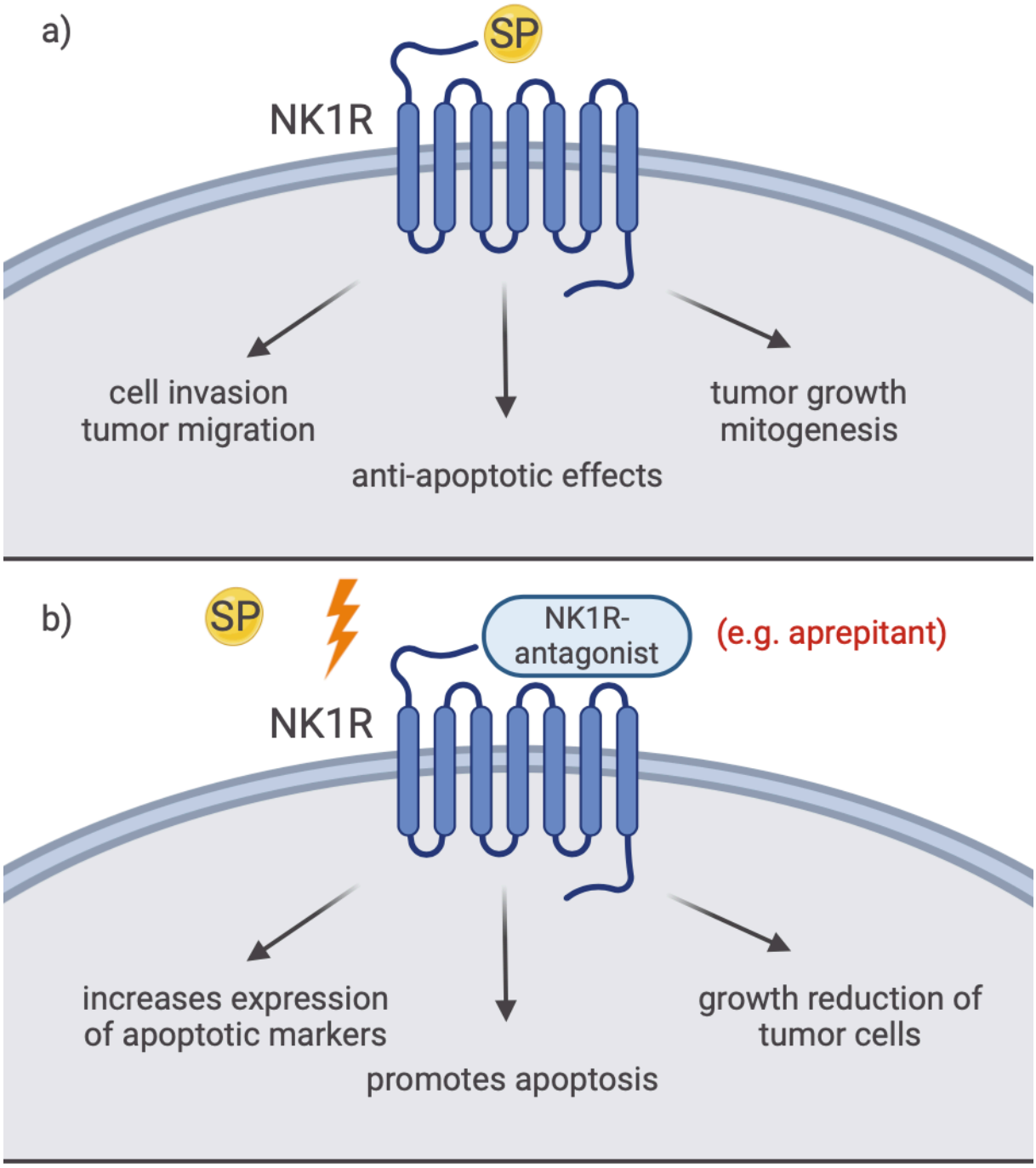

Figure 1: Role of NK1R-/SP-complex (a) and NK1R-antagonist, e.g. aprepitant (b) (based on (Muñoz and Coveñas, 2013, Munoz and Covenas, 2020).

2.1.2 Splice variants of NK1R

Two isoforms of the NK1R have been reported. The full-length version (fl-NK1R, encoded by the gene *TACR1-fl*) contains 407 amino acids and the truncated version (tr-NK1R, encoded by the gene *TACR1-tr*) contains 311 amino acids, lacking 96 amino acids at the C-terminus (Munoz et al., 2019b). Due to this structural difference, both isoforms activate different downstream signaling pathways and overall possess distinct physiological functions. It has been reported that the activation of the tr-NK1R increases metastasis, whereas the fl-NK1R reduces it (Zhou et al., 2013). Furthermore, it has been shown in tumor cells, that tr-NK1R expression levels are higher in comparison to fl-NK1R (Ge et al., 2019).

2.1.3 NK1R-antagonist Aprepitant

There are several antagonists of the NK1R receptor that can be classified as peptide and non-peptide antagonists. The peptide NK1R antagonists (e.g., NY-3460, NY-3238) show low affinity for the NK1R, neurotoxicity and an inability to cross the blood-brain barrier, consequently limiting their clinical application (Munoz et al., 2015). The non-peptide NK1R antagonists (e.g., aprepitant, L-733,969, L-732,138) show a high affinity for the NK1R and can cross the blood-brain barrier due to their lipid solubility and therefore have been used for the treatment of tumors located in the central nervous system (CNS) (Munoz and Covenas, 2020).

The non-peptide NK1R-antagonist aprepitant is a potent and highly selective drug for chemotherapy-induced nausea and vomiting (CINV) in pediatric patients and adults and for postoperative nausea and vomiting (PONV) in adults (Chain et al., 2020). It was approved for oral administration by the *Food and Drug Administration* (FDA) and the *European Medicines Agency* (EMA) in 2003 (Emend®). Interestingly, aprepitant has shown antitumor actions both, in vitro and in vivo, in several human cancer entities, such as hepatoblastoma, neuroblastoma, colon carcinoma, B- and T-cell acute lymphoblastic leukemia, osteosarcoma, acute or chronic myeloid leukemias, melanoma, breast cancer and lung cancer (seen in Figure 2) (Berger et al., 2014, Munoz et al., 2010, Gillespie et al., 2011, Zhou et al., 2013, Munoz et al., 2014, Berger and D, 2017, Molinos-Quintana et al., 2019, Munoz et al., 2019a, Munoz and Covenas, 2020, Munoz et al., 2012, Robinson et al., 2023, Covenas et al., 2023). These antitumor actions range from promoting G2 M-phase cell-cycle arrest and triggering apoptosis by increasing expression of apoptotic markers (such as propidium iodide (PI) and annexin-V) or blocking the canonical Wnt signaling pathway in hepatoblastoma, resulting in a growth reduction of tumor cells (seen in Figure 1b) (Ilmer et al., 2015, Munoz and Covenas, 2020). Furthermore, it is important to notice the safety of the drug aprepitant. Even in high doses, aprepitant is well

tolerated and side effects remain minimal (Munoz and Covenas, 2013). Moreover, when aprepitant is co-administered with cytostatic drugs a decrease of doxorubicin-induced cardiotoxicity, cisplatin-induced-hepatotoxicity and -nephrotoxicity has been shown (Un et al., 2020).

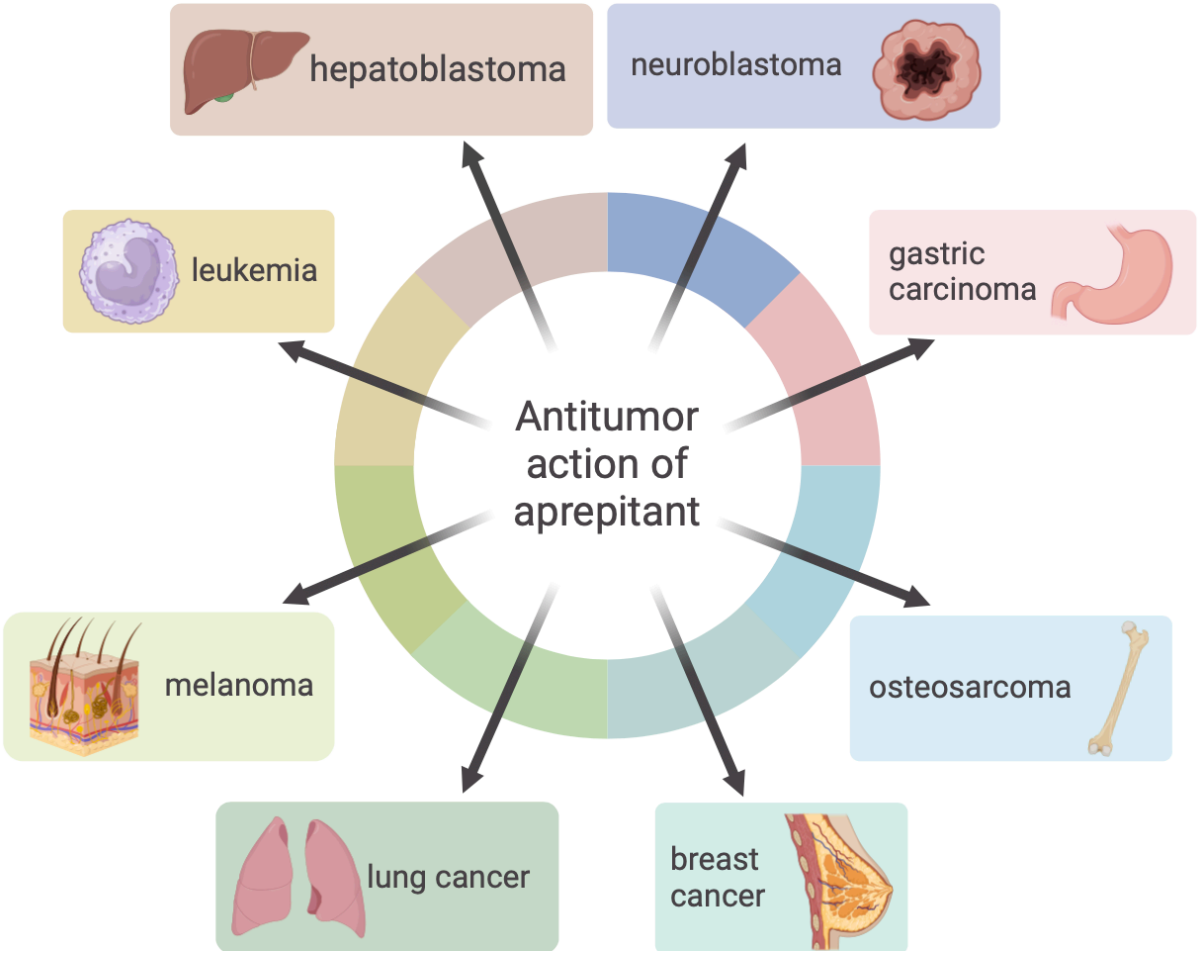

Figure 2: Overview of cancers entities in which aprepitant has been shown to exert antitumor actions, an example (based on (Munoz and Covenas, 2020)

2.2 Rhabdoid Tumor

2.2.1 Epidemiology

The Rhabdoid Tumor (RT) is a rare and highly malignant pediatric tumor that has been described largely in children between the age of 1 and 4 years (Geller et al., 2015, Fazlollahi et al., 2019). The RT can be localized in different organ compartments, such as brain (atypical teratoid/ rhabdoid tumor (AT/RT)), kidney (rhabdoid tumor of the kidney (RTK)), liver or soft tissues (malignant rhabdoid tumor (MRT)) (Chi et al., 2009, Gonzales, 2001). The AT/RT was first described in 1996 (Rorke et al., 1996), and MRT in 1978 (Beckwith and Palmer, 1978). The average annual age-adjusted incidence rate for AT/RTs in the USA was 0.07 per 100,000 (Ostrom et al., 2014) and for MRT in UK was 0.6 per 1 million children (Brennan et al., 2013).

2.2.2 Treatment

Currently there is no standard therapy regimen for RT. Even though the treatment options have been improved immensely over the last couple of years, overall survival is still dismal, which often only occurs at the cost of high toxicity and late adverse effects of chemotherapy and radiation therapy (Richardson et al., 2018). Most treatment regimens are multimodal regimens, including surgical resection of the tumor, adjuvant chemotherapy and sometimes local radiotherapy or high dose chemotherapy with autologous stem-cell rescue (Nemes et al., 2022).

A multimodal treatment approach was tested for MRT and RTK in the *European registry for Rhabdoid Tumors* (EU-RHAB) and showed a 5-year-overall-survival of 45,8 ± 5,4% and an 5-year-event-free-survival of 35,2 ± 5,1 % (Nemes et al., 2021). This approach included primary surgical resection of the tumor, following adjuvant chemotherapy and radiotherapy. High-dose chemotherapy was only used at the treating physician's discretion; however, no survival benefit of high-dose chemotherapy has yet been reported (Nemes et al., 2021).

For the treatment of AT/RT the introduction of an institutionalized multimodal approach has brought immense improvement in overall survival and event-free-survival of patients, such as the *Canadian Pediatric Neuro-Oncology Standards of Practice*, introduced in 2020 (Gastberger et al., 2023, Bennett et al., 2020). The approach is based on the treatment regimen of the *Children´s Oncology Group Trial (*ACSN0333) and the *Children's Cancer Group* (CCG99703), which both consisted of up-front surgery, adjuvant high-dose chemotherapy and sometimes local radiotherapy or autologous stem-cell rescue (Reddy et al., 2020, Bennett et al., 2020). Due to this treatment regimen, four-year event-free-survival is 37% and overall survival is 43%. Chemotherapeutic drugs, that were included in this study were vincristine, methotrexate, etoposide, cyclophosphamide, cisplatin, carboplatin and thiotepa (Reddy et al., 2020).

However, these findings still suggest a pressing requirement for novel targeted therapies to improve overall survival and to reduce toxicity of current treatment options.

2.2.3 SMARCB1 Mutation

Rhabdoid tumors represent a rare and aggressive type of cancer that are distinct by their unique genetic landscape. Their genetic driver mutation is a bi-allelic loss-of-function mutation of the SWI/SNF-related matrix-associated actin-dependent regulator of chromatin subfamily B member 1 (SMARCB1) (Kohashi and Oda, 2017, Xue et al., 2020). This “genetic hallmark” of RT, SMARCB1 is also known as integrase interactor 1 (INI1) and is a core subunit protein in the SWItch/Sucrose non-fermentable (SWI/SNF) ATP-dependent chromatin remodeling complex. SMARCB1/INI1 is expressed in the nuclei of all healthy cells and functions as a tumor suppressor gene by playing an important role in the regulation of cell cycle (Versteege et al., 1998, Hollmann and Hornick, 2011, Brennan et al., 2013). Therefore, a loss-of-function mutation in this tumor suppressor gene drives tumor proliferation in RTs. Currently, three types of aberrant SMARC1/INI1 protein expression patterns are known, which are complete loss (including MRT and AT/RT), mosaic expression and reduced expression (Kohashi and Oda, 2017).

2.3 Pancreatic Ductal Adenocarcinoma

2.3.1 Epidemiology

Pancreatic ductal adenocarcinoma (PDAC) is an aggressive solid tumor with a poor prognosis with an overall five-year survival rate of only 6% (Ilic and Ilic, 2016). It is the most common form of pancreatic cancer and one of the leading causes of cancer-related deaths in the world. The age-standardized incidence rates worldwide in 2020 were 5.7 per 100,000 people for males and 4.1 per 100,000 people for females with an age-standardized mortality rate of 5.3 per 100,000 people, or 3.8 per 100,000 people, for males or females, respectively (Sung et al., 2021). These global age-standardized incidences rates and death rates for PDAC have been steadily rising in the last decades due to several factors including aging of the population, smoking, insufficiency of physical activity and obesity (Shinoda et al., 2022, Collaborators, 2019). It has been calculated that pancreatic cancer will become the second leading cause of cancer-related deaths in high income countries such as the United States and Germany by 2030 (Quante et al., 2016). Hence, new treatment options are urgently needed.

2.3.2 Treatment

Treatment success rates for pancreatic cancer have only slightly improved over the last decades. Diagnosis at an advanced stage and resistance to chemotherapy still lead to poor treatment outcomes (Collaborators, 2019).

The standard therapy regiment for PDAC consists of a multimodal approach including surgery, chemotherapy and sometimes radiotherapy. Standard treatment regimens are based on resectability of the tumor, metastasis at diagnosis, age, medical history, and general condition of the patient (Garajova et al., 2023).

After staging the tumor is characterized as resectable, borderline resectable, locally advanced, or metastatic, whereas surgical resection of the tumor is the only curative treatment. (Conroy et al., 2023). Following curative surgical resection fit patients receive adjuvant chemotherapy with modified FOLFIRINOX (mFOLFIRINOX), whereas older (>75 years) unfit patients receive gemcitabine-based strategies (Conroy et al., 2023). Patients treated with mFOLFIRINOX regime receive fluorouracil, oxaliplatin, leucovorin and irinotecan for a period of 6 months. The median disease-free survival for these patients with resectable PDAC is 21.6 months (mFOLFIRINOX) vs. 12.8 months (gemcitabine), the median overall survival is 54.4 months (mFOLFIRINOX) vs. 35.0 months (gemcitabine), and the overall survival rate at 3 years is 63.4% (mFOLFIRINOX) vs. 48.6 months (gemcitabine), for patients treated with mFOLFIRINOX. Adverse effects were higher in mFOLFIRINOX vs. gemcitabine (75.9% vs. 52.9%) (Conroy et al., 2018).

Treatment options for patients with borderline resectable, locally advanced, and metastatic tumors include induction therapy with chemoradiotherapy and enrolling in clinical trials. Several new treatment strategies, such as a neoadjuvant treatment regimen, immunotherapeutic vaccines, immune checkpoint inhibitors, CDK4/6 inhibitors or KRAS inhibitors are being investigated, however treatment for PDAC minimally improves with a lack of early diagnosis, resistance to therapeutic options and PDAC proving to be a complex tumor entity (Digiacomo et al., 2021, Seufferlein and Ettrich, 2019, Mercanti et al., 2023, Garajova et al., 2023, Halbrook et al., 2023). Thus, novel therapeutic strategies are desperately needed.

2.4 Goal and scope of this study

The goal of this dissertation is to investigate the neurokinin-1 receptor as a target in pediatric rhabdoid tumor and pancreatic ductal adenocarcinoma. The role of the NK1R/SP-complex and its antagonist aprepitant has been described in several tumor entities. However for the first time, we present clinical data for the expression of NK1R, and introducing the NK1R-antagonist aprepitant as a novel therapeutic target for treatment of RT and PDAC (Kolorz et al., 2021, Beirith et al., 2021). The scope of both publications is outlined below.

2.4.1 The Neurokinin-1 Receptor is a Target in Pediatric Rhabdoid Tumors

Since there is no available data on the role of the NK1R in RTs so far, we started our study by analyzing the expression levels of TACR1 (NK1R) and TAC1 (SP) for the most common childhood malignancies (acute myeloid leukemia, acute lymphoblastic leukemia, neuroblastoma, and RT). We obtained publicly available data sets of the above-mentioned cancer entities (acute myeloid leukemia, n=44, acute lymphoblastic leukemia, n=203, neuroblastoma, n=140, RT, n=42 and Wilms´ tumor, n=129) from the cBio Cancer Genomics portal and carried out gene expression analyses (Paper I, Figure 1a-b).

We found that the expression levels of TACR1 were significantly higher in RTs than in other childhood malignancies. Therefore, as a next step, we performed real-time quantitative polymerase chain reaction (RT-qPCR) analysis in RT cell lines (one RTK cell line, two AT/RT cell lines) and in tumor tissue samples, obtained from patients as surgical resectates (Paper I, Figure 1c-h). Interestingly, expression levels for NK1R-variants (TACR1-fl, TACR1-tr) were similar compared to a human hepatoblastoma cell line with a known high expression of TACR1-tr, which was used as a positive control (Berger et al., 2014). TACR1-tr expression levels were significantly elevated in every cell line and TACR1-tr was expressed higher in tumor tissue samples compared to TACR-fl. Two human dermal fibroblasts were used as healthy controls. We also tested TAC1 expression levels in all cell lines. Overall expression levels were detected to be low with the exceptions of adult fibroblasts and, surprisingly, primary patient material from a RT of the kidney.

Next, we analyzed the clinical outcome and the biological characteristics of patients with RT, by utilizing the data retrieved from the cBio Cancer Genomics Portal (tumor stage, gender, age of diagnosis and overall survival). Patient cohorts were divided in TACR1 or TAC1 low-expressing and high-expressing groups, by taking median expression levels as cut out point. Interestingly, we observed no significant differences between high- and low-expressing groups and concluded that the expression of TACR1 and TAC1 is independent of clinical and biological characteristics (Paper I, Figure 1i-l).

To investigate the role of NK1R-targeted therapies in RT, we performed MTT cell viability assays and exposed tumor cells to increasing concentrations of aprepitant (Paper I, Figure 2a). A dose-dependent decrease on tumor cell viability was detected in RT cell lines. Furthermore, we exposed tumor cells to increasing concentrations of cisplatin and the combination of cisplatin and aprepitant to examine possible synergistic effects of conventional chemotherapy and NK1R-targeted therapies (Paper I, Figure 2b-c). We observed trends towards additive effects.

To probe whether SP could reverse the treatment effect of aprepitant, we treated tumor cells with supramaximal dosages of SP and aprepitant and observed that SP did not cause any toxicity for the cells and that it reversed the anti-proliferative effect of aprepitant (Paper I, Figure 2d). This insight highlighted the specificity of NK1R-targeted therapies.

As a next step, we investigated the mechanism of cell death by flow cytometry with Annexin V staining and observed reduction of viable cell populations upon aprepitant-treatment and increasing populations of early and late apoptotic cells, suggesting apoptosis as one mechanism of cell death (Paper I, Figure 3a-b). To confirm this finding, we performed Western blot analysis with apoptotic markers and detected an upregulation of apoptotic signaling pathways in RTs upon treatment with aprepitant (Paper I, Figure 4a-b).

2.4.2 Identification of the Neurokinin-1 Receptor as Targetable Stratification Factor for Drug Repurposing in Pancreatic Cancer

There is limited information available about the effects of the neurokinin-1 receptor in pancreatic ductal adenocarcinoma. Therefore, we started our investigation by analyzing expression levels of NK1R variants (TACR1-fl, TACR1-tr) and SP (TAC1) with RT-qPCR in PDAC cell lines and primary stellate cells (Paper II, Figure 1a). Expression levels of TACR1-tr varied and no expression of TACR1-fl was detected. Later, Enzyme-Linked Immunosorbent Assay (ELISA) was performed, and the presence of SP was shown in all tested cell lines (Paper II, Figure 1b-c).

As a next step, we analyzed data sets from the Cancer Genome Atlas, the Cancer Cell Line Encyclopedia and the Gene Expression Omnibus and observed significant downregulation of TACR1 in tumor cells in comparison to normal cells. Interestingly, tendencies towards a lower expression of TACR1 with tumor stage progression were observed, while high expression of TACR1 correlated with higher overall survival of PDAC patients (Paper II, Figure 2a-f).

To determine the effects of NK1R-targeted therapy on PDAC cells, we carried out MTT cell viability assays, by exposing the cells to increasing concentrations of aprepitant and observed a dose-dependent growth inhibition in PDAC cell lines and cancer stem cell-like cells (CSCs)

(Paper II, Figure 3a-b). Furthermore, functional effects with colony and sphere formation assays were performed, resulting in a dose-dependent treatment response towards aprepitant and demonstrating morphological differences of cell size, shape, and texture after treatment (Paper II, Figure 3c-d)).

Lastly, using flow cytometry with annexin V/ PI staining we were able to measure treatment-induced apoptotic cell populations (Paper II, Figure 4-5). Applying DAPI staining in flow cytometry, we acknowledged that aprepitant exposure leads to cell cycle arrest in PDAC cell lines with TACR1 expression.

3. Zusammenfassung

Das Neurokinin-1-Rezeptor- (NK1R) /Substanz P (SP)-System spielt eine wichtige Rolle bei der Krebsentstehung. Durch die Bindung an seinen Rezeptor induziert SP die Proliferation von Tumorzellen und hemmt apoptotische Mechanismen. Eine zielgerichtete Therapie gegen den NK1R stellt daher einen hoffnungsvollen Ansatz für eine Antitumorstrategie dar. Einer der NK1R-Antagonisten ist das Medikament Aprepitant (Emend®), das normalerweise bei Chemotherapie-induzierter Übelkeit und Erbrechen eingesetzt wird. Aprepitant übt nachweislich anti-proliferative und anti-metastatische Wirkungen aus und verursacht in hohen Dosen wenig bis keine Nebenwirkungen. Diese Antitumorwirkungen wurden bei mehreren Krebserkrankungen in in-vivo- und in-vitro-Studien gezeigt. Es besteht jedoch noch ein Mangel an Wissen über ihre Wirkungen bei RTs und PDACs.

Der Rhabdoidtumor ist ein seltener und bösartiger pädiatrischer Tumor, der hauptsächlich Kinder im Alter zwischen 1 und 4 Jahren betrifft. RTs können an mehreren Stellen des Körpers auftreten, wie z.B. im Gehirn (AT/RT), in der Niere (RTK), in der Leber oder in Weichteilen (extrarenaler rhabdoider Tumor oder MRT). Aufgrund des Fehlens einer wirksamen Standardtherapie werden dringend neue zielgerichtete Therapien benötigt. Darüber hinaus kann es trotz erfolgreicher Remission oft zu Langzeitnebenwirkungen von Chemotherapeutika kommen. In dieser Studie zeigen wir, dass der NK1R in rhabdoiden Tumorzellen exprimiert wird und nicht auf bestimmte klinische oder biologische Eigenschaften beschränkt ist. Darüber hinaus zeigen wir zum ersten Mal, dass Aprepitant das Tumorwachstum wirksam hemmt, die pro-apoptotischen Signalkaskaden in RT-Zellen auslöst und es einen additiven Effekt gibt, wenn es mit dem Standard-Chemotherapeutikum Cisplatin kombiniert wird.

Das duktale Adenokarzinom des Pankreas ist eine aggressive bösartige Erkrankung mit einer schlechten 5-Jahres-Überlebensrate und steigenden Inzidenzen. Es ist die häufigste Form von Bauchspeicheldrüsenkrebs und eine der Hauptursachen für krebsbedingte Todesfälle weltweit. Aufgrund von Adipositas, Typ-II-Diabetes und einem Wandel der Bevölkerungsstruktur ist mit einem weiteren Anstieg der Inzidenz innerhalb der nächsten zehn Jahre zu rechnen. Derzeitige Therapieregime konzentrieren sich auf die chirurgische Resektion gefolgt von einer adjuvanten Chemotherapie, jedoch gibt es nur wenige Patienten mit resektablem duktalem Adenokarzinom des Pankreas. In dieser Veröffentlichung konnten wir erstmals zeigen, dass Aprepitant die Wachstumsreduktion wirksam hemmt und einen Zellzyklusarrest in PDAC-Zelllinien hervorruft. Dementsprechend ist eine NK1R-gerichtete Therapie für PDAC-Patienten auch in einem klinischen Umfeld vorstellbar.

4. Abstract

The neurokinin-1 receptor (NK1R)/ substance P (SP) system plays an important role in cancer development. By binding to its receptor, SP induces proliferation of tumor cells and inhibits apoptotic mechanisms. It has been shown that targeting the NK1R can be a used as a tool in antitumor treatment. One of the NK1R-antagonists is the drug Aprepitant (Emend®), usually used for chemotherapy-induced nausea and vomiting. Aprepitant has been shown to exert antiproliferative and antimetastatic effects and to not cause severe adverse events in high doses. These antitumor effects have been shown in several malignancies in in vivo and in in vitro studies, however there is still a lack of knowledge regarding its effects on RTs and PDACs.

The rhabdoid tumor is a rare and malignant pediatric tumor, primarily affecting children between the age of 1 and 4 years. RTs can occur in several sites such as the brain (ATRT), kidney (RTK), liver or soft tissues (extrarenal rhabdoid tumor or MRT). Due to the lack of a standard effective therapy, new targeted therapies are desperately needed. Additionally, successful remission is often dimmed by late adverse effects due to the high toxicity of chemotherapeutics. In this study, we show that the NK1R is expressed in rhabdoid tumor cells and that it is not restricted to certain clinical or biological characteristics. Furthermore, for the first time, we demonstrate that aprepitant effectively inhibits tumor growth and triggers apoptosis signaling in RT cells and shows an additive effect when combined with standard chemotherapy drug cisplatin.

Pancreatic ductal adenocarcinoma is an aggressive malignancy with a poor 5-year survival rate and rising incidence. It is the most common form of pancreatic cancer and one of the leading causes for cancer-related deaths worldwide. Due to obesity, type II diabetes and a change in demographics its incidence is expected to rise further within the next ten years. Current therapy regiments focus on surgical resection followed by adjuvant chemotherapy, however, only few patients present with resectable PDAC. In this publication, we show that aprepitant effectively inhibits growth reduction and leads to cell cycle arrest in PDAC cell lines. Therefore, a NK1R-targeted therapy for PDAC patients seems plausible.

5. Paper I

Current Oncology

MDPI

Article

The Neurokinin-1 Receptor Is a Target in Pediatric Rhabdoid Tumors

Julian Kolorz [1,†], Salih Demir [1,†], Adrian Gottschlich [2], Iris Beirith [3], Matthias Ilmer [3,4], Daniel Lüthy [1], Christoph Walz [5], Mario M. Dorostkar [6], Thomas Magg [7], Fabian Hauck [7], Dietrich von Schweinitz [1], Sebastian Kobold [2,4,8], Roland Kappler [1] and Michael Berger [1,*]

1 Research Laboratories, Department of Pediatric Surgery, Dr. von Hauner Children's Hospital, Ludwig-Maximilians-University Munich, 80337 Munich, Germany; julian.kolorz@med.uni-muenchen.de (J.K.); salih.demir@med.uni-muenchen.de (S.D.); daniel.luethy@med.uni-muenchen.de (D.L.); dietrich.schweinitz@med.uni-muenchen.de (D.v.S.); roland.kappler@med.uni-muenchen.de (R.K.)
2 Center for Integrated Protein Science Munich (CIPSM) and Division of Clinical Pharmacology, Department of Medicine IV, University Hospital, Ludwig-Maximilians-University Munich, 80337 Munich, Germany; adrian.gottschlich@med.uni-muenchen.de (A.G.); sebastian.kobold@med.uni-muenchen.de (S.K.)
3 Department of General, Visceral, and Transplantation Surgery, University Hospital, Ludwig-Maximilians-University Munich, 81377 Munich, Germany; iris.beirith@med.uni-muenchen.de (I.B.); matthias.ilmer@med.uni-muenchen.de (M.I.)
4 German Center for Translational Cancer Research (DKTK), Partner Site Munich, 81377 Munich, Germany
5 Institute of Pathology, Faculty of Medicine, Ludwig Maximilians-University Munich, 80337 Munich, Germany; christoph.walz@med.uni-muenchen.de
6 Center for Neuropathology, Ludwig-Maximilians-University Munich, 81377 Munich, Germany; mario.dorostkar@med.uni-muenchen.de
7 Department of Pediatrics, Dr. von Hauner Children's Hospital, Ludwig-Maximilians-University Munich, 80337 Munich, Germany; thomas.magg@med.uni-muenchen.de (T.M.); fabian.hauck@med.uni-muenchen.de (F.H.)
8 Einheit für Klinische Pharmakologie (EKLiP), Helmholtz Zentrum München, German Research Center for Environmental Health (HMGU), 85764 Neuherberg, Germany
* Correspondence: michael.berger@med.uni-muenchen.de; Tel.: +49-89-4400-57859
† These authors contributed equally to this work.

check for updates

Citation: Kolorz, J.; Demir, S.; Gottschlich, A.; Beirith, I.; Ilmer, M.; Lüthy, D.; Walz, C.; Dorostkar, M.M.; Magg, T.; Hauck, F.; et al. The Neurokinin-1 Receptor Is a Target in Pediatric Rhabdoid Tumors. *Curr. Oncol.* **2022**, *29*, 94–110. https://doi.org/10.3390/curroncol29010008

Received: 15 November 2021
Accepted: 24 December 2021
Published: 26 December 2021

Publisher's Note: MDPI stays neutral with regard to jurisdictional claims in published maps and institutional affiliations.

Abstract: Rhabdoid tumors (RT) are among the most aggressive tumors in early childhood. Overall survival remains poor, and treatment only effectively occurs at the cost of high toxicity and late adverse effects. It has been reported that the neurokinin-1 receptor/ substance P complex plays an important role in cancer and proved to be a promising target. However, its role in RT has not yet been described. This study aims to determine whether the neurokinin-1 receptor is expressed in RT and whether neurokinin-1 receptor (NK1R) antagonists can serve as a novel therapeutic approach in treating RTs. By in silico analysis using the cBio Cancer Genomics Portal we found that RTs highly express neurokinin-1 receptor. We confirmed these results by RT-PCR in both tumor cell lines and in human tissue samples of various affected organs. We demonstrated a growth inhibitory and apoptotic effect of aprepitant in viability assays and flow cytometry. Furthermore, this effect proved to remain when used in combination with the cytostatic cisplatin. Western blot analysis showed an upregulation of apoptotic signaling pathways in rhabdoid tumors when treated with aprepitant. Overall, our findings suggest that NK1R may be a promising target for the treatment of RT in combination with other anti-cancer therapies and can be targeted with the NK1R antagonist aprepitant.

Keywords: rhabdoid tumor; NK-1 receptor; NK-1 receptor antagonist; substance P; cancer; apoptosis

1. Introduction

Rhabdoid tumors (RT) are rare and highly aggressive tumors primarily affecting infants and young children [1–3]. They have been reported to be located in several organ compartments, such as the central nervous system (CNS) (referred to as atypical

teratoid/rhabdoid tumor [AT/RT]), kidneys (RT of the kidney [RTK]), the liver, and soft tissue (extrarenal RT, malignant RT [MRT]) [1,3–7]. One of the genetic hallmarks of RTs is a loss-of-function mutation of the SWI/SNF-related matrix-associated actin-dependent regulator of chromatin subfamily B member 1 (SMARCB1), also named integrase interactor 1 (INI1). INI1 acts as a component of the SWItch/Sucrose Non-Fermentable (SWI/SNF) chromatin-remodeling complex, which functions as a tumor suppressor [1,8]. Prognosis of children with RT has improved, but overall survival remains unsatisfactory with less than 50% for AT/RTs and less than 40% for MRTs [9–12]. The lack of standard effective therapy, considerable concern about the toxicity of the chemotherapeutics, and late adverse effects require an improvement in the treatment of RT [1,2,9,12–14].

The involvement of the neurokinin-1 receptor (NK1R; *TACR1*)/substance P (SP; *TAC1*) complex in cancer has been described previously [15–19]. By binding to NK1R, SP promotes a variety of functions to improve the growth and survival of tumor cells [20]. Thus, the use of NK1R antagonists can serve as a desirable target for cancer treatment.

Two isoforms of NK1R have been reported. Full-length (fl-) NK1R contains 407 amino acids, whereas truncated (tr-) NK1R only consists of 311 amino acids, lacking 96 amino acids at the cytoplasmic C-terminus of the receptor [19,21]. It has been demonstrated that the truncated isoform is expressed higher in the tumor in comparison to the full-length isoform [17]. Furthermore, the full-length form has been associated with slow growth of cells, whereas an upregulation of the truncated version has been related with rapid growth and more aggressive behavior of tumor cells [22,23].

The non-peptide NK1R antagonist aprepitant is approved by the *Food and Drug Administration (FDA)* for the treatment of chemotherapy-induced nausea and vomiting. However, it has been shown to exert antiemetic, antipruritic, antiviral, and a broad variety of antitumor actions as well [20]. Importantly, the side effects of aprepitant are minimal, and even high doses do not seem to influence the proliferative capacity of healthy cells [24–26].

Until now, the role of the NK1R/SP complex in rhabdoid tumors remained unknown. For the first time, we describe the expression of NK1R and its truncated splice variant in rhabdoid tumors, and that it can be targeted with NK1R antagonist aprepitant, serving as a novel target for the treatment of RT.

2. Materials and Methods

2.1. Cell Culture

Two AT/RT cell lines, BT-12 and CHLA-266, one RTK cell line, G-401, and one hepatoblastoma (HB) cell line, HepG2, were used throughout this study. The two cell lines BT-12 and CHLA-266 were obtained from the Childhood Cancer Repository of the Children's Oncology Group at Texas Tech University Health Sciences Center (Lubbock, TX, USA). Both AT/RT cell lines were grown in Iscove's Modified Dulbecco's Medium (Gibco, Carlsbad, CA, USA) supplemented with 20% heat-inactivated fetal calf serum (FCS) and 100 µg/mL streptomycin 100 U/mL penicillin. G-401 was purchased from the ATCC (Manassas, VA, USA) and was grown in McCoy-5A-Medium (ATCC, Manassas, VA, USA) supplemented with 10% FCS and 100 µg/mL streptomycin 100 U/mL penicillin. HepG2 was grown in RPMI (Gibco, Carlsbad, CA, USA) supplemented with 10% FCS and 100 µg/mL streptomycin 100 U/mL penicillin as previously described [19,27]. The two primary dermal fibroblasts PCS-201-012 (Adult) and PCS-201-010 (Neonatal) were both obtained from the ATCC (Manassas, VA, USA) and grown in DMEM (Gibco, Carlsbad, CA, USA) with 10% FCS and 100 µg/mL streptomycin 100 U/mL penicillin. All cells were grown at 37 °C in a humidified incubator with 5% CO_2. Mycoplasma contamination was regularly excluded using mycoplasma-specific polymerase chain reactions protocols.

2.2. Drugs

The NK1R antagonist aprepitant and the cytostatic compound cisplatin were purchased from Selleck Chemicals (Houston, TX, USA) and were dissolved in DMSO. SP

(NK1R agonist) was purchased from Sigma-Aldrich (St. Louis, MO, USA) and dissolved in 0.1 mol/L acetic acid and purified water.

2.3. Proliferation Assays (MTT Assay)

MTT (3-(4,5-dimethylthiazol-2-yl)-2,5-diphenyltetrazolium bromide) salt was purchased from Sigma-Aldrich (St. Louis, MO, USA) and dissolved in PBS (MTT solution; 5 mg/mL). 5×10^4 cells/well were seeded into a 96-well plate and were incubated overnight in culturing media for attachment. The cells were exposed to 10 different increasing concentrations of the corresponding compounds (from 0.02 μM to 100 μM) for 48 h. For combination treatment, the cells were exposed to the corresponding compounds for 48 h. After exposure, culturing media was replaced with the MTT solution for 4 h at 37 °C. Then, MTT solution was replaced with 10% SDS in 0.01 M HCl for overnight incubation in the incubator. 96-well plates were measured using a FLUOstar Omega microplate reader (BMG LABTECH Inc., Cary, NC, USA) at 595 nm wavelength.

2.4. In Vitro Analysis of Apoptosis

The determination of apoptotic cell populations was performed by flow cytometry. Annexin V staining was performed according to manufacturer's instructions. 5×10^4 cells/well were seeded into a 96-well plate. The cells were incubated overnight in the culturing media for attachment and then were exposed to the corresponding compounds for 48h. Cells were stained with 2 μL Pacific Blue Annexin V (BioLegend, San Diego, CA, USA) for 15 min at RT in dark. Annexin V-binding buffer (10× Binding Buffer: 10 mM HEPES/NaOH, 140 mM NaCl, 2.5 mM CaCl2) was used for respective staining and washing steps. Fixable Viability Dye eFluor™ 780 (FVD, eBioscience, Inc., San Diego, CA, USA) was used to discriminate viable and dead cell populations. Staining was carried out at 4 °C for 30 min in the dark. Percentages of viable, apoptotic and necrotic cells were measured with a BD FACSCanto II (BD Biosciences, Franklin Lanes, NY, USA) and results were analyzed using FlowJo 10.0 Software (Tree Star, Inc., Ashland, OR, USA).

2.5. Western Blot Analysis

Protein expression of PARP-1 (rabbit, 1:1000 dilution; Cell Signaling Technologies, Danvers, MA, USA) and α-tubulin (mouse, 1:5000 dilution; Sigma-Aldrich, St. Louis, MO, USA) was analyzed by Western blot analysis. Cells were lysed for 30 min on ice with lysis buffer (tris-HCL 30 mM, NaCl 150 mM, tritonX 1% and glycerol 10%) and then underwent high-speed centrifugation. Protein concentration was assessed by Bradford assay (Bio-Rad Laboratories, Hercules, CA, USA). 20 mg protein per well was separated by Novex WedgeWell 4 to 20%, Tris-Glycine, 1.0 mm, mini protein gels (Invitrogen, Carlsbad, CA, USA) and electroblotted onto 0.2 μm PVDF membranes using Trans-Blot Turbo mini transfer packs (Bio-Rad Laboratories, Hercules, CA, USA). After blocking for 1 h in phosphate-buffered saline supplemented with 5% milk and 0.1% Tween 20 (Sigma-Aldrich, St. Louis, MO, USA), immunodetection was performed using polyclonal goat anti-mouse IgG (P0447; 1:20,000) and polyclonal goat anti-rabbit IgG (P0448; 1:2000) antibodies (both from DakoCytomation Denmark A/S, Glostrup, Denmark). Enhanced chemiluminescence was used for detection (GE Healthcare Amersham™ ECL™ Prime Western blotting detection reagents, Thermo Scientific, Waltham, MA, USA) and imaging was performed at ChemiDoc XRS+ (Bio-Rad Laboratories, Hercules, CA, USA). The size of proteins on Western blots was identified by PageRuler Prestained Protein Ladder (Thermo Scientific, Waltham, MA, USA).

2.6. RT-PCR (Reverse Transcription Polymerase Chain Reaction)

RNA extraction, complementary DNA synthesis, and quantitative polymerase chain reaction (qPCR) analysis were performed as previously described [27]. Specific primers were as follows: *TACR1-fl* (NM_001058.3; forward 5′-AACCCCATCATCTACTGCTGC-3′ and reverse 5′-ATTTCCAGCCCCTCATAGTCG-3′), *TACR1-tr* (forward 5′-

CAGGGGCCACAAGACCATCTA-3′ and reverse 5′-ATAAGTTAGCTGCAGTCCCCAC-3′), *TAC1* (forward 5′-AAGCCTCAGCAGTTCTTTGG-3′ and reverse 5′-TCTGGCCATGTCCATAAAGAG-3′) and *TBP* (forward 5′-GCCCGAAACGCCGAATAT-3′ and reverse 5′-CCGTGGTTCGTGGCTCTCT-3′).

2.7. Patients and Tumor Samples

A total of 6 tumor specimens were obtained from pediatric patients. Three rhabdoid tumors of the liver and one rhabdoid tumor of the kidney were resected at the Department of Pediatric Surgery, LMU and preserved in liquid nitrogen. Two formalin-fixed and paraffin-embedded AT/RT tumor samples on slides were obtained from the Center for Neuropathology, LMU. RNA from the former samples was extracted using TRIzol reagent (Invitrogen, Karlsruhe, Germany), from the latter using High Pure FFPET RNA Isolation Kit from Roche Diagnostics Deutschland GmbH (Mannheim, Germany) according to manufacturer's instructions. The study protocol was approved by the Committee of Ethics of the LMU (Munich) and written informed consent was obtained from each patient in accordance with the Declaration of Helsinki.

2.8. Data Base Analysis

Data sets were derived from the cBio Cancer Genomics Portal (http://cbioportal.org; accessed on 2 December 2021) [28–30]. Five pediatric cancer studies on acute myeloid leukemia (AML; phs000465), acute lymphoblastic leukemia (ALL; phs000464), neuroblastoma (NB; phs000467), rhabdoid tumors (RT; phs0004709), and Wilms tumor (WT; phs000471) were selected from the Therapeutically Applicable Research to Generate Effective Treatments (https://ocg.cancer.gov/programs/target; accessed on 2 December 2021) initiative and the mRNA expression of 2 genes was analyzed (*TACR1*, *TAC1*).

2.9. Statistical Analysis

Results are expressed as the mean ± standard error of the mean (SEM). All statistical comparisons were made with an unpaired parametric t-test comparing two groups, an ordinary one-way ANOVA or a Tukey´s multiple comparison test, with a single pooled variance using GraphPad Prism (San Diego, CA, USA). The significance was considered as: $p < 0.05$ (*), $p < 0.01$ (**), $p < 0.001$ (***) and $p < 0.0001$ (****) for all comparisons.

3. Results

3.1. Expression of TACR1 and TAC1 in Pediatric Cancer

It has been previously demonstrated that the NK1R/SP complex serves as a target in a large variety of cancers, including pediatric malignancies such as neuroblastoma and hepatoblastoma [19,20,31–33]. Nothing was known of the expression of this potent target in rhabdoid tumors. Therefore, as a first step we assessed expression levels for the NK1R/SP complex (TACR1, TAC1) of the most common childhood malignancies from the cBio Cancer Genomics Portal, focusing on acute myeloid leukemia, acute lymphoblastic leukemia, neuroblastoma, and Wilms' tumor, and compared them to the expression levels in rhabdoid tumors [28]. Database analysis showed that the TACR1 gene is expressed significantly higher in rhabdoid tumors in comparison to the aforementioned tumors (Figure 1a). TAC1 mRNA (which codes for SP and is the natural ligand of NK1R) expression levels were high in rhabdoid tumors and neuroblastoma, but not significantly different to the other tumors (Figure 1b). As this in silico analysis did not allow for a sub-analysis between the expression levels of the full-length and truncated splice variant of NK1R, we next determined their gene expression levels in RT cell lines by RT-PCR (Figure 1c–f). The RTK cell line G-401 and the two AT/RT cell lines BT-12 and CHLA-266 are known to carry loss-of-function mutation of INI1 [34,35] and their characteristics are summarized in Table 1. Interestingly, expression levels of TACR1-fl and TACR1-tr genes in G-401, BT-12, and CHLA-266 were similar to HepG2, a human hepatoblastoma (HB) cell line with a known high expression of TACR1-tr [19] used as a positive control. The adult and neonatal

primary dermal fibroblasts expressed significantly less TACR1-tr than G-401 and were used as a negative control (Figure 1e). TACR1-tr was significantly overexpressed in every cell line compared to TACR1-fl (Figure 1c). Then, expression levels of TAC1 were tested in the different cell lines. The expression levels of TAC1 were detected to be very low in all cell lines analyzed except for the primal dermal fibroblasts (Figure 1d). Of the tumor cell lines, G-401 showed the highest expression of TAC1, while HepG2 cells have no detectable expression of TAC1 in mRNA levels.

Table 1. Summary of characteristics of cell lines.

Cell Line	Disease	Origin	INI1-Mutation
BT-12	AT/RT	Female, 2 months, Caucasian	Loss-of-function
CHLA-266	AT/RT	Female, 30 months, Caucasian	Loss-of-function
G-401	RTK	Male, 3 months, Caucasian	Loss-of-function
HepG2	HB	Male, 15 years, Caucasian	–

AT/RT—atypical teratoid/rhabdoid tumor; RTK—rhabdoid tumor of the kidney; HB—hepatoblastoma; INI1—integrase interactor 1.

Next, we analyzed the expression levels of TACR1 in six rhabdoid tumor tissue samples by RT-PCR. As rhabdoid tumors can arise at different sites throughout the body, we analyzed tissue samples of three MRTs of the liver, one RT of the kidney, and two AT/RTs. The patient characteristics are summarized in Table 2. The age at the time of diagnosis ranged from 0–127 months (median, 18 months). INI1 alterations were detected in all tested samples. Five out of six tumor samples showed a loss-of-function mutation of INI. Interestingly, one patient (T190) was found to carry an INI1 germ line mutation (Table 2). The respective patient was first diagnosed with an AT/RT, and after initial successful treatment, subsequently developed a RTK. In line with the expression pattern observed in AT/RT and RTK cell lines, splice variant TACR1-tr was expressed higher than TACR1-fl. Expression levels of TACR1-tr were found the highest in an RT of the liver tumor tissue sample (T125II), and the lowest in AT/RT tumor tissue samples (T16, T12IC). TACR1-fl expression was found to be very low in all tumor samples analyzed. Surprisingly, the analysis of TAC1 expression revealed that the RT of the kidney (T190) had the highest expression, whereas the other tumor tissue samples showed almost no expression (Figure 1g,h).

In conclusion, we were able to demonstrate the expression of TACR1 in both RT cell lines and primary patient material, with TACR1-tr being significantly higher expressed than TACR1-fl in all tested samples. Importantly, both cell lines and patient tissue samples originated from different compartments of the body, modelling the heterogenicity of rhabdoid tumors.

3.2. Clinical Outcome and Biological Characteristics of Patients with Rhabdoid Tumors

Next, we made use of the pediatric rhabdoid tumor study from The cBio Cancer Genomics Portal to understand in detail whether TACR1 or TAC1 expression in rhabdoid tumors correlates with biological or clinical characteristics [28]. The gene expression patterns of 42 patients were analyzed and correlated to tumor stage, gender, age of diagnosis and overall survival (Table 3, Figure 1i–l). Tumor stages were classified by the American Joint Committee on Cancer [36]. mRNA expression for TACR1 showed similar expression in every stage, whereas mRNA expression for TAC1 was slightly elevated in stages I–II. Gender was distributed similarly for TACR1 and TAC1 (45% male vs. 55% female) and no

significant differences in the mRNA expression levels of the genes were observed. Age of diagnosis was prominently represented within the first year of life for both TACR1 and TAC1 (<6 months, 22.5%; 6–12 months, 37.5%). Overall survival of rhabdoid tumor patients with low expression (n = 20) of TACR1 or TAC1 was compared to the patients with high expression (n = 19) based on the median of TAC1 or TACR1 expression. For three patients, overall survival data was not available. We could not observe any significant differences between TACR1 or TAC1 low-expressing and high-expressing groups.

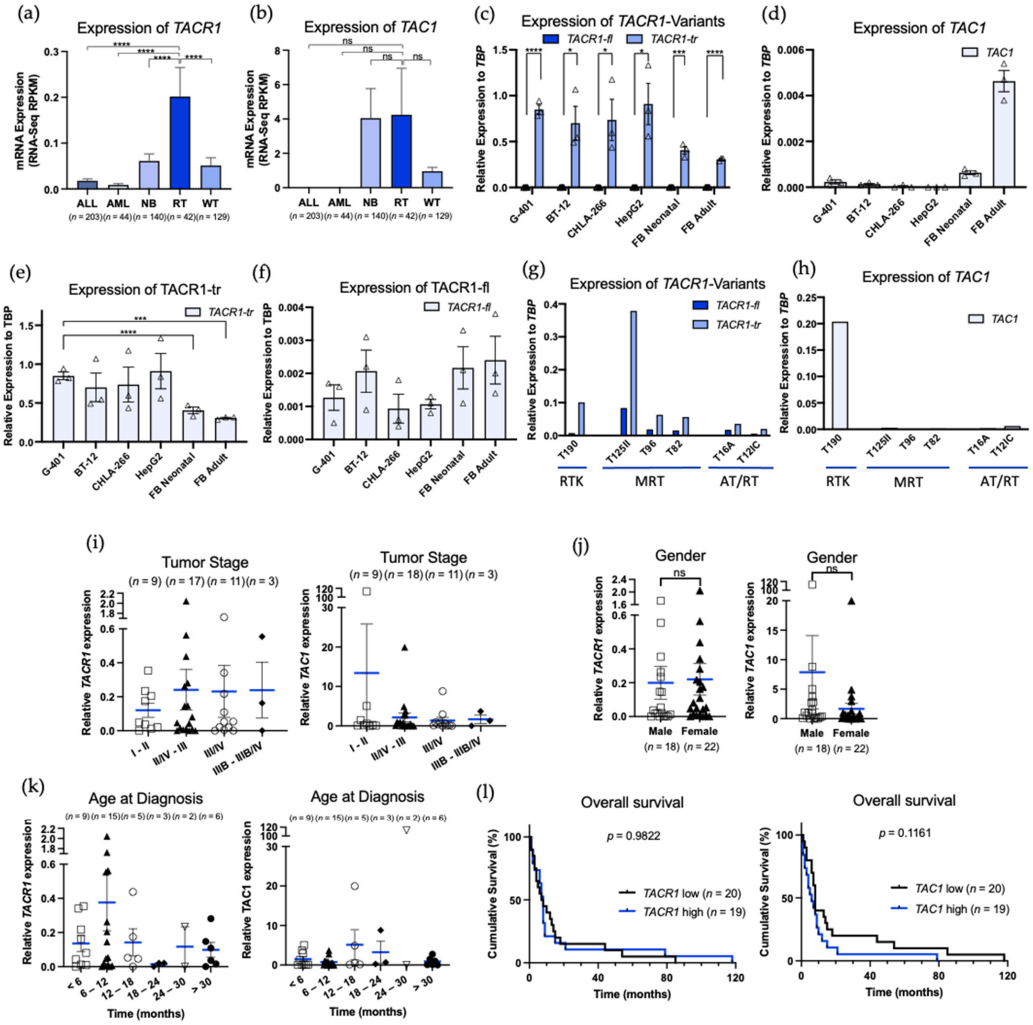

Figure 1. Expression of *TACR1* and *TAC1* and biological and clinical parameters of rhabdoid tumors. (**a**,**b**) mRNA expression of *TACR1* and *TAC1* in ALL (n = 203), AML (n = 44), NB (n = 140), RT (n = 42), and WT (n = 129). Relative expression was correlated to the (**i**) tumor stage by the Neoplasm American Joint Committee on Cancer (I-II n = 9; II/IV-III n = 17 for TACR1, n = 18 for TAC1; III/IV

n = 11; IIIB-IIIB/IV n = 3), (**j**) gender (Male n = 18; Female n = 22), (**k**) age at diagnosis (months) (<6 months n = 9; 6–12 months n = 15; 12–18 months n = 5; 18–24 months n = 3; 24–40 months n = 2; >30 months n = 6), (**l**) overall survival (months) (TACR1 low n = 20; TACR1 high n = 19; TAC1 low (n = 20), TAC1 high n = 19), and (**c**–**f**) mRNA expression of *TACR1-fl*, *TACR1-tr,* and *TAC1* in G-401, BT-12, CHLA-266, HepG2, and in FB Neonatal (=fibroblasts neonatal, PCS-201-120) and in FB Adult (=fibroblasts adult, PCS-201-012) normalized to the housekeeping gene *TBP*. (**g**,**h**) mRNA expression of *TACR1-fl*, *TACR1-tr* and *TAC1* in tumor samples normalized to *TBP*. Results are expressed as the mean ± standard error of the mean (SEM). All statistical comparisons were made with an unpaired parametric t-test comparing two groups, an ordinary one-way ANOVA or a Tukey's multiple comparison test, with a single pooled variance. ns = not significant. $p < 0.05$ (*), $p < 0.001$ (***) and $p < 0.0001$ (****) for all comparisons.

Table 2. Summary of the characteristics of tumor samples.

Case	Name	Subtype of RT (Organ Compartment)	Gender (M/F)	Age at Diagnosis (Months)	INI1-Mutation	Treatment	Relapse
1	T190	AT/RT → RTK *	M	<23 *	Germline mutation	Chemotherapy, Resection, Stem-cell therapy	Yes
2	T125II	MRT (liver)	M	10	Loss-of-function	Chemotherapy, Resection	Yes
3	T96	MRT (liver)	F	13	Loss-of-function	Chemotherapy, Resection, Stem-cell therapy	No
4	T82	MRT (liver)	M	33	Loss-of-function	Chemotherapy, Resection	No
5	T16A	AT/RT	M	5	Loss-of-function	-	-
6	T12IC	AT/RT	M	127	Loss-of-function	Chemotherapy, Radiotherapy	Yes

M—male; F—female; RTK—rhabdoid tumor of the kidney; AT/RT—atypical teratoid/rhabdoid tumor; MRT—malignant rhabdoid tumor; INI1—integrase interactor 1; * Relapse.

Table 3. Summary of clinical outcome and biological characteristics of the patients from database analysis.

Characteristics	TACR1 *	TAC1 *
Tumor Stage		
I–II	9 (22.5)	9 (22.0)
II/IV–III	17 (42.5)	18 (43.9)
III/IV	11 (27.5)	11 (26.8)
IIIB–IIIB/IV	3 (7.5)	3 (7.3)
Gender		
Male	18 (45.0)	18 (45.0)
Female	22 (55.0)	22 (55.0)
Age at Diagnosis (months)		
<6	9 (22.5)	9 (22.5)
6–12	15 (37.5)	15 (37.5)
12–18	5 (12.5)	5 (12.5)
18–24	3 (7.5)	3 (7.5)
24–30	2 (5.0)	2 (5.0)
>30	6 (15.0)	6 (15.0)

* Patients, n (%); data sets were derived from the cBio Cancer Genomics Portal.

Overall, we observed that TACR1 and TAC1 were expressed across different tumor stages and independent of gender or age of diagnosis. This conserved expression highlights the functionality of the NK1R/SP axis in rhabdoid tumors independent of clinical or

biological characteristics of the patient. Thus, NK1R redirected targeted therapies would not be restricted to a certain subset of patient suffering from rhabdoid tumors.

3.3. Aprepitant Inhibits Tumor Growth in Rhabdoid Tumor Cell Lines and Shows Increased Activity with Cisplatin

To probe the role of NK1R-SP-targeted therapies in rhabdoid tumors, we next investigated the effect of aprepitant on the RT tumor cell lines G-401, BT-12, and CHLA-266 with the human HB cell line HepG2 as a positive control and the primary dermal fibroblasts as a negative control for aprepitant response [19]. Tumor cells were exposed to nine different increasing concentrations of aprepitant (ranging from 10 μM to 100 μM) for 48 h and viability was determined using MTT cell proliferation assay. All RT cells showed a dose-dependent decrease in cell viability after aprepitant treatment in comparison to solvent-treated controls. The neonatal and adult primary dermal fibroblasts showed no strong dose-dependent decrease and were used as a negative control. G-401, BT-12, CHLA-266 and HepG2 cells exhibited similar response towards aprepitant (G-401 and BT-12, 50 μM; CHLA-266, 40 μM; HepG2 15 μM) (Figure 2a).

In order to investigate possible synergism of conventional treatment regimens and NK1R-targeted therapies, we combined aprepitant with cisplatin, a commonly used cytostatic chemotherapeutic agent for the treatment of rhabdoid tumors [1,37]. First, we investigated the viability of the tumor cells upon cisplatin exposure, using MTT assay as described (10 different increasing concentrations, ranging from 0.02 μM to 100 μM). We observed dose-dependent response towards cisplatin in all tumor cells with the exception of the G-401 cells (Figure 2b).

Next, G-401, BT-12, CHLA-266, and HepG2 cells were exposed to aprepitant, cisplatin, and a combination of both (Figure 2c). Lower cisplatin concentrations were used to evaluate possible synergism between the treatments. We observed significant additive effects in HepG2 and the AT/RT cell line CHLA-266. Similar trends were observed for BT-12 and G-401, but the effect was not statistically significant.

In summary, we were able to demonstrate a dose-dependent reduction in the viability of the rhabdoid tumor cell lines G-401, BT-12, and CHLA-266 after treatment with aprepitant and highlight possible additive effects of combinatory treatment approaches combining aprepitant with a conventional cytostatic drug.

3.4. Substance P Reverses Anti-Proliferative Effect of Aprepitant

In order to investigate the specificity of aprepitant, we tested whether treatment with the NK1R-ligand substance P could abrogate the observed treatment effects. Thus, G-401, BT-12, and CHLA-266 cells were exposed to a saturating concentration of substance P (200 nM, 48 h). As aprepitant acts as a competitive inhibitor of NK1R [38], high dose treatment with SP should prevent the binding of aprepitant to NK1R, diminishing the treatment effect as previously described for other tumors, including hepatoblastoma [19]. Our experiments revealed that substance P does not cause any toxicity for the cells, as no changes in cell viability were observed (Figure 2d). Importantly, aprepitant and substance P co-exposure significantly inhibited the anti-proliferative effect of aprepitant in BT-12 (Figure 2d). A similar trend was observed for G-401 and CHLA-266, however the effect was not statistically significant.

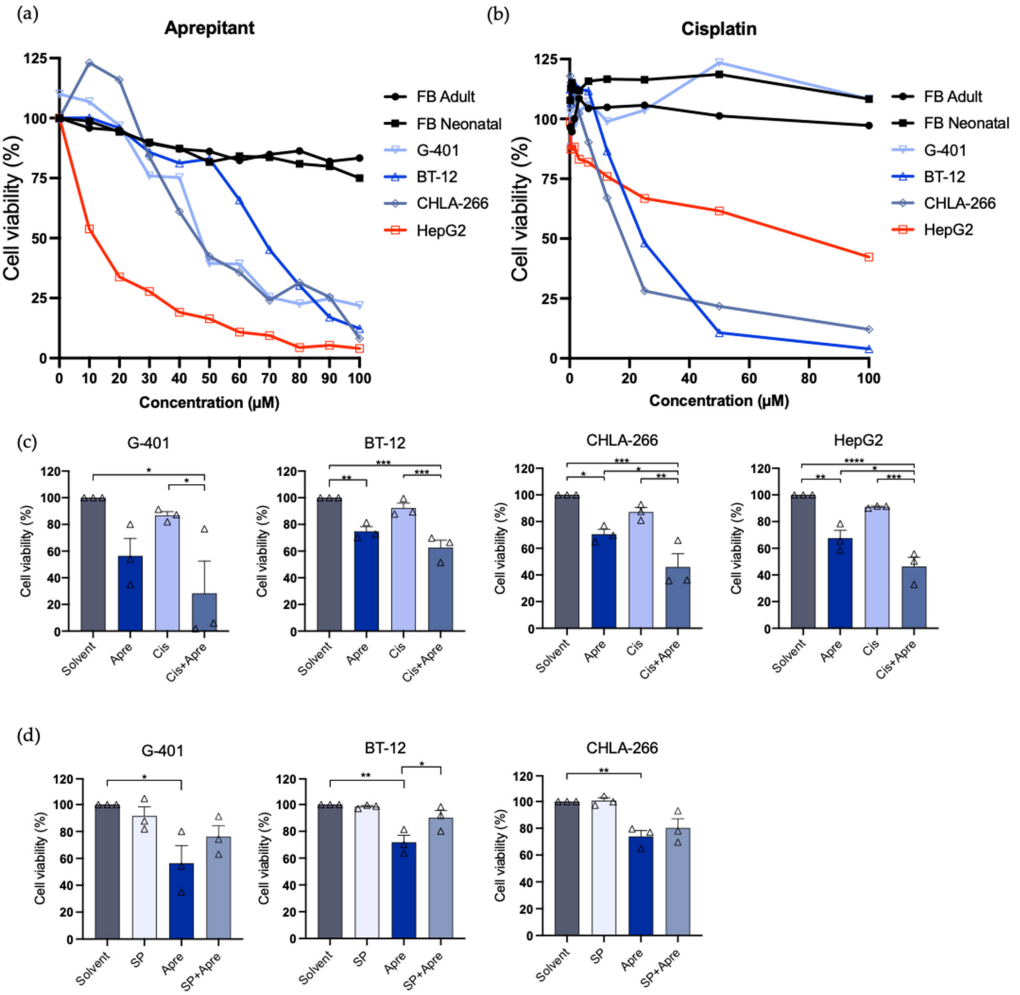

Figure 2. Cell proliferation analysis of G-401, BT-12, CHLA-266, HepG2, FB Neonatal, and FB Adult upon treatment with different compounds. (**a**) MTT assay measuring cell viability upon treatment with aprepitant (10–100 μM) for 48 h. (**b**) MTT assay measuring cell viability upon treatment with cisplatin (0.02–100 μM) for 48 h. (**c**) Combination MTT assay measuring cell viability upon treatment of aprepitant (aprepitant concentrations for G-401 and BT-12, 50 μM; CHLA-266, 40 μM; HepG2 15 μM), cisplatin (Cis, 20 μM) and aprepitant + cisplatin (Combi) for 48 h. (**d**) MTT assay measuring cell viability upon treatment of aprepitant (G-401 and BT-12, 50 μM; CHLA-266, 40 μM; HepG2 15 μM) and stimulation with Substance P (SP, 200 nM) and combination of Apre and SP. Pooled data of three independent experiments. Results are expressed as the mean ± standard error of the mean (SEM). All statistical comparisons were made with an ordinary one-way ANOVA or a Tukey's multiple comparison test, with a single pooled variance. $p < 0.05$ (*), $p < 0.01$ (**), $p < 0.001$ (***) and $p < 0.0001$ (****) for all comparisons.

In conclusion, treatment with a supramaximal dosage of substance P reversed the observed therapeutic effect of aprepitant, highlighting the specificity of NK1R-targeted therapies and emphasizing the role of the NK1R/SP complex as a pro-tumorigenic signaling pathway in rhabdoid malignancies.

3.5. Aprepitant Triggers Apoptosis Signaling in Rhabdoid Tumor Cell Lines

To investigate the mechanism of cell death induced by aprepitant in tumor cells, we focused on important effector cascades that are known to take part in cell death induction.

First, we carried out Annexin V staining by using flow cytometry. We observed reduction of viable cell populations upon exposure to aprepitant, comparable to previous experiments. Moreover, we observed increasing fractions of early and late apoptotic cells in rhabdoid tumor cells after 48 h exposure to aprepitant, suggesting apoptosis as the mechanism of aprepitant-induced-cell death. (Figures 3a,b, S1 and S2). Treatment with cisplatin was used as a positive control. Furthermore, a combination of both compounds showed similar effect of increasing apoptotic cell populations.

To confirm these results, we used immunoblotting to analyze the expression of the key pro-apoptotic effector protein poly (ADP-ribose) polymerase 1 (PARP-1). Whole cell lysates from rhabdoid tumor cells were isolated after treatment with aprepitant, cisplatin, or the combination of both. Interestingly, we observed strong expression of the cleaved products of PARP-1 in rhabdoid cells upon aprepitant exposure, in line with the results obtained from flow cytometric Annexin V staining (Figures 4a,b, S3 and S4).

Altogether, these findings show an upregulation of apoptotic signaling pathways in rhabdoid cells when treated with aprepitant, emphasizing the potential efficacy of an aprepitant treatment in RTs.

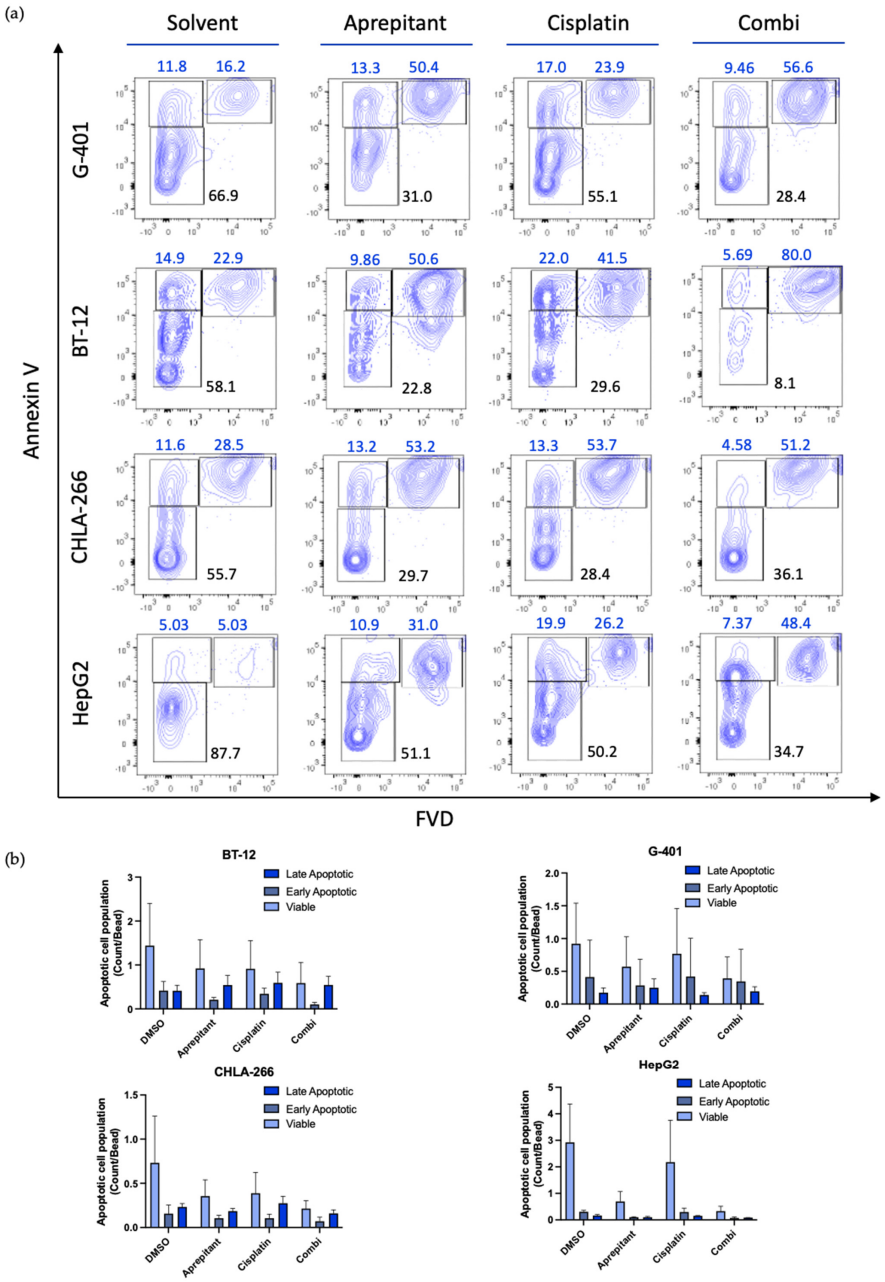

Figure 3. (**a**) Determination of apoptotic cell populations of G-401, BT-12, CHLA-266, and HepG2 was performed by staining with annexin V and fixable viability dye (FVD) and assessed through

fluorescence-activated cell sorting. Cells were treated with aprepitant (aprepitant concentrations for G-401 and BT-12, 50 µM; CHLA-266, 40 µM; HepG2, 15 µM), cisplatin (Cis, 20 µM) and aprepitant + cisplatin (Combi) for 48 h. DMSO was used as treatment control. Shown is one representative of three experiments. Numbers represent the percentages of the cell populations; black: viable; blue: apoptotic. (**b**) Quantification of viable and apoptotic cell populations. Shown are results from three independent experiments (n = 3).

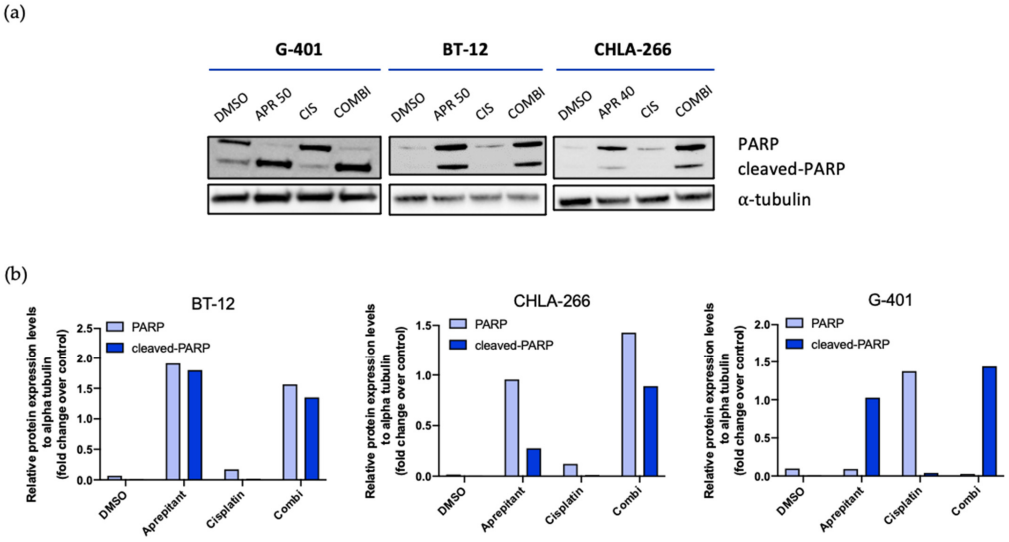

Figure 4. (**a**) Western blot analysis of G-401, BT-12 and CHLA-266 upon treatment with aprepitant (G-401 and BT-12, 50 µM; CHLA-266, 40 µM), cisplatin (CIS 20 µM) and aprepitant + cisplatin (COMBI) (48 h). DMSO used as a treatment control. Blots are representative of n = 2. (**b**) Densitometry analysis of Western blots. Relative protein expression levels were normalized to alpha tubulin expression.

4. Discussion

Rhabdoid tumors are rare but highly aggressive cancer types of early childhood [1]. Due to the lack of an effective conventional therapy regimen and the high toxicity of chemotherapy, patients suffering from rhabdoid tumors have poor overall survival rates (less than 50%) [11,12]. In order to improve treatment options and increase the chances of survival, novel targeted therapies must be investigated.

To the best of our knowledge, the expression and the role of the NK1R/SP complex in rhabdoid tumors has not been described so far. In this study, we present for the first time the expression of *TACR1* and *TAC1* in rhabdoid tumors. It has been shown that the *TACR1* expression pattern for hepatoblastoma does not correlate with clinical characteristics [39]. Similar to our recent study in hepatoblastoma, we here demonstrated for rhabdoid tumors that the expressions of *TACR1* and *TAC1* do not seem to correlate to parameters such as stage of disease, gender, and age of diagnosis. Hence, this conserved expression appears to be independent of any biological or clinical characteristics and highlights the broad applicability of NK1R-targeted therapies for treating pediatric rhabdoid tumors.

The NK1R antagonist aprepitant has been in clinical use against chemotherapy induced nausea and vomiting [40]. Furthermore, the antitumor effects of aprepitant have been described in several cancer types, including osteosarcoma, hepatoblastoma, and lung cancer [39,41,42]. It should be highlighted that the safety and the tolerability of aprepitant has been demonstrated in clinical trials, with high dose treatment leading to mild side

effects at most [24]. In this study, we investigated the cancer cell killing effects of aprepitant, and demonstrated that rhabdoid tumor growth is inhibited by blocking the NK1R, in vitro.

We were able to demonstrate the anti-tumor activity of aprepitant in three different rhabdoid tumor cell lines using at least two established procedures (e.g., MTT, FACS). To model the heterogeneity of rhabdoid tumors, which arise at different sites in the body, we used 2 AT/RT cell lines and 1 RTK cell line. All cell lines carry the characteristic loss-of-function INI1 mutation, thus closely reflecting the developing pediatric malignancies. Furthermore, in combination with a platin-derived cytostatic cisplatin, an additive effect was observed.

It has been shown in breast cancer and hepatoblastoma that the anti-tumor effect of aprepitant is induced by activation of apoptotic signaling pathways [19,43]. In order to unravel the mechanism of cell death in rhabdoid tumors, we investigated apoptosis by using both Annexin V staining and Western blot analysis. Similar to the previous studies, our data reveal increasing portions of late and early apoptotic cell populations upon aprepitant exposure. Using Western blot analysis, we could confirm the induction of apoptotic signal on protein level. More precisely, we observed cleaved products of PARP-1 in RT cells upon incubation with aprepitant. Altogether, these findings reveal that aprepitant exposure induces cell death by upregulating apoptotic signaling pathways.

New treatment regimens of RTs, such as intense multimodal therapy, have shown significant survival improvements [12]. However, due to considerable concerns over severe cytotoxicity and late adverse effects, further intensification of cytostatic compounds is not feasible. Therefore, novel therapeutic approaches are desperately needed. As such, just recently, Theruvath et al. presented an approach utilizing B7-H3-targeted chimeric antigen receptor (CAR) T cells for the treatment of AT/RTs [44], highlighting recent efforts to generate targeted therapies for the treatment of rhabdoid tumors. Our data beg the question of whether this novel target can potentially be included into more sophisticated future therapies, such as CAR T cell design. We have recently started to bring such efforts on the way, even though they are sophisticated, expensive and time consuming. Either way, we believe that it is worthwhile to further investigate the role of targeting the NK1R in the treatment of rhabdoid tumors.

Our approach presented here, on the other hand, is much more straightforward and merely involves the application of a small molecule already approved by the FDA, although for other indications. Also, it is important to note that in order to achieve antitumor effects to be triggered via NK1R-antagonists, much higher doses are expected to be needed compared to what is needed for the treatment of nausea and vomiting. It is generally understood that the doses of aprepitant for an anticancer effect must likely be 10-fold higher, which then would correspond to the μM doses used in the experiments presented here.

There exists some evidence that aprepitant will likely be tolerated in higher doses. For example, there have been several large prospective randomized clinical trials investigating the role of NK1R antagonists as antidepressants, with mixed results [45,46]. Importantly, the safety and tolerability of the NK-1 receptor antagonist aprepitant was demonstrated in a placebo-controlled trial in patients with moderate-to-severe major depression. At a dose of 300 mg/day (several times higher than for antiemesis), aprepitant was well tolerated, and no statistically significant difference in the frequency of adverse events was observed as compared to placebo [45].

Further, we are currently using aprepitant as an off-label drug for some (desperate) cases in children with hepatocellular carcinoma or hepatoblastoma, although to this point not for rhabdoid tumors. We use doses five times higher than what is normally given to children as an antiemetic, in general up to 10 mg/kg or higher. In our case, we did not see general side effects that we could attribute to the NK1R-antagonist alone, with one important exception. Children on whom we had performed a liver transplant (for hepatoblastoma) and who are on immunosuppression show a strong interaction with their tacrolimus levels, which in some cases immediately become sky high and can trigger kidney disfunction. This reaction is likely due to inhibition of the cytochrome p450 system.

Therefore, caution is warranted in children who are on tacrolimus and related medications when giving aprepitant in high doses.

There are several limitations to our study. The patient cohort (n = 43) of the analyzed database is rather small. Given that the age-standardized incidence for extracranial rhabdoid tumors and for AT/RTs in children is 0.6 per 1 million and 0.07 per 100,000, respectively, this small sample size reflects the rarity of the disease. Nevertheless, we confirmed our findings using primary patient material obtained from children treated at our hospital. Again, we could only obtain a few tissue samples, but we argue that the number is sufficient to allow for further investigation of our hypothesis [47,48]. Also, we did not correlate our findings in two liver tumor specimens with corresponding cell lines. The reason is that, different from the two other organ systems presented, no viable cell line exists for rhabdoid tumors of the liver. Furthermore, in our study, we do not investigate the in vivo efficacy of the treatment. However, the efficacy of aprepitant treatment in cancer cells has already been presented in experimental mouse models for other tumors [19,42].

5. Conclusions

For the first time, we present the expression of *TACR1* and *TAC1* in rhabdoid tumors, the potent inhibitory effect of the NK1R antagonist aprepitant in this tumor entity and the analysis of apoptotic pathways of rhabdoid tumor cells upon treatment with aprepitant. Our results strongly suggest further studies of the NK1R/SP complex and its antagonist in rhabdoid tumors to implement this novel therapeutic approach in its treatment.

Supplementary Materials: The following are available online at https://www.mdpi.com/article/10.3390/curroncol29010008/s1. Figure S1: Determination of apoptotic cell populations of G-401, BT-12, CHLA-266 and HepG2 (second representative); Figure S2: Determination of apoptotic cell populations of G-401, BT-12, CHLA-266 and HepG2 (third representative); Figure S3: Western blot analysis of G-401, BT-12 and CHLA-266 upon treatment with aprepitant and densitometry analysis of Western blots (first representative); Figure S4: Western blot analysis of G-401, BT-12 and CHLA-266 upon treatment with aprepitant and densitometry analysis of western blots (second representative).

Author Contributions: Conceptualization, M.B.; methodology, M.B., S.D., A.G., J.K. and R.K.; validation, J.K., S.D. and A.G.; formal analysis, J.K., S.D., A.G.; investigation, J.K., S.D., A.G., D.L.; resources, R.K., M.M.D., C.W., D.v.S., T.M., F.H., S.K.; data curation, J.K., S.D., A.G.; writing—original draft preparation, J.K. and S.D.; writing—review and editing, M.B., S.D., R.K., S.K., A.G., M.I. and I.B.; visualization, J.K., S.D., A.G. and D.L.; supervision, M.B.; project administration, M.B.; funding acquisition, M.B., R.K. and S.K. All authors have read and agreed to the published version of the manuscript.

Funding: This research was funded by the "Promotionsstudium Förderung für Forschung und Lehre" program from the University of Munich, LMU (to J.K. and M.B.). M.B. was also funded by the Friedrich-Baur Institute. Additionally, this study was supported by the Marie-Sklodowska-Curie Program Training Network for the Immunotherapy of Cancer funded by the H2020 Program of the European Union (Grant 641549, to S.K.), the Marie-Sklodowska-Curie Program Training Network for Optimizing Adoptive T Cell Therapy of Cancer funded by the H2020 Program of the European Union (Grant 955575, to S.K.), the Hector foundation, the International Doctoral Program i-Target: Immunotargeting of Cancer funded by the Elite Network of Bavaria (S.K.); Melanoma Research Alliance Grants 409510 (to S.K.); the Else Kröner-Fresenius-Stiftung (S.K.); the German Cancer Aid (S.K.); the Ernst-Jung-Stiftung (S.K.); LMU Munich's Institutional Strategy LMUexcellent within the framework of the German Excellence Initiative (to S.K.); the Bundesministerium für Bildung und Forschung Project Oncoattract (to S.K.); by the European Research Council Grant 756017, ARMOR-T (to S.K.), by the German Research Foundation (DFG to S.K.), the Fritz-Bender Foundation (to S.K.) and the José-Carreras Foundation (to S.K.). Fabian Hauck is funded by the Care-for-Rare Foundation (C4R, 160073), the Else Kröner-Fresenius Stiftung (EKFS, 2017_A110), and the German Federal Ministry of Education and Research (BMBF, 01GM1910C).

Institutional Review Board Statement: The study was conducted according to the guidelines of the Declaration of Helsinki and approved by the Institutional Review Board (or Ethics Committee) of Ludwig-Maximilians-University Munich, Germany (protocol code 19-115 and 21-0191).

Informed Consent Statement: Informed consent for surgical tissue sampling was obtained from all subjects involved in the study. The tissue samples used in this study represent leftover tissue from previous diagnostic workup. Given that tissue samples date back as far as 20 years from the original sampling and that tissue samples were available in an anonymous format, additional informed consent was waived.

Data Availability Statement: The data presented in this study are openly available in the cBio Cancer Genomics Portal (http://cbioportal.org, accessed on 2 December 2021) [28,29]. Five pediatric cancer studies on acute myeloid leukemia (AML; phs000465), acute lymphoblastic leukemia (ALL; phs000464), neuroblastoma (NB; phs000467), rhabdoid tumors (RT; phs0004709), and Wilms tumor (WT; phs000471) were selected from the Therapeutically Applicable Research to Generate Effective Treatments (https://ocg.cancer.gov/programs/target, accessed on 2 December 2021) initiative and mRNA expression of 2 genes was analyzed (*TACR1*, *TAC1*).

Acknowledgments: The authors would like to thank A. Hotes and T. Schmidt for excellent technical assistance. We thank the iFlow Core Facility of the university hospital Munich for assistance with the generation of flow cytometry data. We thank T. Magg and F. Hauck for providing the fibroblast cell lines.

Conflicts of Interest: S.K. has received honoraria from Novartis, TCR2 and GSK. S.K. is an inventor of several patents in the field of immuno-oncology. S.K. received research support from TCR2 Inc and Arcus Bioscience for work unrelated to this manuscript.

References

1. Geller, J.I.; Roth, J.J.; Biegel, J.A. Biology and Treatment of Rhabdoid Tumor. *Crit. Rev. Oncog.* **2015**, *20*, 199–216. [CrossRef] [PubMed]
2. Chi, S.N.; Zimmerman, M.A.; Yao, X.; Cohen, K.J.; Burger, P.; Biegel, J.A.; Rorke-Adams, L.B.; Fisher, M.J.; Janss, A.; Mazewski, C.; et al. Intensive multimodality treatment for children with newly diagnosed CNS atypical teratoid rhabdoid tumor. *J. Clin. Oncol.* **2009**, *27*, 385–389. [CrossRef] [PubMed]
3. Fazlollahi, L.; Hsiao, S.J.; Kochhar, M.; Mansukhani, M.M.; Yamashiro, D.J.; Remotti, H.E. Malignant Rhabdoid Tumor, an Aggressive Tumor Often Misclassified as Small Cell Variant of Hepatoblastoma. *Cancers* **2019**, *11*, 1992. [CrossRef] [PubMed]
4. Chao, M.F.; Su, Y.F.; Jaw, T.S.; Chiou, S.S.; Lin, C.H. Atypical teratoid/rhabdoid tumor of lumbar spine in a toddler child. *Spinal Cord Ser. Cases* **2017**, *3*, 16026. [CrossRef]
5. Bourdeaut, F.; Freneaux, P.; Thuille, B.; Bergeron, C.; Laurence, V.; Brugieres, L.; Verite, C.; Michon, J.; Delattre, O.; Orbach, D. Extra-renal non-cerebral rhabdoid tumours. *Pediatr. Blood Cancer* **2008**, *51*, 363–368. [CrossRef]
6. Biggs, P.J.; Garen, P.D.; Powers, J.M.; Garvin, A.J. Malignant rhabdoid tumor of the central nervous system. *Hum. Pathol.* **1987**, *18*, 332–337. [CrossRef]
7. Rorke, L.B.; Packer, R.J.; Biegel, J.A. Central nervous system atypical teratoid/rhabdoid tumors of infancy and childhood: Definition of an entity. *J. Neurosurg.* **1996**, *85*, 56–65. [CrossRef]
8. Kohashi, K.; Oda, Y. Oncogenic roles of SMARCB1/INI1 and its deficient tumors. *Cancer Sci.* **2017**, *108*, 547–552. [CrossRef]
9. Richardson, E.A.; Ho, B.; Huang, A. Atypical Teratoid Rhabdoid Tumour: From Tumours to Therapies. *J. Korean Neurosurg. Soc.* **2018**, *61*, 302–311. [CrossRef] [PubMed]
10. Fruhwald, M.C.; Biegel, J.A.; Bourdeaut, F.; Roberts, C.W.; Chi, S.N. Atypical teratoid/rhabdoid tumors-current concepts, advances in biology, and potential future therapies. *Neuro Oncol.* **2016**, *18*, 764–778. [CrossRef]
11. Brennan, B.; De Salvo, G.L.; Orbach, D.; De Paoli, A.; Kelsey, A.; Mudry, P.; Francotte, N.; Van Noesel, M.; Bisogno, G.; Casanova, M.; et al. Outcome of extracranial malignant rhabdoid tumours in children registered in the European Paediatric Soft Tissue Sarcoma Study Group Non-Rhabdomyosarcoma Soft Tissue Sarcoma 2005 Study-EpSSG NRSTS 2005. *Eur. J. Cancer* **2016**, *60*, 69–82. [CrossRef] [PubMed]
12. Reddy, A.T.; Strother, D.R.; Judkins, A.R.; Burger, P.C.; Pollack, I.F.; Krailo, M.D.; Buxton, A.B.; Williams-Hughes, C.; Fouladi, M.; Mahajan, A.; et al. Efficacy of High-Dose Chemotherapy and Three-Dimensional Conformal Radiation for Atypical Teratoid/Rhabdoid Tumor: A Report From the Children's Oncology Group Trial ACNS0333. *J. Clin. Oncol.* **2020**, *38*, 1175–1185. [CrossRef]
13. Tomlinson, G.E.; Breslow, N.E.; Dome, J.; Guthrie, K.A.; Norkool, P.; Li, S.; Thomas, P.R.; Perlman, E.; Beckwith, J.B.; D'Angio, G.J.; et al. Rhabdoid tumor of the kidney in the National Wilms' Tumor Study: Age at diagnosis as a prognostic factor. *J. Clin. Oncol.* **2005**, *23*, 7641–7645. [CrossRef] [PubMed]
14. Ahmed, H.U.; Arya, M.; Levitt, G.; Duffy, P.G.; Sebire, N.J.; Mushtaq, I. Part II: Treatment of primary malignant non-Wilms' renal tumours in children. *Lancet Oncol.* **2007**, *8*, 842–848. [CrossRef]
15. Munoz, M.; Covenas, R.; Esteban, F.; Redondo, M. The substance P/NK-1 receptor system: NK-1 receptor antagonists as anti-cancer drugs. *J. Biosci.* **2015**, *40*, 441–463. [CrossRef]
16. Muñoz, M.; Coveñas, R. Involvement of substance P and the NK-1 receptor in cancer progression. *Peptides* **2013**, *48*, 1–9. [CrossRef]

17. Munoz, M.; Covenas, R. Involvement of substance P and the NK-1 receptor in human pathology. *Amino Acids* **2014**, *46*, 1727–1750. [CrossRef]
18. Munoz, M.; Rosso, M.; Covenas, R. Neurokinin-1 Receptor Antagonists against Hepatoblastoma. *Cancers* **2019**, *11*, 1258. [CrossRef]
19. Berger, M.; Neth, O.; Ilmer, M.; Garnier, A.; Salinas-Martin, M.V.; de Agustin Asencio, J.C.; von Schweinitz, D.; Kappler, R.; Munoz, M. Hepatoblastoma cells express truncated neurokinin-1 receptor and can be growth inhibited by aprepitant in vitro and in vivo. *J. Hepatol.* **2014**, *60*, 985–994. [CrossRef]
20. Munoz, M.; Covenas, R. The Neurokinin-1 Receptor Antagonist Aprepitant: An Intelligent Bullet against Cancer? *Cancers* **2020**, *12*, 2682. [CrossRef] [PubMed]
21. Kage, R.; Leeman, S.E.; Boyd, N.D. Biochemical characterization of two different forms of the substance P receptor in rat submaxillary gland. *J. Neurochem.* **1993**, *60*, 347–351. [CrossRef] [PubMed]
22. Zhou, Y.; Zhao, L.; Xiong, T.; Chen, X.; Zhang, Y.; Yu, M.; Yang, J.; Yao, Z. Roles of full-length and truncated neurokinin-1 receptors on tumor progression and distant metastasis in human breast cancer. *Breast Cancer Res. Treat.* **2013**, *140*, 49–61. [CrossRef]
23. Gillespie, E.; Leeman, S.E.; Watts, L.A.; Coukos, J.A.; O'Brien, M.J.; Cerda, S.R.; Farraye, F.A.; Stucchi, A.F.; Becker, J.M. Truncated neurokinin-1 receptor is increased in colonic epithelial cells from patients with colitis-associated cancer. *Proc. Natl. Acad. Sci. USA* **2011**, *108*, 17420–17425. [CrossRef]
24. Munoz, M.; Covenas, R. Safety of neurokinin-1 receptor antagonists. *Expert Opin. Drug Saf.* **2013**, *12*, 673–685. [CrossRef] [PubMed]
25. Munoz, M.; Covenas, R. The Neurokinin-1 Receptor Antagonist Aprepitant, a New Drug for the Treatment of Hematological Malignancies: Focus on Acute Myeloid Leukemia. *J. Clin. Med.* **2020**, *9*, 1659. [CrossRef] [PubMed]
26. Molinos-Quintana, A.; Trujillo-Hacha, P.; Piruat, J.I.; Bejarano-Garcia, J.A.; Garcia-Guerrero, E.; Perez-Simon, J.A.; Munoz, M. Human acute myeloid leukemia cells express Neurokinin-1 receptor, which is involved in the antileukemic effect of Neurokinin-1 receptor antagonists. *Investig. New Drugs* **2019**, *37*, 17–26. [CrossRef] [PubMed]
27. Eichenmüller, M.; Gruner, I.; Hagl, B.; Häberle, B.; Müller-Höcker, J.; von Schweinitz, D.; Kappler, R. Blocking the hedgehog pathway inhibits hepatoblastoma growth. *Hepatology* **2009**, *49*, 482–490. [CrossRef]
28. Cerami, E.; Gao, J.; Dogrusoz, U.; Gross, B.E.; Sumer, S.O.; Aksoy, B.A.; Jacobsen, A.; Byrne, C.J.; Heuer, M.L.; Larsson, E.; et al. The cBio cancer genomics portal: An open platform for exploring multidimensional cancer genomics data. *Cancer Discov.* **2012**, *2*, 401–404. [CrossRef]
29. Gao, J.; Aksoy, B.A.; Dogrusoz, U.; Dresdner, G.; Gross, B.; Sumer, S.O.; Sun, Y.; Jacobsen, A.; Sinha, R.; Larsson, E.; et al. Integrative analysis of complex cancer genomics and clinical profiles using the cBioPortal. *Sci. Signal.* **2013**, *6*, pl1. [CrossRef]
30. The cBio Cancer Genomics Portal. Available online: http://cbioportal.org (accessed on 2 December 2021).
31. Pohl, A.; Kappler, R.; Muhling, J.; Von Schweinitz, D.; Berger, M. Expression of Truncated Neurokinin-1 Receptor in Childhood Neuroblastoma is Independent of Tumor Biology and Stage. *Anticancer Res.* **2017**, *37*, 6079–6085. [CrossRef]
32. Berger, M.; Von Schweinitz, D. Therapeutic Innovations for Targeting Childhood Neuroblastoma: Implications of the Neurokinin-1 Receptor System. *Anticancer Res.* **2017**, *37*, 5911–5918. [CrossRef] [PubMed]
33. Henssen, A.G.; Odersky, A.; Szymansky, A.; Seiler, M.; Althoff, K.; Beckers, A.; Speleman, F.; Schäfers, S.; De Preter, K.; Astrahanseff, K.; et al. Targeting tachykinin receptors in neuroblastoma. *Oncotarget* **2017**, *8*, 430–443. [CrossRef]
34. Brenca, M.; Rossi, S.; Lorenzetto, E.; Piccinin, E.; Piccinin, S.; Rossi, F.M.; Giuliano, A.; Dei Tos, A.P.; Maestro, R.; Modena, P. SMARCB1/INI1 genetic inactivation is responsible for tumorigenic properties of epithelioid sarcoma cell line VAESBJ. *Mol. Cancer Ther.* **2013**, *12*, 1060–1072. [CrossRef] [PubMed]
35. Xue, Y.; Zhu, X.; Meehan, B.; Venneti, S.; Martinez, D.; Morin, G.; Maiga, R.I.; Chen, H.; Papadakis, A.I.; Johnson, R.M.; et al. SMARCB1 loss induces druggable cyclin D1 deficiency via upregulation of MIR17HG in atypical teratoid rhabdoid tumors. *J. Pathol.* **2020**, *252*, 77–87. [CrossRef] [PubMed]
36. Edge, S.B.; Compton, C.C. The American Joint Committee on Cancer: The 7th edition of the AJCC cancer staging manual and the future of TNM. *Ann. Surg. Oncol.* **2010**, *17*, 1471–1474. [CrossRef]
37. Nesvick, C.L.; Nageswara Rao, A.A.; Raghunathan, A.; Biegel, J.A.; Daniels, D.J. Case-based review: Atypical teratoid/rhabdoid tumor. *Neurooncol. Pract.* **2019**, *6*, 163–178. [CrossRef] [PubMed]
38. Yin, J.; Chapman, K.; Clark, L.D.; Shao, Z.; Borek, D.; Xu, Q.; Wang, J.; Rosenbaum, D.M. Crystal structure of the human NK1 tachykinin receptor. *Proc. Natl. Acad. Sci. USA* **2018**, *115*, 13264–13269. [CrossRef]
39. Garnier, A.; Ilmer, M.; Becker, K.; Haberle, B.; Schweinitz, D.V.; Kappler, R.; Berger, M. Truncated neurokinin-1 receptor is an ubiquitous antitumor target in hepatoblastoma, and its expression is independent of tumor biology and stage. *Oncol. Lett.* **2016**, *11*, 870–878. [CrossRef]
40. Hesketh, P.J. Chemotherapy-Induced Nausea and Vomiting. *N. Engl. J. Med.* **2008**, *358*, 2482–2494. [CrossRef]
41. Munoz, M.; Crespo, J.C.; Crespo, J.P.; Covenas, R. Neurokinin-1 receptor antagonist aprepitant and radiotherapy, a successful combination therapy in a patient with lung cancer: A case report. *Mol. Clin. Oncol.* **2019**, *11*, 50–54. [CrossRef]
42. Munoz, M.; Berger, M.; Rosso, M.; Gonzalez-Ortega, A.; Carranza, A.; Covenas, R. Antitumor activity of neurokinin-1 receptor antagonists in MG-63 human osteosarcoma xenografts. *Int. J. Oncol.* **2014**, *44*, 137–146. [CrossRef]
43. Munoz, M.; Gonzalez-Ortega, A.; Salinas-Martin, M.V.; Carranza, A.; Garcia-Recio, S.; Almendro, V.; Covenas, R. The neurokinin-1 receptor antagonist aprepitant is a promising candidate for the treatment of breast cancer. *Int. J. Oncol.* **2014**, *45*, 1658–1672. [CrossRef] [PubMed]

44. Theruvath, J.; Sotillo, E.; Mount, C.W.; Graef, C.M.; Delaidelli, A.; Heitzeneder, S.; Labanieh, L.; Dhingra, S.; Leruste, A.; Majzner, R.G.; et al. Locoregionally administered B7-H3-targeted CAR T cells for treatment of atypical teratoid/rhabdoid tumors. *Nat. Med.* **2020**, *26*, 712–719. [CrossRef]
45. Kramer, M.S.; Cutler, N.; Feighner, J.; Shrivastava, R.; Carman, J.; Sramek, J.J.; Reines, S.A.; Liu, G.; Snavely, D.; Wyatt-Knowles, E.; et al. Distinct mechanism for antidepressant activity by blockade of central substance P receptors. *Science* **1998**, *281*, 1640–1645. [CrossRef]
46. Varty, G.B.; Cohen-Williams, M.E.; Hunter, J.C. The antidepressant-like effects of neurokinin NK1 receptor antagonists in a gerbil tail suspension test. *Behav. Pharmacol.* **2003**, *14*, 87–95. [CrossRef] [PubMed]
47. Ostrom, Q.T.; Chen, Y.; de Blank, P.M.; Ondracek, A.; Farah, P.; Gittleman, H.; Wolinsky, Y.; Kruchko, C.; Cohen, M.L.; Brat, D.J.; et al. The descriptive epidemiology of atypical teratoid/rhabdoid tumors in the United States, 2001–2010. *Neuro Oncol.* **2014**, *16*, 1392–1399. [CrossRef] [PubMed]
48. Brennan, B.; Stiller, C.; Bourdeaut, F. Extracranial rhabdoid tumours: What we have learned so far and future directions. *Lancet Oncol.* **2013**, *14*, e329–e336. [CrossRef]

6. Paper II

cancers

MDPI

Article

Identification of the Neurokinin-1 Receptor as Targetable Stratification Factor for Drug Repurposing in Pancreatic Cancer

Iris Beirith [1], Bernhard W. Renz [1,2], Shristee Mudusetti [1], Natalja Sergejewna Ring [1], Julian Kolorz [3], Dominik Koch [1], Alexandr V. Bazhin [1,2], Michael Berger [3,4], Jing Wang [1,5], Martin K. Angele [1], Jan G. D'Haese [1], Markus O. Guba [1], Hanno Niess [1], Joachim Andrassy [1], Jens Werner [1,2] and Matthias Ilmer [1,2,*]

[1] Department of General, Visceral and Transplantation Surgery, University Hospital, Ludwig-Maximilians-University Munich, 81377 Munich, Germany; iris.beirith@med.uni-muenchen.de (I.B.); bernhard.renz@med.uni-muenchen.de (B.W.R.); shristee.mudusetti@med.uni-muenchen.de (S.M.); natalja.ring@med.uni-muenchen.de (N.S.R.); dominik.koch@med.uni-muenchen.de (D.K.); alexandr.bazhin@med.uni-muenchen.de (A.V.B.); drjwang@ustc.edu.cn (J.W.); martin.angele@med.uni-muenchen.de (M.K.A.); jan.dhaese@med.uni-muenchen.de (J.G.D.); markus.guba@med.uni-muenchen.de (M.O.G.); Hanno.niess@med.uni-muenchen.de (H.N.); joachim.andrassy@med.uni-muenchen.de (J.A.); jens.werner@med.uni-muenchen.de (J.W.)
[2] German Center for Translations Cancer Research (DKTK), Partner Site Munich, 80336 Munich, Germany
[3] Department of Pediatric Surgery, Research Laboratories, von Hauner Children's Hospital, Ludwig-Maximilians-University Munich, 80337 Munich, Germany; julian.kolorz@med.uni-muenchen.de (J.K.); michael.berger@med.uni-muenchen.de (M.B.)
[4] Department of General, Abdominal and Transplant Surgery, Essen University Hospital, 45417 Essen, Germany
[5] Department of General Surgery, The First Affiliated Hospital of USTC, Division of Life Sciences and Medicine, University of Science and Technology of China, Hefei 230036, China
* Correspondence: matthias.ilmer@med.uni-muenchen.de; Tel.: +49-089-4400-711218

Simple Summary: Pancreatic ductal adenocarcinoma is the most common form of pancreatic cancer. It is known for low life expectancies after diagnosis and very limited treatment options. The identification of new therapeutic molecular targets is urgent as it might allow faster development of new treatment strategies. Targeting the neurokinin-1 receptor with small molecules has previously shown anti-tumoral effects in a large variety of cancers. Here, we found specific types of pancreatic cells to express the neurokinin-1 receptor while at the same time showing positive treatment response represented by cell growth reduction in number and size when treated with aprepitant. Our results suggest the neurokinin-1 receptor as a promising targetable structure and therefore interesting in the concept of personalized medicine.

Abstract: The SP/NK1R-complex plays an important role in tumor proliferation. Targeting of the neurokinin-1 receptor in previous studies with its antagonist aprepitant (AP) resulted in anti-tumoral effects in colorectal cancer and hepatoblastoma. However, there is still a lack of knowledge regarding its effects on pancreatic cancer. Therefore, we treated human pancreatic ductal adenocarcinoma (PDAC) cell lines (Capan-1, DanG, HuP-T3, Panc-1, and MIA PaCa-2) and their cancer stem cell-like cells (CSCs) with AP and analyzed functional effects by MTT-, colony, and sphere formation assays, respectively; moreover, we monitored downstream mechanisms by flow cytometry. NK1R inhibition resulted in dose-dependent growth reduction in both CSCs and non-CSCs without induction of apoptosis in most PDAC cell lines. More importantly, we identified striking AP dependent cell cycle arrest in all parental cells. Furthermore, gene expression and the importance of key genes in PDAC tumorigenesis were analyzed combining RT-qPCR in eight PDAC cell lines with publicly available datasets (TCGA, GEO, CCLE). Surprisingly, we found a better overall survival in patients with high NK1R levels, while at the same time, NK1R was significantly decreased in PDAC tissue compared to normal tissue. Interestingly, there is currently no differentiation between the isoforms of NK1R (truncated and full; NK1R-tr and -fl) in any of the indicated public transcriptomic records, although many publications already emphasize on important regulatory differences between the two isoforms of NK1R in many cancer entities. In conclusion, analysis of splice variants might potentially

check for updates

Citation: Beirith, I.; Renz, B.W.; Mudusetti, S.; Ring, N.S.; Kolorz, J.; Koch, D.; Bazhin, A.V.; Berger, M.; Wang, J.; Angele, M.K.; et al. Identification of the Neurokinin-1 Receptor as Targetable Stratification Factor for Drug Repurposing in Pancreatic Cancer. *Cancers* **2021**, *13*, 2703. https://doi.org/10.3390/cancers13112703

Academic Editors: Rafael Coveñas Rodríguez and Miguel Muñoz Sáez

Received: 17 April 2021
Accepted: 25 May 2021
Published: 30 May 2021

lead to a stratification of PDAC patients for NK1R-directed therapies. Furthermore, we presume PDAC patients with high expressions of NK1R-tr might benefit from treatment with AP to improve chemoresistance. Therefore, analysis of splice variants might potentially lead to a stratification of PDAC patients for NK1R-directed therapies.

Keywords: pancreatic ductal adenocarcinoma; PDAC; neurokinin-1 receptor; NK1R; TACR1; substance P; aprepitant; SP/NK1R-complex

1. Introduction

Pancreatic ductal adenocarcinoma (PDAC) is known for its frequent late diagnosis at advanced stages of cancer progression. With a 5-year survival rate of less than 10%, it is the most aggressive form of pancreatic cancer [1,2]. The incidences are expected to rise about 3% per year, causing scientists to expect PDAC to be the second leading cause of cancer-related death by 2030 [3,4].

The pancreas is characterized by highly complex interactions between the nervous system and disease [5]. With PDAC being innervated by both sympathetic, parasympathetic, and sensory nerves, its hallmarks comprise increased neural density as well as neural hypertrophy [6–8]. Currently, the recruitment of nerves is an emerging hallmark of cancer, and multiple pharmacological approaches are investigated to influence their signaling in the tumor microenvironment serving as a promising novel therapeutic strategy in the treatment of cancer [9].

The targeted inhibition of the substance P/neurokinin 1 receptor (SP/NK1R) system with its critical role in neuroinflammation has been considered as a promising drug target within the scope of personalized medicine [10,11]. SP, released by primary sensory nerve fibers, is a member of the tachykinin family [11,12]. These intensively studied and structurally related neuropeptides are known for being expressed throughout the nervous and immune system and are involved in a myriad of biological and physiological processes, including inflammation and proliferation [10,12,13]. Furthermore, they contribute to multiple pathological conditions, including acute and chronic inflammation, infection, and cancer, among others [12].

SP is encoded by *TAC1* and binds to three tachykinin receptors of which NK1R shows the highest binding affinity [10]. NK1R, also referred to as tachykinin receptor 1 (*TACR1*), is a G-protein coupled (GCPR), seven-transmembrane domain receptor [14]. The human receptor exists in two distinct isoforms, evoking diverse functionalities and differential expression across the body. As such, the full-length version consists of 407 aa (NK1R-fl) and is to be found at certain sites in the human brain [15]. SP mediated activation of NK1R-fl results in the assembly of a scaffolding complex incorporating β-arrestin, ERK1/2, and p38MAPK among others promoting proliferative and anti-apoptotic effects [16]. In contrast, the truncated isoform (311 aa; NK1R-tr) lacks at the C-terminus (exon 5), and is predominantly expressed in the central nervous system, as well as in peripheral tissues [15,17]. Receptor truncation leads to a decrease of SP binding affinity by at least 10-fold and inhibits β-arrestin-involved complex formation through failure of NK1R endocytosis [18].

The NK1R antagonist aprepitant (AP) has been approved by the FDA for the treatment of chemotherapy-induced nausea and vomiting in low dosage. Latest publications suggest higher dosages of AP to act as anti-tumoral agent through the inhibition of proliferation and induction of apoptosis in a variety of malignant cells [19,20]. We have previously shown that targeting of the SP/NK1R signaling cascade with AP successfully inhibits canonical Wnt signaling, while at the same time causing significant growth reduction in human colon cancer and hepatoblastoma cells [21,22]. However, the mechanisms of AP treatment in pancreatic tumorigenesis are poorly explored. Therefore, we aimed to investigate the effects

of treatment with AP and SP on cancer stem-like cells (CSCs) and multiple heterogenic pancreatic cancer cell lines regarding cell proliferation and intracellular mechanisms.

2. Materials and Methods

2.1. Cell Culture

We used the following pancreatic cancer cell lines: BxPC-3, Capan-1, DanG, HuP-T3, Panc-1, MIA PaCa-2, PSN-1, and AsPC-1. All cell lines were cultured in the appropriate media according to the ATCC recommendations (Gibco® RPMI 1640 for BxPC-3, Capan-1, DanG, PSN-1, and AsPC-1 or Gibco® Dulbecco's Modified Eagle's Medium (DMEM) for the remaining), supplemented with 10% fetal bovine serum (FBS; Corning, Wiesbaden, Germany), and 1% streptomycin/penicillin (PAN-Biotech, Aidenbach, Germany) at 37 °C in a humidified incubator with 5% CO_2. For all experiments, cell lines were used up to passage number 20. Cell culture medium for pancreatic stellate cells (PSCs) consisted of Gibco® DMEM/F-12, 1% amphotericin B (PAN-Biotech, Aidenbach, Germany), 10% FBS, and 1% streptomycin/penicillin. Detection of mycoplasma was conducted regularly using conventional PCR technique. All cells tested negative for mycoplasma contamination. All cells were authenticated commercially by IDEX BioResearch (Ludwigsburg, Germany).

2.2. Preparation of PSC Conditioned Media

PSC conditioned media (CM) were obtained by culturing primary PSCs for 24 h at approximately 70% confluency. CM were collected and filtered before through a 0.4 µM filter. PDAC cell lines were cultured in a 1:1 ratio of appropriate cell line media and CM for the indicated time.

2.3. Drugs

Aprepitant (Tocris Bioscience, Bristol, UK) (NK1R antagonist) was dissolved at 50 mM in DMSO. Substance P (Tocris Bioscience, Bristol, UK) (NK1R agonist) was dissolved at 1 mM in distilled water. Drugs were stored at −20 °C.

2.4. Viability Assay

Cell viability was assessed using a 3-(4,5-Dimethylthiazol-2-yl)-2,5-Diphenyltertazolium Bromide (MTT) (Invitrogen, Carlsbad, CA, USA) assay, and 15,000 cells were seeded into 96-well plates (NUNC, Langenselbold, Germany). After 24 h, cells were treated with increasing doses of AP (5–50 µM) for 24 h. To assess cell viability, 50 µL of MTT lysis solution with a final concentration of 0.5 mg/mL in 1X PBS (AppliChem, Darmstadt, Germany) was first added to each well followed by 30 min incubation at 37 °C. The MTT solution was discarded and 50 µL of DMSO (Sigma-Aldrich, Taufkirchen, Germany) was added to each well. For the readout, a multi-scanner micro-plate reader (VersaMax Microplate Reader, Molecular Diagnostics, CA, USA) was used to measure the absorbance at 570 nm with a background absorbance of 670 nm.

2.5. Sphere and Colony Formation Culture

Sphere culture and assays were performed as previously described [23]. Briefly, sphere formation medium was prepared with Advanced DMEM/F-12, 1% penicillin/streptomycin, and 1% methylcellulose (Sigma-Aldrich, Taufkirchen, Germany), further supplemented by 10 ng/mL human recombinant βFGF, 20 ng/mL human recombinant EGF, and 1× B27 serum-free supplement (supplies obtained from Invitrogen, Carlsbad, CA, USA). PDAC cells were trypsinized and washed twice with DPBS. An amount of 500 cells were seeded into 96-well ultra-low attachment plates (Corning, Wiesbaden, Germany) in 100 µL sphere formation medium. Before counting, spheres were cultivated for 10–14 days in media containing additives as mentioned in the text (20 µM AP, 100 ng/mL SP or DMSO). Medium was replenished twice per week.

For colony formation, 500 c/w cells were seeded onto 6-well plates. After incubation for 24 h, treatments with different concentrations of aprepitant and SP (1 µM, 10 µM, 20 µM,

40 µM plus combinations with 20 nM of SP) were started. Colonies were counted after 12 days by staining with crystal violet (CV) (0.1% CV in 20% Methanol) for 20 min, dried overnight and measured at 570/670 nm with Versa Max microplate reader (Molecular Diagnostics, CA, USA).

2.6. RNA Isolation and RT-qPCR

Isolation of RNA was performed using RNeasy Mini Kit (Qiagen, Hilden, Germany). This was followed by cDNA synthesis, realized through QuantiTect Reverse Transcription Kit (Qiagen, Hilden, Germany) using 1 µg of the respective isolated RNA. Thermal cycling during cDNA synthesis was realized by Eppendorf Mastercycler gradient.

PCR reaction was set up employing QuantiNova SYBR Green PCR Kit (Qiagen, Hilden, Germany). qPCR thermal cycling was done through StepOne Real-Time PCR System (Applied Biosystems, Carlsbad, CA, USA) and consisted of 40 cycles with denaturation at 95 °C for 5 s, annealing at 60 °C for 10 s, and elongation at 60 °C for 60 s. All experimental conditions were assessed in triplicates. The primers were used as follows: *TACR1-tr* forward, 5′-CAGGGGCCACAAGACCATCTA-3′; *TACR1-tr* reverse, 5′-ATAAGTTAGCTGCAGTCCCCAC-3′; *TACR1-fl* forward, 5′-AACCCCATCATCTACT GCTGC-3′; *TACR1-fl* reverse, 5′-ATTTCCAGCCCCTCATAGTCG-3′; TAC1 forward, 5′-TCGTGGCCTTGGCAGTCTTT-3′; *TAC1* reverse, 5′-CTGGTCGCTGTCGTACCAGT-3, *GAPDH* forward, 5′-GTCTCCTCTGACTTCAACAGC-3′; *GAPDH* reverse, 5′-ACCACCCT GTTGCTGTAGCCAA-3′. *ZEB1* forward, 5′-TTCACAGTGGAGAGAAGCCA-3′; *ZEB1* reverse, 5′-GCCTGGTGATGCTGAAAGAG-3′; *CDH1* forward, 5′-GAACGCATTGCCACAT ACAC-3′; *CDH1* reverse, 5′-ATTCGGGCTTGTTGTCATTC-3′. All kits were used according to the manufacturer's instructions. Primer functionality was confirmed in the hepatoblastoma cell line Hep G2 for *TACR1-tr*, *TACR1-fl*, and *TAC1*. Hep G2 cDNA was obtained from Kolorz et al., 2021 [24].

2.7. Apoptosis Detection Assay

Cells were seeded at 500,000 cells per well in a 6-well plate and incubated for 24 h at 37 °C, 5% CO_2. The treatments, aprepitant (Tocris Bioscience, Bristol, UK) and substance P (Tocris Bioscience, Bristol, UK), were applied to the wells at their respective concentrations and incubated for 24 h at 37 °C, 5% CO_2. Post treatment, the cells were observed for morphological changes under the microscope. The supernatants from each well were individually collected into 5 mL round bottom polystyrene test tubes (Falcon, Corning, Wiesbaden, Germany). The cells were carefully washed with 1 mL of DPBS (PAN-Biotech, Aidenbach, Germany) per well. The cells were then detached using 300 µL of accutase (Sigma-Aldrich, Taufkirchen, Germany) and incubated for 3 min at 37 °C, 5% CO_2. Accutase was inactivated by adding 1.5 mL of medium with 10% FBS (Falcon, Corning, Wiesbaden, Germany). The cells were carefully collected into their respective FACS tubes and centrifuged (Hettich, Rotina 380R) at 500 rpm for 5 min. The pellet was resuspended in 1 mL of DPBS and the centrifugation step was repeated. The cell pellet was stained for 15 min at 37 °C, 5% CO_2 with 100 µL of working solution (96 µL DPBS + 3 µL Annexin V + 1 µL propidium iodide (FITC Annexin V Apoptosis Detection Kit I, BD Biosciences, Heidelberg, Germany)). The staining was stopped by washing cells with 900 µL 1× ABB. The cells were measured using flow cytometry (LSRFortessa, BD Biosciences, Heidelberg, Germany). Further analysis was performed using FlowJo software (BD Biosciences, version 10).

2.8. Caspase Detection Assay

Cells were seeded at 500,000 cells per well in a 6-well plate and incubated for 24 h at 37 °C, 5% CO_2. The treatments, aprepitant (Tocris Bioscience, Bristol, UK) and substance P (Tocris Bioscience, Bristol, UK), were applied as indicated. Post treatment, the cells were observed for morphological changes under the microscope. The supernatants from each well were individually collected into 5 mL round-bottom polystyrene test tubes

(Falcon, Corning, Wiesbaden, Germany). The cells were carefully washed with 1 mL of DPBS (PAN-Biotech, Aidenbach, Germany) per well. The cells were then detached using 500 µL of trypsin (PAN-Biotech, Aidenbach, Germany) and incubated for 3 min at 37 °C, 5% CO_2. The trypsinization was stopped by adding 1.5 mL of medium with 10% FBS. The cells were carefully collected into 5 mL round-bottom polystyrene test tubes (Falcon, Corning, Wiesbaden, Germany) and centrifuged at 500 rpm for 5 min. The cell pellet was re-suspended in 1 mL of DPBS and the centrifugation step was repeated. The cell pellet was stained for 30 min at 37 °C, 5% CO_2 with 100 µL of working solution (99 µL DPBS + 5% FBS + 1 µL FITC–VAD-FMK (Apostat intracellular caspase detection, R&D Systems, Minneapolis, MN, USA). The staining was stopped by washing cells with 1 mL DPBS and centrifugation. The cell pellet was re-suspended in 1 mL DPBS and analyzed using flow cytometry. Further analysis was performed using Flowjo software (version 10) by BD.

2.9. Cell Cycle Detection

Cells were seeded at 500,000 cells per well in a 6-well plate and incubated for 24 h at 37 °C, 5% CO_2. The treatments, aprepitant and substance P, were applied to the wells at their respective concentrations and incubated for 24 h. The supernatants from each well were individually collected into 5 mL round-bottom polystyrene test tubes. The cells were carefully washed with 1 mL of DPBS per well. The cells were then detached using 500 µL of trypsin and incubated for 3 min at 37 °C, 5% CO_2. The trypsin was inactivated by adding 1.5 mL of medium with 10% FBS. The cells were carefully collected into their respective FACS tubes and centrifuged at 500 rpm for 5 min. The pellet was resuspended in 1 mL of DPBS and the centrifugation step was repeated. The cells were fixed by dropwise addition of 70% ice cold ethanol. The cells were incubated overnight at 4 °C to aid fixation. The cells were then centrifuged to remove the traces of ethanol and washed repeatedly with 1 ml DPBS. The cell pellets were stained with 1 mL 4′,6-Diamidin-2-phenylindol, Dihydrochlorid (DAPI) working solution (1 µg/mL DAPI (Invitrogen, Carlsbad, CA, USA) + 1% Triton X (Merck, Darmstadt, Germany) in DPBS) for 15 min in the dark. The cells were analyzed using flow cytometry. Further analysis was performed using FlowJo software (version 10) by BD Biosciences (San Jose, CA, USA).

2.10. ELISA

Conditioned media from the cell lines, MIA Paca-2, Panc-1, DanG, and HuP-T3, were collected after 24 h of culture to evaluate them for residual substance P concentration. The study was also extended to include sera from cancer patients and from control groups. This was approved by the ethics committee of the Ludwig-Maximilian-University (LMU) Munich, Germany (approval number 19–233). The supernatants were centrifuged at 4 °C, 16,000× g for 10 min. An amount of 100 µL of the test samples were applied to a pre-coated plate and the further steps were performed as recommended by the manufacturer (Substance P ELISA Kit, My BioSource, San Diego, CA, USA). The absorbance was detected at 450 nm using a spectrophotometer (VersaMax, Molecular Diagnostics, CA, USA). The minimum detectable concentration of SP was 0.175 ng/mL.

2.11. Statistical Analysis

Results are expressed as the mean ± standard error of the mean (SEM). All statistical comparisons were performed via one way ANOVA or unpaired parametric t-test comparing two groups using the biostatistics software GraphPad Prism (version 9.0.0, 86, San Diego, CA, USA). p-values shown as *, $p \leq 0.05$; **, $p \leq 0.01$; *** $p \leq 0.001$; ****, $p \leq 0.0001$.

3. Results

3.1. Transcriptome Data Analysis Reveals Diverging Expression of TACR1 and TAC1 in PDAC and Normal Pancreatic Tissue

To obtain an overview regarding the importance of the SP/NK1R-complex in PDAC, we first conducted expression analysis of complex-related genes via RT-qPCR. The assay

was performed on eight PDAC cell lines as indicated in Figure 1a, targeting both NK1R isoforms (*TACR1-tr* and *-fl*) separately, as well as *TAC1*. Additionally, we used the same for expression analysis on primary stellate cells. While no expression of *TACR1-fl* was detected consistently throughout all RT-qPCR experiments, we observed fluctuations in *TACR1-tr* expression between the pancreatic cancer cells. No expression could be detected in Capan-1 and HuP-T3, however, we observed *TACR1-tr* in the remaining six PDAC cell lines and, with low levels, in PSCs. In comparison to the positive control (hepatoblastoma cell line Hep G2) [20], we found significantly lower *TACR1-tr* levels in all tested PDAC cells (p-value < 0.0001). Although differences in *TAC1* expression were not within a significant range, it is noteworthy that Panc-1, MIA PaCa-2, Hep G2, and PSCs were positive for the presence of the SP encoding gene, whereas all other PDAC cell lines were categorized as non-detects (Figure 1a).

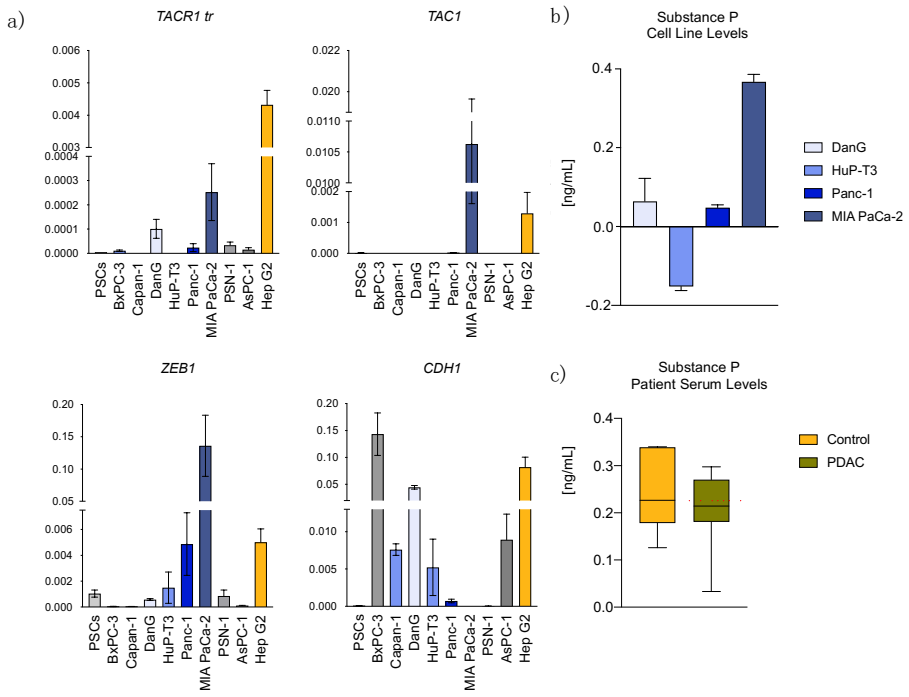

Figure 1. Expression of the SP/NK1R complex varies in established cell lines and PDAC patient serum. (**a**) Transcript abundance analyzed through RT-qPCR illustrated in ΔCt with standard deviation (SD) in the indicated cell lines. (**b**) ELISA for quantitative analysis of Substance P levels in PDAC cell lines and (**c**) serum of control (n = 7) vs. PDAC patients (n = 7).

In contrast to the RT-qPCR results, quantification of SP employing Enzyme-Linked Immunosorbent Assay (ELISA) in cell lines did show SP presence in all tested cell lines, with highest levels also in MIA PaCa-2 (Figure 1b). We performed the same assay on human serum for comparison of SP levels between control and PDAC patients. Here, we found a lower SP blood serum level in PDAC patients in comparison to a control group, although not with a significant level (Figure 1c).

Next, we collected publicly available bioinformatical data sets for further validation of SP/NK1R complex related gene expressions. The comparison of the PDAC data sets obtained from Gene Expression Omnibus (GEO), the Cancer Genome Atlas (TCGA), and Cancer Cell Line Encyclopedia (CCLE) allowed identification of a significant downregula-

tion of *TACR1* in tumor vs. normal cells (Figure 2a). However, these public records did not allow for the differentiation between the two receptor splice variants.

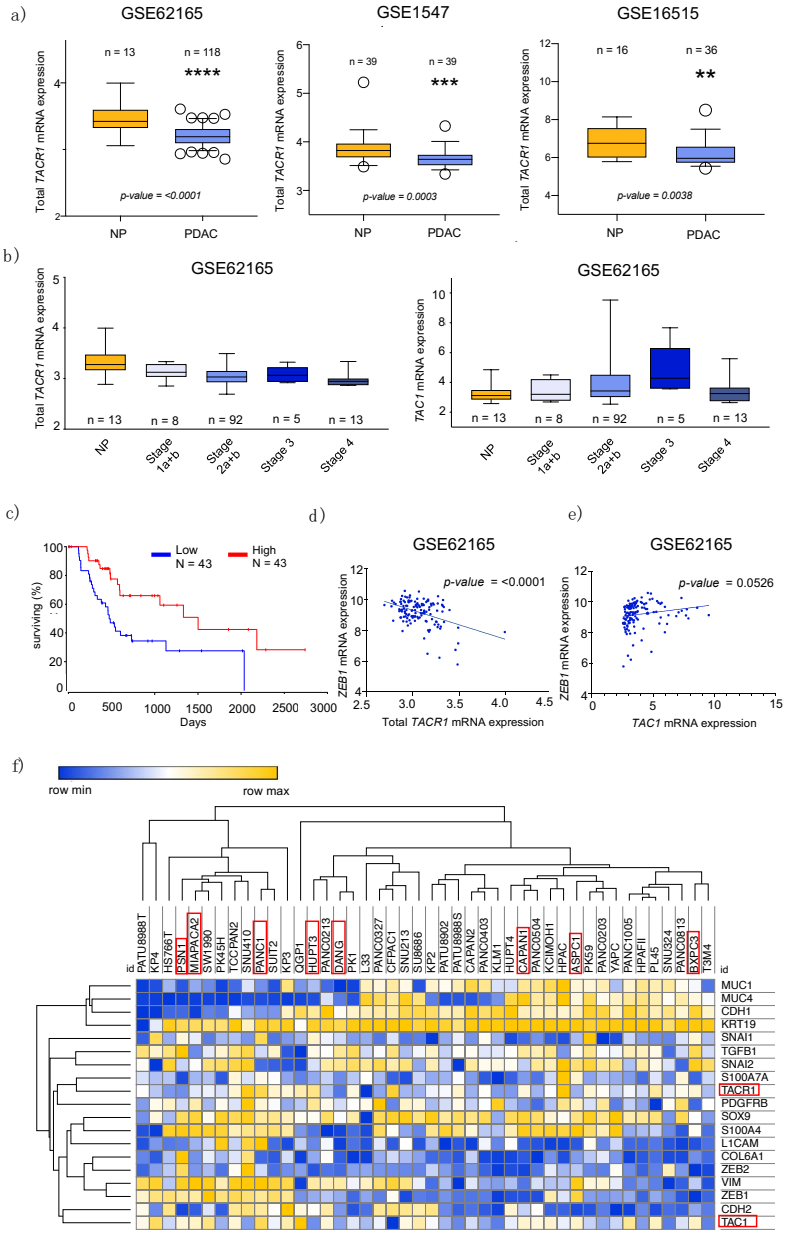

Figure 2. Transcriptome-based data analysis. (**a**) Boxplots demonstrating significantly lower mRNA expression levels of *TACR1* in PDAC compared to normal tissue (NP) in the indicated transcriptomic data series. *p*-values were calculated using

unpaired *t*-test. (**b**) *TACR1-total* and *TAC1* gene expression in different pancreatic cancer stages obtained from the indicated GEO data set. (**c**) Prognostic significance of *TACR1-tr* (top and bottom 25% gene expression) in PDAC, assessed by OncoLnc. (**d**) Inverse correlation between the EMT marker *ZEB1* and *TACR1* in the indicated transcriptomic data set. The *p*-value is based on Pearson's Correlation. (**e**) Correlation between *ZEB1* and *TAC1* in the indicated transcriptomic data set. (**f**) Visualization of CCLE gene expression across PDAC cell lines. The SP/NK1R coding genes are highlighted in red, as well as the cell lines used for further analysis. Hierarchical clustering based on one minus Pearson's Correlation.

Interestingly, GEO data indicates differential gene expression with tumor progression. Precisely, GSE micro array data shows tendencies towards a decreasing expression of total *TACR1* with tumor stage progression, while *TAC1* tends to increase with higher stages (Figure 2b). In addition, in survival analysis, higher expressions of *TACR1* correlated significantly with higher overall survival for PDAC patients (Figure 2c, via OncoLnc.org).

3.2. Epithelial to Mesenchymal Transition State Correlates with Expression of TACR1 and TAC1

Epithelial-mesenchymal plasticity (EMP) describes the disruption of tissue homeostasis, which further contributes to cellular transformation and heterogeneity, particularly in PDAC [25]. Recent biological experimental data, as well as transcriptomic bioinformatical analysis, support the strong association between high expression of mesenchymal markers, such as the zinc finger E-box binding homeobox 1 (*ZEB1*), and worse prognosis in patients [26]. Interestingly, inverse correlation of gene expression of *TACR1-total* and *ZEB1* demonstrates a significant relationship between high expression of *ZEB1* and low expression of *TACR1-total* (Figure 2d). However, we found a positive correlation between *ZEB1* and *TAC1* expression (Figure 2e). Gene clustering revealed *TACR1* and *TAC1* to form two distinct clusters, each with a group of different EMT markers. Hereby, *TACR1* clustered with genes associated with epithelial characteristics (e.g., *S100A7A*, *SNAI2*, *KRT19*, *CDH1*), while *TAC1* clustered closely to mesenchymal markers (e.g., *ZEB1*, *CDH2*, *VIM*, *ZEB2*) corroborating before mentioned data. Representing the heterogenic nature of PDAC for our further investigations, we used PDAC cell lines (Capan-1, DanG, HuP-T3, Panc-1, and MIA PaCa-2) that differ in their classification regarding epithelial-to-mesenchymal-transition (EMT) state as well as based on their *TACR1* and *TAC1* gene expression according to the CCLE data base (Figures 1a and 2f, and Table 1). To provide an overview on those cell line characteristics relevant to this study, Table 1 shows the EMT state of eight cell lines as well as a simplified classification model of gene expression based on CCLE data (see also Figure 2f).

Table 1. PDAC cell line characteristics and CCLE gene expressions.

PDAC Cell Line	EMT State	*TAC1*	*TACR1*
BxPC-3	epithelial	+	+
Capan-1	epithelial	+	+
DanG	epithelial	− −	− −
HuP-T3	epithelial/mesenchymal	− −	+ +
Panc-1	epithelial/mesenchymal	+ +	+ +
MIA PaCa-2	mesenchymal	+	−
PSN-1	mesenchymal	+	−
AsPC-1	mesenchymal	+	+

− − = very low expression; − = low expression; + = high expression; + + = very high expression.

To validate EMT state and expression levels of EMT markers, we employed primers for *ZEB1* and epithelial cadherin-1 *(CDH1*), additionally to the aforementioned primer sets in all RT-qPCR runs. We found the expression of EMT markers in our data to match the indicated classifications in previous literature [27]. In more detail, *CDH1* expression in DanG was significantly higher in comparison to the other PDAC cell lines with no expression in MIA PaCa-2 and PSN-1. *ZEB1* was detected in BxPC-3, AsPC-1, PSN-1, DanG, HuP-T3, Panc-1, Hep G2 (sorted in ascending order), and, with the significantly highest expression, in MIA PaCa-2 (Figure 1a).

3.3. Aprepitant Significantly Reduces Growth in PDAC Cell Lines and Cancer Stem Cell-Like Cells

To investigate the effects of NK1R-targeted therapy on the growth of PDAC cells, we tested treatment with the NK1R antagonist AP followed by the determination of 50% inhibitory concentration by MTT cell viability assay. The IC50 value for Hep G2, obtained by Kolorz et al., 2021 [24], functioned as positive control [20]. Exposure to AP resulted in dose-dependent growth inhibition of PDAC cells over a time period of 24 h. The lowest sensitivity to AP was detected in PSCs (32 μM), followed by Panc-1 (30 μM), Capan-1 (30 μM), HuP-T3 (29 μM), DanG (26 μM), and MIA PaCa-2 (19 μM) (Figure 3a). Similar IC50 values have been previously detected [28].

PSC-conditioned media is known to fuel pancreatic cancer cell metabolism and stimulate tumor cell proliferation and colony formation [29]. To exclude potential discrepancies through potential SP secretions of the immediate PDAC microenvironment represented by PSCs, we determined IC50 values (MTT) for both normal and PSC conditioned media for all cell lines. Interestingly, we observed higher susceptibility to AP treatment in cells cultured in PSC-conditioned media (Figure 3b). A significant difference between the two growth conditions was not ascertainable (unpaired *t*-test).

An in vitro surrogate functional marker and technique to identify cell lines enriched of cells with stem-like characteristics is the establishment of colonies and spheroids [23,30,31]. Treatment of colonies and spheres resulted in exceptional dose-dependent treatment response to AP after 14 days of culture. In the presence of SP, effects were partially smoothened, especially in co-treatments with higher concentrations of AP, particularly in MIA PaCa-2. In addition, MIA PaCa-2 robustly showed the highest sensitivity to AP treatment. Remarkably, we found a profound and significant inability of colony and spheroid formation at a concentration of 40 μM consistently in all cell lines ($p < 0.0001$). Addition of SP seemed to profit Panc-1 as the only cell line under CFA growth conditions ($p = 0.0005$), whereas effects of AP seemed to be alleviated by additions of SP in SFAs with MIA PaCa-2. There was no significant difference between control and SP-only treatment in SFA (Figure 3c).

In addition to changes in the number of colonies and spheroids, we also observed morphological differences after the treatments. Figure 3d illustrates spheroids obtained from DanG, MIA PaCa-2, and Panc-1. Distinct phenotypic features, including size, shape, and texture were monitored. Specifically, manipulation of the SP/NK1R system led to a loss of tightly packed shape in all cases, with blebbing at the surface of the spheres indicative of apoptosis initiation after antagonistic treatment (Figure 3d, right panels).

In summary, we observed a dose-dependent decrease in PDAC cell viability reflected by reductions in the size of spheres and numbers of cells as well as changes in cell morphology after exposure to the NK1R antagonist AP.

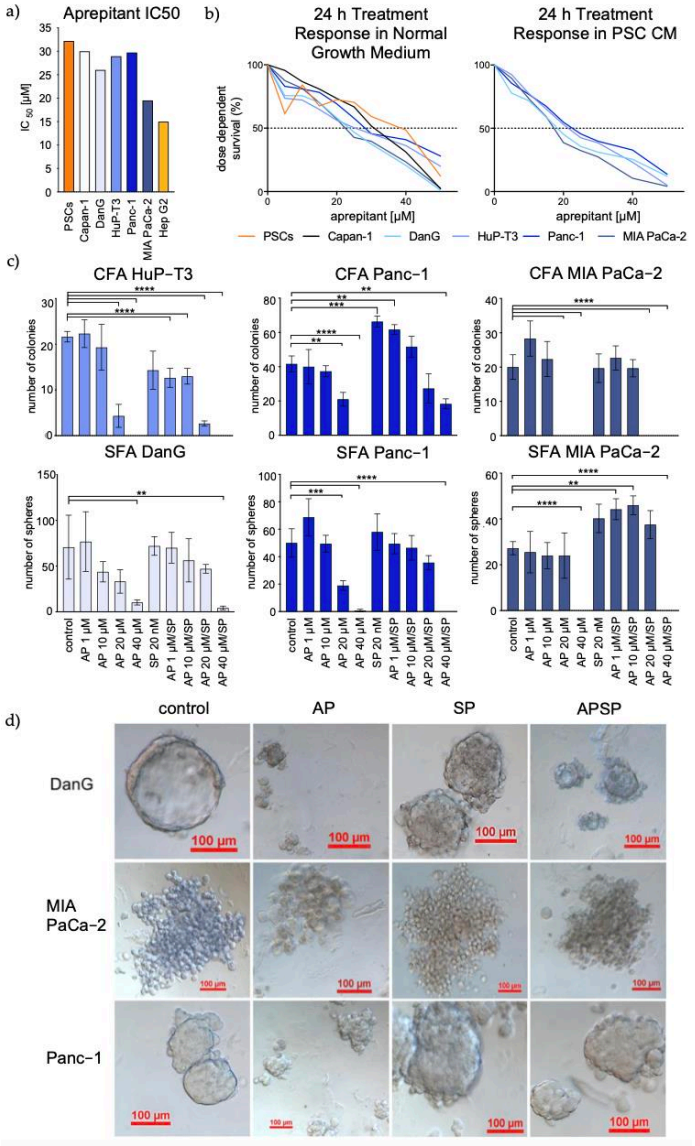

Figure 3. Aprepitant treatment response in PDAC cells, spheres, and colonies. (**a**) IC50 for all tested PDAC cell types as indicated. (**b**) AP dose-dependent survival curves for the indicated PDAC cells in normal (left) or PSC-conditioned media (right). (**c**) Bar charts illustrating number of colonies (upper panel) or spheroids (lower panel) under different treatment conditions as specified on the x-axis. (**d**) Images of SFA under treatment conditions showing morphological changes in the cell lines DanG (upper panel), MIA PaCa-2 (middle panel), and Panc-1 (lower panel).

3.4. Aprepitant Affects Cell Cycle Progression in PDAC Cells

We performed FITC Annexin V/PI staining to measure treatment-induced apoptosis rates (Figure 4a) as well as pan caspase labeling for determination of caspase activity via flow cytometry (Figure 4b). For apoptosis detection, our experiments revealed no differences between the treatment regimens in all cell lines. Moreover, caspase detection solely indicated a slight left shift in MIA PaCa-2, suggesting low pan caspase contribution with respect to apoptosis (Figure 4b). On the basis of these results, we performed DAPI staining for flow cytometry analysis to explore cell cycle progression in treated vs. untreated PDAC cell lines. The collected data showed drastic AP-induced changes of events in the phases G1 and S in the three cell lines DanG, Panc-1, and MIA PaCa-2 comparing AP-treated cells to controls. However, Capan-1 and HuP-T3, which had no expression of *TACR1-tr* and *-fl*, showed no reaction regarding AP-induced cell cycle arrest. We observed no effect of SP in terms of cell cycle modulation in all cells. For more detailed information, we added the histograms illustrating changes in cell cycle progression after AP treatment into the appendix. Taken together, blockage of NK1R in *TACR1-tr* expressing PDAC cells lead to prominent cell cycle arrest with an emphasis on G1 and S phase (Figure 5).

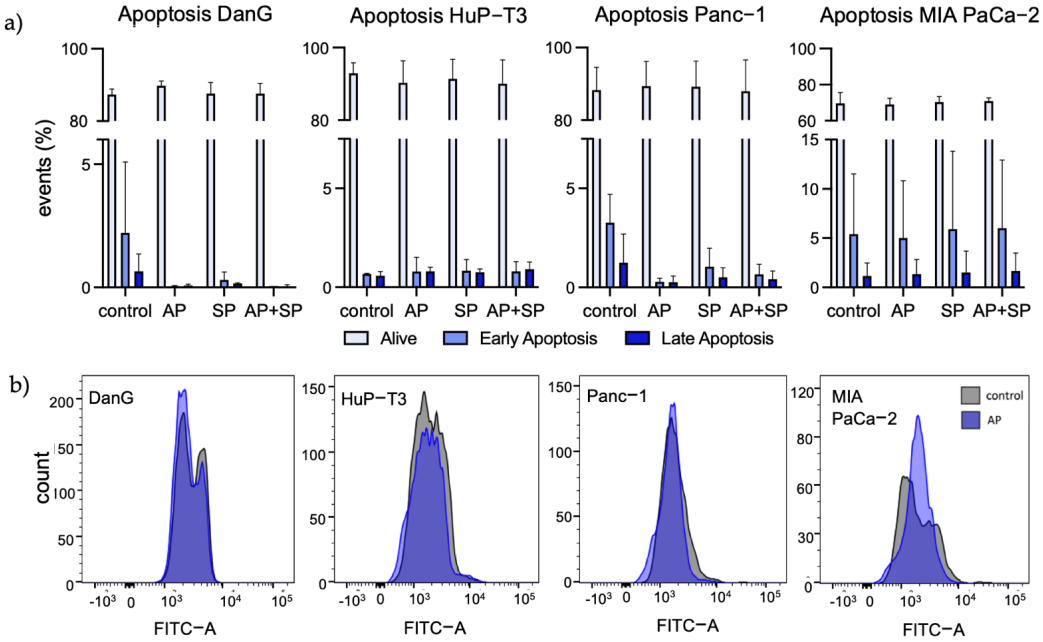

Figure 4. Apoptosis detection and caspase detection analysis. (**a**) FITC Annexin V/PI flow cytometry for detection of AP-mediated apoptosis in untreated and SP-treated cells. Drugs were applied in the following concentrations: AP 25 µM and SP 20 nM. Statistical analysis revealed no significant differences between treatments regarding Annexin V-positive cells. (**b**) FITC-VAD-FMK accumulation in the indicated cell lines measured via flow cytometry. Slight left shift after AP-treatment indicates small, but not significant changes in intracellular caspase activation. Bar charts and univariate histogram sorted left to right from epithelial to mesenchymal transition state.

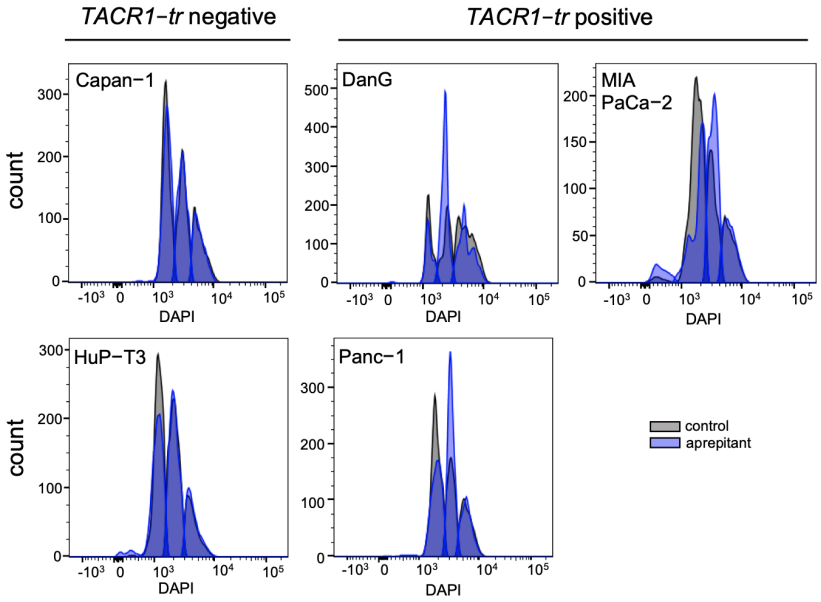

Figure 5. Evaluation of cell cycle progression in PDAC cells. Flow cytometry univariate histogram of DAPI staining in control vs. AP-treated cells showing number of events for cell cycle phases. Left panels: *NK1R-tr* negative cell lines demonstrate no difference in treatment. Right panels: a clear shift in cell cycle progression could be observed in *NK1R-tr* positive cell lines. The histogram of cell cycle distribution was generated from 10,000 events per sample. Appendix A provide more detailed information regarding the AP-induced shifts in cell cycle progression. Drugs were applied in the concentrations 25 μM of AP and 20 nM of SP.

4. Discussion

The SP/NK1R complex, especially the involvement of NK1R-tr, is known to play a pivotal role in different solid cancer entities, such as the childhood cancers hepatoblastoma (HB) and neuroblastoma as well as colon and breast cancer. Our latest publications firstly demonstrated the robust efficacy of the NK1R antagonist AP concerning the inhibition of pediatric liver cancer in vitro and in vivo [20]. Secondly, we demonstrated AP-induced modulation of AKT and Wnt pathways for the same cancer type [22]. Similarly, we reported the Wnt/β-catenin signaling activity to be significantly inhibited in colorectal cancer cells, thus decreasing cancer stemness [21]. To expand on these findings, in this study, we investigated the role of the SP/NK1R complex in the tumorigenesis of PDAC with a focus on the potential anti-tumoral effects of the NK1R antagonist AP.

A number of studies has already investigated splice variant subordinate differences between normal and malignant tissues, proving the homogenic and tissue specific presence of either one of the two isoforms [14,20,32]. Whereas the full transcript was commonly identified in areas of the central and peripheral nervous system, the truncated form is expressed in several tissues and cells [33]. We hypothesized PDAC cells to predominantly express NK1R-tr over the full-length version, which was confirmed through RT-qPCR analysis, while also providing proof for the absence of NK1R-fl in all tested PDAC cells.

In contrast to our results suggesting no expression of *TACR1* in some cell lines, such as Capan-1, other publications have reported contradictory results in Capan-1 via RT-qPCR and Western blot [34,35]. Depending on the method employed, RT-qPCR performance can yield different results and thus show discrepancies between the measures of standard error [36]. Additionally, Friess et al. (2003) [35] employed a primer set binding to the

first exon of the gene, thus detecting both variants at the same time. In contrast, our primers were designed to specifically distinguish between the NK1R isoforms [TACR1-fl,20], thus, a decrease in expression might be expected compared to mRNA of total NK1R (full and truncated combined). However, the absence of the gene on a transcriptional level might also be explained through features associated with the truncated isoform of NK1R. In contrast to NK1R-fl, following endocytosis, the carboxy-terminally truncated, and thus internalization-defective, NK1R-tr fails β-arrestin-mediated dephosphorylation. This can cause unsuccessful desensitization of NK1R-tr to SP [11,16]. The prolonged exposure of NK1R to substance P has been shown to lead to the decrease of NK1R on a transcriptional level with concurrent increase of regulatory microRNAs (miRNA) [37]. As such, the presence of the protein might also explain the strong AP-induced effects we observed in our experiments despite the here-observed low or absent transcriptional expression. Furthermore, variations between transcriptional and protein levels are a phenomenon frequently observed [38,39]. For further investigation and determination of gene expression, we suggest Western blot analysis for the specific protein of interest. However, with respect to this method, it seems to be difficult to distinguish between the two isoforms so far.

Varying expression of *TACR1-tr* and *TAC1* release is in line with the TCGA data, where we found trends related to tumor stages. Such intermittent transcriptomic expression could be required for tumor stage development; however, definite assertions require further investigation. Another explanation that needs to be considered, is the downregulation of *TACR1* due to genomic alterations with progressing EMT [27]. As such, cells might try to counterbalance the loss of function of NK1R by upregulating its activator SP on a transcriptomic level. In a first step to understand circulating SP serum levels in patients, we screened SP levels in PDAC patients in comparison to patients without an underlying malignancy and found a slight tendency towards a decrease of SP serum levels in the former. However, to increase the predictive significance of this data, a higher number of samples would be required to determine differences in SP serum levels. Our data let us assume that local transcriptomic data of *TAC1* and circulating protein release measurements in serum do not necessarily correlate and might therefore not be helpful for monitoring of PDAC. Therapeutic stratification or monitoring of therapeutic success with NK1R inhibition will have to be investigated in future trials.

Data mining in publicly available datasets, such as TCGA, GEO, and CCLE, with additional consideration of OncoLnc survival data, allowed for linkage of differential expression of *TACR1* and *TAC1* to tumor progression and EMT state of cancer cells. EMT is an act of tumor progression, in which epithelial cells lose their cell polarity and cell-cell adhesion in order to gain migratory and invasive properties to become more mesenchymal [25,40,41]. Significant decline of *TACR1* in PDAC tumor tissues in the course of tumor progression is in line with survival curves demonstrating lower expression of *TACR1* to correlate with poorer survival. On top of that, low expression of *TACR1* in PDAC (expression compared to other tissues) significantly relates to high expression of *ZEB1* (Figure 2d). *ZEB1* overexpression is known to facilitate tumor progression, invasion, and metastasis [40]. In summary, exponential decline of *TACR1* seems to correlate with exponential increase of *ZEB1* expression. Clustering of gene expression revealed grouping of *TACR1* and *TAC1* into two distinct sets. More precisely, *TACR1* showed closer relation to epithelial markers, whereas *TAC1* was clustered into a group of genes associated with mesenchymal properties. Positive correlation of *ZEB1* and *TAC1* also showed high levels of these genes to correlate with a close to significant *p*-value. It remains particularly intriguing, whether the transition of high *TACR1* and low *TAC1* might act as an indicator of tumor progression, especially as links between substance P and activation of mesenchymal stem cells were previously described [42]. However, the presented results require biological conformation as being based solely on bioinformatical analysis. At this point, we do not consider *TAC1* as a molecular marker for PDAC diagnosis, but we hypothesize that the decrease of SP in

patient sera might be caused by increased SP consumption by malignant cells and might be an object for further exploration.

In a previous study [35], mRNA expression of NK1R in pancreatic tissue was analyzed via RT-qPCR. According to these results, gene expression indicates higher expression of NK1R in tumor versus normal tissue. Additionally, they found increasing NK1R levels with tumor progression, as well as higher expression of NK1R to correlate with lower patient survival. Surprisingly, the data sets analyzed in this study (Figure 2; TCGA, GSE62165, GSE15471, and GSE16515) clearly show contradictory results. Although both results are based on transcriptomic analysis, contradictory results might still occur through differences in the methodology, as GEO data sets for instance are microarray-based. Furthermore, bioinformatical analysis conducted in our study employed four large independent data sets with a total of 193 tumor patients and 68 normal controls in the GEO data set, and another 86 patients through OncoLnc. Thus, discrepancies might occur through a much smaller population size in the aforementioned publication.

High expression of truncated *TACR1* and high sensitivity to AP seem to correlate. Interestingly, we found strikingly higher expressions of truncated *TACR1* in MIA PaCa-2, which also exhibited the highest values regarding the presence of *TAC1*. Furthermore, we found the mesenchymal cell line to be the most sensitive for AP treatment in terms of growth interference in all experiments, including CFA and SFA. Additionally, we observed a small increase in pan caspase activity solely in this cell line, suggesting AP to have a particular effect on this strongly undifferentiated cancer cell. Similar trends observed in MIA PaCa-2 were found in DanG, which showed the second highest level of *TACR1-tr*. Taken together, our investigation suggests cancer subgroups with higher expression of *TACR1-tr* to be more susceptible for AP. For future studies, we therefore believe that PDAC patients with higher *TACR1-tr* expression might potentially benefit from treatment with AP as an anti-cancer treatment. Hence, we propose a prospective trial to investigate the implementation of *TACR1-tr* measurement for therapeutic stratification of PDAC.

The establishment of tumor-derived spheroids from anoikis-resistant cells is commonly used as an in vitro surrogate functional marker for cancer stemness [23]. It enables for sensitive identification of cells possessing CSC-like properties while at the same time allowing drug testing in a 3D in vitro culturing model [23,30,31]. CSCs are rare tumor initiators with strong chemoresistance [30,31]. The potential to inhibit CSC growth is therefore considered a very attractive method to improve therapy effects in cancer patients. Not only did most of the here-tested cell lines show the ability for CFA and SFA, but also, we observed exceptional dose-dependent treatment responses to AP in colonies and spheroids after 14 days of culture. In addition, cells in colony and spheroid formation exhibited even higher sensitivity to AP than parental cells, indicating lower concentrations to be required for successful growth inhibition. This suggests NK1R blockage to show high efficacy in targeting CSC-like cells, thus owning high potential for tumor initiator inhibition. In order to gain more knowledge regarding this mechanism, further analysis is required at this point to determine potential changes in the expression of SP/NK1R-related genes.

Another crucial discovery is the effect of AP on PSCs, where we found a lower sensitivity. PSCs are the major contributor to aggressive stromal fibrosis and closely interact with cancer cells, which in turn stimulates pancreatic tumor growth [43,44]. Activation of quiescent PSCs during PDAC development promotes several factors associated with proliferation and tumor progression. Additionally, linkage to genomic instability and capability of induction of EMT has been reported [44]. The ability to silence cell signaling of such cells might drastically improve a patient's outcome through inhibiting reoccurring tumor growth after surgery.

Due to the markedly decreased viability in all assays after AP exposure, we examined the cells regarding AP-induced mechanisms. Intriguingly, we found very low indication for activated apoptotic processes. With both apoptosis assays uniformly suggesting the exclusion of apoptotic mechanisms in AP-induced growth inhibition, we refocused on a different mechanism to determine the effect of NK1R antagonistic growth inhibition. One

way to eliminate cancer cells is interference with cell cycle progression, the key process for cell replication. Quantification of cell cycle progression allowed the identification of AP-induced cell cycle arrest with the most striking effects in G1 and S phase. To further uncover the mechanisms behind AP-induced cell cycle arrest, deeper investigations are of priority including, among others, cell-cycle-related proteins.

Relative overall mRNA expression of *TACR1* splice variants led us to question the mechanism through which AP exhibits its significant anti-proliferative effect on pancreatic cancer cells, which we expected to be mediated by the SP/NK1R complex. Next to binding to NK1R with high affinity, AP also shows little to no affinity to corticosteroid receptors, serotonin, or dopamine [45]. For further investigation, it might be of interest whether aprepitant could exhibit anti-tumoral effects through binding to the mentioned receptors in case of NK1R absence.

5. Conclusions

Current research strongly supports the idea of the SP/NK1R complex being involved in cancer progression. Additionally, it has been shown in multiple ways that blockage of the NK1R receptor results in the inhibition of cancer cell growth. In this study, we identified the SP/NK1R complex as a potent target in PDAC and aprepitant to inhibit cell cycle progression. NK1R blockage resulted in dose-dependent growth reduction in CSC-like cells, parental PDAC cells, and to a lesser degree in primary PSCs, whereby the highest sensitivity was observed in aggressive cancer cell types and subgroups expressing higher levels of the truncated *TACR1* variant. *TACR1-tr* was also the predominantly expressed isoform in PDAC cells. In conclusion, we suggest antagonistic NK1R-blockage as a potential therapeutic option for PDAC subgroups with high *TACR1-tr* expressions.

However, with respect to the heterogenic nature of PDAC, deeper investigation of splice variants appearing in PDAC patients is necessary and might help to distinguish between PDAC subgroups. Especially with the currently increasing identification of isoform-guided differential mechanisms being prominently involved in tumor progression, increased understanding might be gained through public availability of transcriptomic differentiation between splice variants. So far, only a very small number of studies has investigated the effects of AP in cancer patients on a molecular level regarding its role as a potential cancer drug. Emphasizing on PDAC being a very heterogenic tumor with no dominant druggable mutation [46,47], investigating the mechanisms on a transcriptional level has high potential in highlighting crucial differences between tumor subtypes and their underlying mechanisms in tumor progression. With no substantial improvements in PDAC treatments over the past 30 years [48,49], such information has the power to lead to new therapeutic developments.

Author Contributions: Conceptualization, B.W.R. and M.I.; Data curation, I.B., S.M., N.S.R., J.K. and J.W. (Jing Wang); Formal analysis, I.B., S.M., J.K., M.B., J.G.D., J.A. and M.I.; Funding acquisition, B.W.R., M.K.A. and M.I.; Investigation, I.B., S.M., N.S.R., M.K.A. and H.N.; Methodology, S.M., N.S.R., J.K., D.K. and M.B.; Project administration, N.S.R. and M.I.; Resources, B.W.R., M.K.A., J.G.D., M.O.G., J.A. and J.W. (Jens Werner); Supervision, B.W.R., A.V.B., M.O.G., J.W. (Jens Werner) and M.I.; Validation, I.B., D.K., A.V.B. and J.G.D.; Writing–original draft, I.B.; Writing–review & editing, B.W.R., D.K., A.V.B., M.B., J.W. (Jing Wang), M.O.G., H.N., J.A., J.W. (Jens Werner) and M.I. All authors have read and agreed to the published version of the manuscript.

Funding: Research from M.I. was funded by the "Bayerisches Zentrum für Krebsforschung" (BZKF), the Else Kröner-Fresenius Stiftung (Grant 2019_A130 to M.I.), and the Wilhelm Sander-Stiftung (Grant 2019.022.01 to M.I.). Further, this work was supported by the Promotionsstudium "Förderung für Forschung und Lehre" program from the University of Munich, LMU (to J.K. and M.B.). B.W.R. and M.K.A. received funding from the Roche Foundation. Last, M.I. and B.W.R. were supported by grants of the German Center for Translations Cancer Research (DKTK).

Institutional Review Board Statement: The study was conducted according to the guidelines of the Declaration of Helsinki and approved on 23 June 2020, by the Institutional Review Board (or Ethics Committee) of Ludwig-Maximilians-University Munich, Germany (protocol code 19-233).

Informed Consent Statement: Informed consent was obtained from all subjects involved in the study.

Data Availability Statement: TCGA at https://portal.gdc.cancer.gov, last accessed on 6 March 2021; GEO at https://www.ncbi.nlm.nih.gov/geo/, last accessed on 6 March 2021; CCLE at https://portals.broadinstitute.org/ccle, last accessed on the 14 April 2021; OncoLnc at http://www.oncolnc.org, last accessed on the 14 April 2021.

Acknowledgments: We apologize to the authors whose work we were not able to cite due to restrictions to the size of this article.

Conflicts of Interest: The authors declare no conflict of interest.

Appendix A

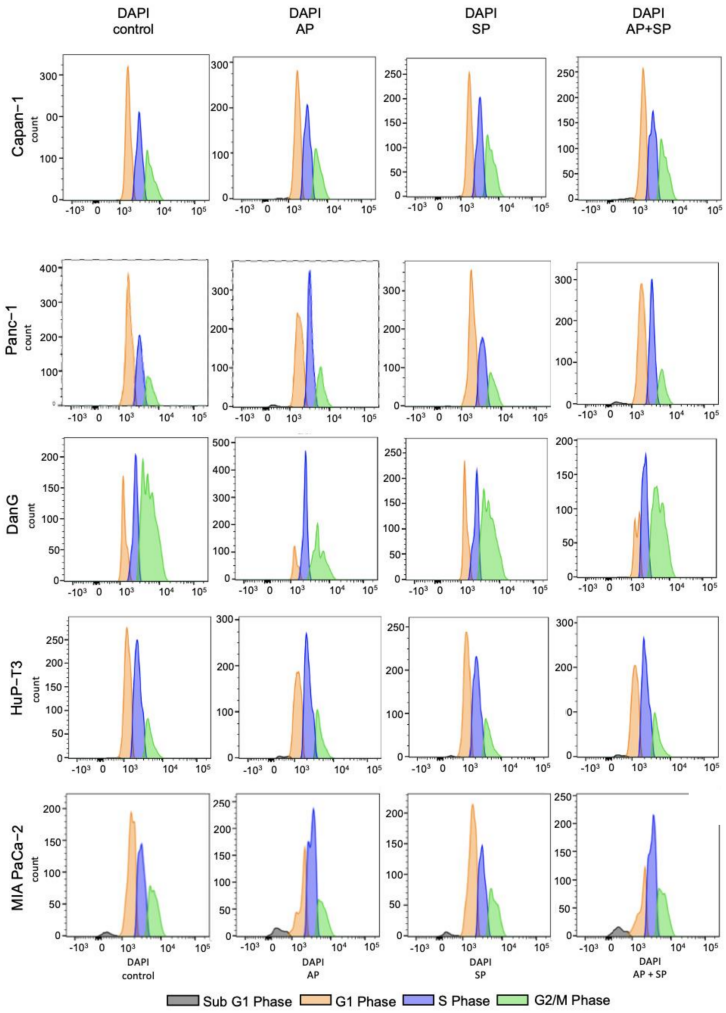

Figure A1. Histogram extension of Figure 5. Histograms showing treatment reaction to AP, SP, and AP+SP after DAPI staining in the indicated cell lines for cell cycle analysis.

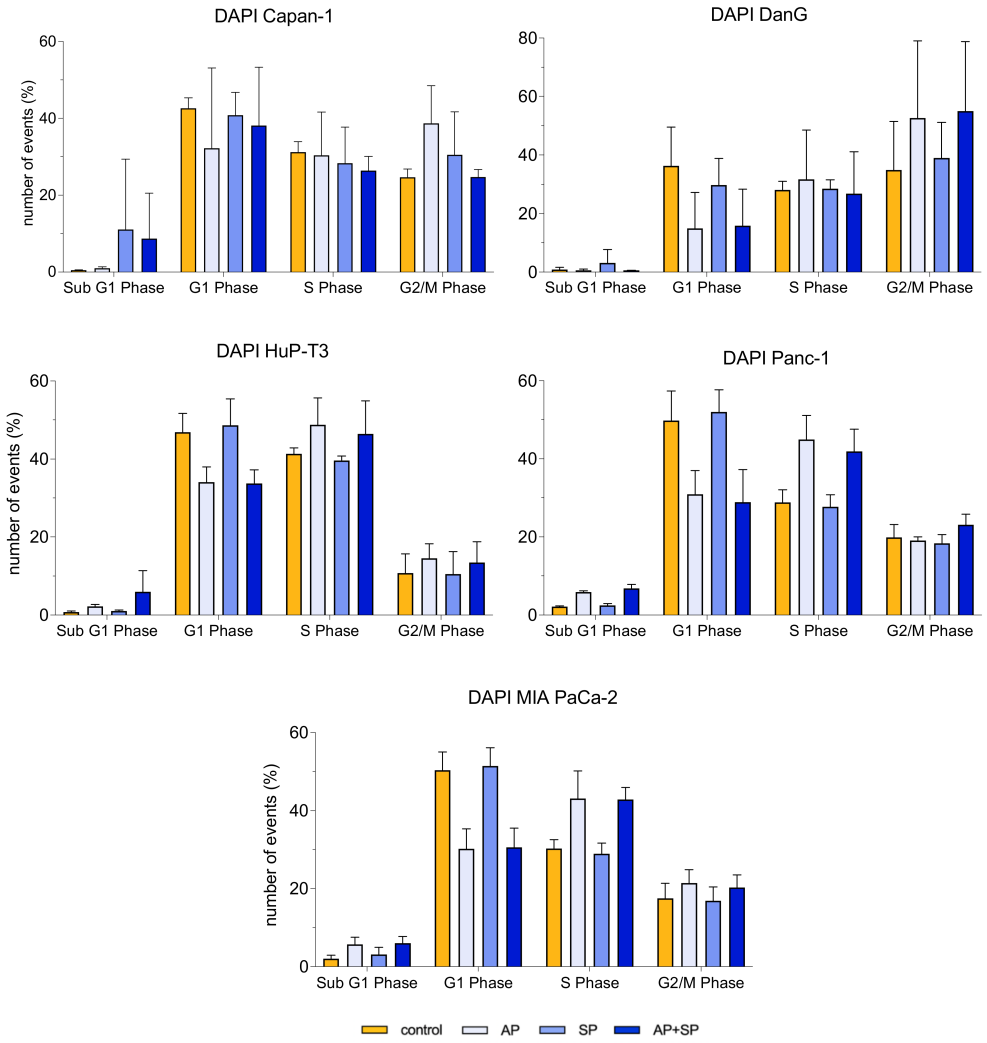

Figure A2. Bar Chart extension of Figure 5. DAPI staining results displayed in % for all cell cycle phases in the indicated cell lines.

References

1. Ariston Gabriel, A.N.; Jiao, Q.; Yvette, U.; Yang, X.; Al-Ameri, S.A.; Du, L.; Wang, Y.-S.; Wang, C. Differences between KC and KPC pancreatic ductal adenocarcinoma mice models, in terms of their modelling biology and their clinical relevance. *Pancreatology* **2020**, *20*, 79–88. [CrossRef] [PubMed]
2. Siegel, R.L.; Miller, K.D.; Jemal, A. Cancer statistics. *Cancer J. Clin.* **2019**, *69*, 7–34. [CrossRef] [PubMed]
3. McGuigan, A.; Kelly, P.; Turkington, R.C.; Jones, C.; Coleman, H.G.; McCain, R. Pancreatic cancer: A review of clinical diagnosis, epidemiology, treatment and outcomes. *World J. Gastroenterol.* **2018**, *24*, 4846–4861. [CrossRef] [PubMed]
4. Quante, A.S.; Ming, C.; Rottmann, M.; Engel, J.; Boeck, S.; Heinemann, V.; Westphalen, C.B.; Strauch, K. Projections of cancer incidence and cancer-related deaths in Germany by 2020 and 2030. *Cancer Med.* **2016**, *5*, 2649–2656. [CrossRef]
5. Gasparini, G.; Pellegatta, M.; Crippa, S.; Schiavo Lena, M.; Belfiori, G.; Doglioni, C.; Taveggia, C.; Falconi, M. Nerves and Pancreatic Cancer: New Insights into A Dangerous Relationship. *Cancers* **2019**, *11*, 893. [CrossRef]

6. Renz, B.W.; Takahashi, R.; Tanaka, T.; Macchini, M.; Hayakawa, Y.; Dantes, Z.; Maurer, H.C.; Chen, X.; Jiang, Z.; Westphalen, C.B.; et al. β2 adrenergic-neurotrophin feed-forward loop promotes pancreatic cancer. *Cancer Cell.* **2018**, *33*, 75–90. [CrossRef]
7. Renz, B.W.; Tanaka, T.; Sunagawa, M.; Takahashi, R.; Jiang, Z.; Macchini, M.; Dantes, Z.; Valenti, G.; White, R.A.; Middelhoff, M.A.; et al. Cholinergic Signaling via Muscarinic Receptors Directly and Indirectly Suppresses Pancreatic Tumorigenesis and Cancer Stemness. *Cancer Discov.* **2018**, *8*, 1458–1473. [CrossRef]
8. Saloman, J.L.; Albers, K.M.; Li, D.; Hartman, D.J.; Crawford, H.C.; Muha, E.A.; Rhim, A.D.; Davis, B.M. Ablation of sensory neurons in a genetic model of pancreatic ductal adenocarcinoma slows initiation and progression of cancer. *Proc. Natl. Acad. Sci. USA* **2016**, *113*, 3078–3083. [CrossRef]
9. Zahalka, A.H.; Frenette, P.S. Nerves in cancer. *Nat. Rev. Cancer.* **2020**, *20*, 143–157. [CrossRef]
10. Martinez, A.N.; Philipp, M.T. Substance P and Antagonists of the Neuokinin-1 Receptor in Neuroinflammation Associated with Infectious and Neurodegenerative Diseases of the Central Nervous System. *J. Neurol. Neuromed.* **2016**, *1*, 29–36.
11. Li, X.; Ma, G.; Ma, Q.; Li, W.; Liu, J.; Han, L.; Duan, W.; Xu, Q.; Liu, H.; Wang, Z.; et al. Neurotransmitter substance P mediates pancreatic cancer perineural invasion via NK-1R in cancer cells. *Mol. Cancer Res.* **2013**, *11*, 294–302. [CrossRef]
12. Steinhoff, M.S.; von Mentzer, B.; Geppetti, P.; Pothoulakis, C.; Bunnett, N.W. Tachykinins and their receptors: Contributions to physiological control and the mechanisms of disease. *Physiol. Rev.* **2014**, *94*, 265–301. [CrossRef]
13. Krause, J.E.; Takeda, Y.; Hershey, A.D. Structure, functions, and mechanisms of substance P receptor action. *J. Investig. Dermatol.* **1992**, *98*, 2S–7S. [CrossRef]
14. Garnier, A.; Ilmer, M.; Becker, K.; Häberle, B.; von Schweinitz, D.; Kappler, R.; Berger, M. Truncated neurokinin-1 receptor is an ubiquitous antitumor target in hepatoblastoma, and its expression is independent of tumor biology and stage. *Oncol. Lett.* **2016**, *11*, 870–878. [CrossRef]
15. Lai, J.-P.; Lai, S.; Tuluc, F.; Tansky, M.F.; Kilpatrick, L.E.; Leeman, S.E.; Douglas, S.D. Differences in the length of the carboxyl terminus mediate functional properties of neurokinin-1 receptor. *Proc. Natl. Acad. Sci. USA* **2008**, *105*, 12605–12610. [CrossRef]
16. DeFea, K.A.; Vaughn, Z.D.; O'Bryan, E.M.; Nishijima, D.; Déry, O.; Bunnett, N.W. The proliferative and antiapoptotic effects of substance P are facilitated by formation of a β-arrestin dependent scaffolding complex. *Proc. Natl. Acad. Sci. USA* **2000**, *97*, 11086–11091. [CrossRef]
17. Tuluc, F.; Lai, J.P.; Kilpatrick, L.E.; Evans, D.; Douglas, S.D. Neurokinin 1 receptor isoforms and the control of innate immunity. *Trends Immunol.* **2009**, *30*, 271–276. [CrossRef]
18. Fong, T.M.; Anderson, S.A.; Yu, H.; Huang, R.R.; Strader, C.D. Differential activation of intracellular effector by isoforms of human neurokinin-1 receptor. *Mol. Pharmacol.* **1992**, *41*, 24–30.
19. Muñoz, M.; Crespo, J.C.; Crespo, J.P.; Coveñas, R. Neurokinin-1 receptor antagonist aprepitant and radiotherapy, a successful combination therapy in a patient with lung cancer: A case report. *Mol. Clin. Oncol.* **2019**, *11*, 50–54.
20. Berger, M.; Neth, O.; Ilmer, M.; Garnier, A.; Salinas-Martin, M.V.; de Agustín Ascencio, J.C.; von Schweinitz, D.; Kappler, R.; Muñoz, M. Hepatoblastoma cells express truncated neurokinin-1 receptor and can be growth inhibited by aprepitant in vitro and in vivo. *J. Hepatol.* **2014**, *60*, 985–994. [CrossRef]
21. Garnier, A.; Vykoukal, J.; Hubertus, J.; Alt, E.; von Schweinitz, D.; Kappler, R.; Berger, M.; Ilmer, M. Targeting the neurokinin-1 receptor inhibits growth of human colon cancer cells. *Int. J. Oncol.* **2015**, *47*, 151–160. [CrossRef]
22. Ilmer, M.; Garnier, A.; Vykoukal, J.; Alt, E.; von Schweinitz, D.; Kappler, R.; Berger, M. Targeting the Neurokinin-1 Receptor Compromises Canonical Wnt Signaling in Hepatoblastoma. *Mol. Cancer Ther.* **2015**, *14*, 2712–2721. [CrossRef]
23. Ilmer, M.; Boiles, A.R.; Regel, I.; Yokoi, K.; Michalski, C.W.; Wistuba, I.I.; Rodriguez, J.; Alt, E.; Vykoukal, J. RSpo2 enhances canonical Wnt signaling to confer stemness associated traits to susceptible pancreatic cancer cells. *Cancer Res.* **2015**, *75*, 1883–1896. [CrossRef]
24. Kolorz, J.; Demir, S.; Gottschlich, A.; Beirith, I.; Ilmer, M.; Lüthy, D.; Walz, C.; Dorostkar, M.; von Schweinitz, D.; Kobold, S.; et al. The Neurokinin-1 receptor is a target in pediatric rhabdoid tumors. Department of Pediatric Surgery, Research Laboratories, Dr. von Hauner Children's Hospital, Ludwig-Maximilians-University Munich, 80337 Munich, Germany. Unpublished work. 2021.
25. Monkman, J.H.; Thompson, E.W.; Nagaraj, S.H. Targeting Epithelial Mesenchymal Plasticity in Pancreatic Cancer: A Compendium of Preclinical Discovery in a Heterogeneous Disease. *Cancers* **2019**, *11*, 1745. [CrossRef]
26. Dijk, F.; Veenstra, V.L.; Soer, E.C.; Dings, M.P.G.; Zhao, L.; Halfwerk, J.B.; Hooijer, G.K.; Damhofer, H.; Marzano, M.; Steins, A.; et al. Unsupervised class discovery in pancreatic ductal adenocarcinoma reveals cell intrinsic mesenchymal features and high concordance between existing classification systems. *Sci. Rep.* **2020**, *10*, 337. [CrossRef]
27. Sinha, A.; Cherba, D.; Bartlam, H.; Lenkiewicz, E.; Evers, L.; Barrett, M.T.; Haab, B.B. Mesenchymal-like pancreatic cancer cells harbor specific genomic alterations more frequently than their epithelial-like counterparts. *Mol. Oncol.* **2014**, *8*, 1253–1265. [CrossRef]
28. Muñoz, M.; Rosso, M. The NK-1 receptor antagonist aprepitant as a broad spectrum antitumor drug. *Investig. New Drugs* **2010**, *28*, 187–193. [CrossRef]
29. Sousa, C.M.; Biancur, D.E.; Wang, X.; Halbrook, C.J.; Sherman, M.H.; Zhang, L.; Kremer, D.; Hwang, R.F.; Witkiewicz, A.K.; Ying, H.; et al. Pancreatic stellate cells support tumour metabolism through autophagic alanine secretion. *Nature* **2016**, *536*, 479–483. [CrossRef] [PubMed]
30. Ishiguro, T.; Ohata, H.; Sato, A.; Yamawaki, K.; Enomoto, T.; Okamoto, K. Tumor-derived spheroids: Relevance to cancer stem cells and clinical applications. *Cancer Sci.* **2017**, *108*, 283–298. [CrossRef] [PubMed]

31. Rajendran, V.; Vilas Jain, M. In Vitro Tumorigenic Assay: Colony Forming Assay for Cancer Stem Cells. *Methods Mol. Biol.* **2018**, *1692*, 89–95. [PubMed]
32. Zhou, Y.; Zhao, L.; Xiong, T.; Chen, X.; Zhang, Y.; Yu, M.; Yang, J.; Yao, Z. Roles of full-length and truncated neurokinin-1 receptors on tumor progression and distant metastasis in human breast cancer. *Breast Cancer Res. Treat.* **2013**, *140*, 49–61. [CrossRef]
33. Spitsin, S.; Pappa, V.; Douglas, S.D. Truncation of neurokinin-1 receptor—Negative regulation of substance P signaling. *J. Leukoc. Biol.* **2018**, *103*, 1043–1051. [CrossRef]
34. Muñoz, M.; Rosso, M.; Conveñas, R. The NK-1 Receptor is Involved in the Antitumoral Action of L-733,060 and in the Mitogenic Action of Substance P on Human Pancreatic Cancer Cell Lines. *Lett. Drug Des. Discov.* **2006**, *3*, 323–329. [CrossRef]
35. Friess, H.; Zhu, Z.; Liard, V.; Shi, X.; Shrikhande, S.V.; Wang, L.; Lieb, K.; Korc, M.; Palma, C.; Zimmermann, A.; et al. Neurokinin-1 receptor expression and its potential effects on tumor growth in human pancreatic cancer. *Lab Investig.* **2003**, *83*, 731–742. [CrossRef]
36. Wong, M.L.; Medrano, J.F. Real-time PCR form RNA quantification. *Biotechniques* **2005**, *39*, 75–85. [CrossRef]
37. Edfors, F.; Danielsson, F.; Hallström, B.M.; Käll, L.; Lundberg, E.; Pontén, F.; Forsström, B.; Uhlén, M. Gene-specific correlation of RNA and protein levels in human cells and tissues. *Mol. Syst Biol.* **2016**, *12*, 883. [CrossRef]
38. Guo, Y.; Xiao, P.; Lei, S.; Deng, F.; Xiao, G.G.; Liu, Y.; Chen, X.; Li, L.; Wu, S.; Chen, Y.; et al. How is mRNA expression predictive for protein expression? A correlation study on human circulating monocytes. *Acta Biochim. Biophys. Sin.* **2008**, *40*, 426–436. [CrossRef]
39. Freire, V.S.; Burkhard, F.C.; Kessler, T.M.; Kuhn, A.; Draegger, A.; Monastyrskaya, K. MicroRNAs May Mediate the Down-Regulation of Neurokinin-1 Receptor in Chronic Bladder Pain Syndrome. *Am. J. Pathol.* **2010**, *176*, 288–303. [CrossRef]
40. Timaner, M.; Tsai, K.K.; Shaked, Y. The multifaceted role of mesenchymal stem cells in cancer. *Semin. Cancer Biol.* **2020**, *60*, 225–237. [CrossRef]
41. Zhang, P.; Sun, Y.; Ma, L. ZEB1: At the crossroads of epithelial-mesenchymal transition, metastasis and therapy resistance. *Cell Cycle* **2015**, *14*, 481–487. [CrossRef]
42. Jin, Y.; Hong, H.S.; So, Y. Substance P enhances mesenchymal stem cells-mediated immune modulation. *Cytokine* **2015**, *71*, 145–153. [CrossRef]
43. Ferdek, P.E.; Jakubowska, M.A. Biology of pancreatic stellate cells-more than just pancreatic cancer. *Pflug. Arch.* **2017**, *469*, 1039–1050. [CrossRef]
44. Schnittert, J.; Bansal, R.; Prakash, J. Targeting Pancreatic Stellate Cells in Cancer. *Trends Cancer.* **2019**, *5*, 128–142. [CrossRef]
45. Pojawa-Golab, M.; Jaworecka, K.; Reich, A. NK-1 Receptor Antagonists and Pruritus: Review of Current Literature. *Dermatol. Ther.* **2019**, *9*, 391–405. [CrossRef]
46. Hayashi, H.; Kohno, T.; Hiraoka, N.; Sakamoto, Y.; Kondo, S.; Morizane, C.; Saito, M.; Shimada, K.; Ichikawa, H.; Komatsu, Y.; et al. Gene Mutation Profile Of Pancreatic Cancer Obtained Using Targeted Deep Sequencing And Its Association With Prognosis. *Ann. Oncol.* **2014**, *25*, iv210–iv253. [CrossRef]
47. Yan, W.; Liu, X.; Wang, Y.; Shuqing, H.; Wang, F.; Liu, X.; Xiao, F.; Guang, H. Identifying Drug Targets in Pancreatic Ductal Adenocarcinoma Through Machine Learning, Analyzing Biomolecular Networks, and Structural Modeling. *Front. Pharmacol.* **2020**, *11*, 534. [CrossRef]
48. Melisi, D.; Calvetti, L.; Frizziero, M.; Tortora, G. Pancreatic cancer: Systemic combination therapies for a heterogeneous disease. *Curr. Pharm. Des.* **2014**, *20*, 6660–6669. [CrossRef]
49. David, M.; Lepage, C.; Jouve, J.-L.; Jooste, V.; Chauvenet, M.; Faivre, J.; Bouvier, A.M. Management and prognosis of pancreatic cancer over a 30-year period. *Br. J. Cancer* **2009**, *101*, 215–218. [CrossRef]

7. References

BECKWITH, J. B. & PALMER, N. F. 1978. Histopathology and prognosis of Wilms tumors: results from the First National Wilms' Tumor Study. *Cancer,* 41**,** 1937-48.

BEIRITH, I., RENZ, B. W., MUDUSETTI, S., RING, N. S., KOLORZ, J., KOCH, D., BAZHIN, A. V., BERGER, M., WANG, J., ANGELE, M. K., D'HAESE, J. G., GUBA, M. O., NIESS, H., ANDRASSY, J., WERNER, J. & ILMER, M. 2021. Identification of the Neurokinin-1 Receptor as Targetable Stratification Factor for Drug Repurposing in Pancreatic Cancer. *Cancers (Basel),* 13.

BENNETT, J., ERKER, C., LAFAY-COUSIN, L., RAMASWAMY, V., HUKIN, J., VANAN, M. I., CHENG, S., COLTIN, H., FONSECA, A., JOHNSTON, D., LO, A., ZELCER, S., ALVI, S., BOWES, L., BROSSARD, J., CHARLEBOIS, J., EISENSTAT, D., FELTON, K., FLEMING, A., JABADO, N., LAROUCHE, V., LEGAULT, G., MPOFU, C., PERREAULT, S., SILVA, M., SINHA, R., STROTHER, D., TSANG, D. S., WILSON, B., CROOKS, B. & BARTELS, U. 2020. Canadian Pediatric Neuro-Oncology Standards of Practice. *Front Oncol,* 10**,** 593192.

BERGER, M. & D, V. S. 2017. Therapeutic Innovations for Targeting Childhood Neuroblastoma: Implications of the Neurokinin-1 Receptor System. *Anticancer Res,* 37**,** 5911-5918.

BERGER, M., NETH, O., ILMER, M., GARNIER, A., SALINAS-MARTIN, M. V., DE AGUSTIN ASENCIO, J. C., VON SCHWEINITZ, D., KAPPLER, R. & MUNOZ, M. 2014. Hepatoblastoma cells express truncated neurokinin-1 receptor and can be growth inhibited by aprepitant in vitro and in vivo. *J Hepatol,* 60**,** 985-94.

BRENNAN, B., STILLER, C. & BOURDEAUT, F. 2013. Extracranial rhabdoid tumours: what we have learned so far and future directions. *The Lancet Oncology,* 14**,** e329-e336.

CHAIN, A., WRISHKO, R., VASILININ, G. & MOUKSASSI, S. 2020. Modeling and Simulation Analysis of Aprepitant Pharmacokinetics in Pediatric Patients With Postoperative or Chemotherapy-Induced Nausea and Vomiting. *J Pediatr Pharmacol Ther,* 25**,** 528-539.

CHI, S. N., ZIMMERMAN, M. A., YAO, X., COHEN, K. J., BURGER, P., BIEGEL, J. A., RORKE-ADAMS, L. B., FISHER, M. J., JANSS, A., MAZEWSKI, C., GOLDMAN, S., MANLEY, P. E., BOWERS, D. C., BENDEL, A., RUBIN, J., TURNER, C. D., MARCUS, K. J., GOUMNEROVA, L., ULLRICH, N. J. & KIERAN, M. W. 2009. Intensive multimodality treatment for children with newly diagnosed CNS atypical teratoid rhabdoid tumor. *J Clin Oncol,* 27**,** 385-9.

COLLABORATORS, G. B. D. P. C. 2019. The global, regional, and national burden of pancreatic cancer and its attributable risk factors in 195 countries and territories, 1990-2017: a systematic analysis for the Global Burden of Disease Study 2017. *Lancet Gastroenterol Hepatol,* 4**,** 934-947.

CONROY, T., HAMMEL, P., HEBBAR, M., BEN ABDELGHANI, M., WEI, A. C., RAOUL, J. L., CHONE, L., FRANCOIS, E., ARTRU, P., BIAGI, J. J., LECOMTE, T., ASSENAT, E., FAROUX, R., YCHOU, M., VOLET, J., SAUVANET, A., BREYSACHER, G., DI FIORE, F., CRIPPS, C., KAVAN, P., TEXEREAU, P., BOUHIER-LEPORRIER, K., KHEMISSA-AKOUZ, F., LEGOUX, J. L., JUZYNA, B., GOURGOU, S., O'CALLAGHAN, C. J., JOUFFROY-ZELLER, C., RAT, P., MALKA, D., CASTAN, F., BACHET, J. B., CANADIAN CANCER TRIALS, G. & THE UNICANCER, G. I. P. G. 2018. FOLFIRINOX or Gemcitabine as Adjuvant Therapy for Pancreatic Cancer. *N Engl J Med,* 379**,** 2395-2406.

CONROY, T., PFEIFFER, P., VILGRAIN, V., LAMARCA, A., SEUFFERLEIN, T., O'REILLY, E. M., HACKERT, T., GOLAN, T., PRAGER, G., HAUSTERMANS, K., VOGEL, A., DUCREUX, M. & CLINICALGUIDELINES@ESMO.ORG, E. G. C. E. A. 2023. Pancreatic cancer: ESMO Clinical Practice Guideline for diagnosis, treatment and follow-up. *Ann Oncol,* 34**,** 987-1002.

COVENAS, R., RODRIGUEZ, F. D., ROBINSON, P. & MUNOZ, M. 2023. The Repurposing of Non-Peptide Neurokinin-1 Receptor Antagonists as Antitumor Drugs: An Urgent Challenge for Aprepitant. *Int J Mol Sci,* 24.

DIGIACOMO, G., VOLTA, F., GARAJOVA, I., BALSANO, R. & CAVAZZONI, A. 2021. Biological Hallmarks and New Therapeutic Approaches for the Treatment of PDAC. *Life (Basel),* 11.

FAZLOLLAHI, L., HSIAO, S. J., KOCHHAR, M., MANSUKHANI, M. M., YAMASHIRO, D. J. & REMOTTI, H. E. 2019. Malignant Rhabdoid Tumor, an Aggressive Tumor Often Misclassified as Small Cell Variant of Hepatoblastoma. *Cancers (Basel),* 11.

GARAJOVA, I., PERONI, M., GELSOMINO, F. & LEONARDI, F. 2023. A Simple Overview of Pancreatic Cancer Treatment for Clinical Oncologists. *Curr Oncol,* 30**,** 9587-9601.

GASTBERGER, K., FINCKE, V. E., MUCHA, M., SIEBERT, R., HASSELBLATT, M. & FRÜHWALD, M. C. 2023. Current Molecular and Clinical Landscape of ATRT - The Link to Future Therapies. *Cancer Manag Res,* 15**,** 1369-1393.

GE, C., HUANG, H., HUANG, F., YANG, T., ZHANG, T., WU, H., ZHOU, H., CHEN, Q., SHI, Y., SUN, Y., LIU, L., WANG, X., PEARSON, R. B., CAO, Y., KANG, J. & FU, C. 2019. Neurokinin-1 receptor is an effective target for treating leukemia by inducing oxidative stress through mitochondrial calcium overload. *Proceedings of the National Academy of Sciences,* 116**,** 19635-19645.

GELLER, J. I., ROTH, J. J. & BIEGEL, J. A. 2015. Biology and Treatment of Rhabdoid Tumor. *Crit Rev Oncog,* 20**,** 199-216.

GILLESPIE, E., LEEMAN, S. E., WATTS, L. A., COUKOS, J. A., O'BRIEN, M. J., CERDA, S. R., FARRAYE, F. A., STUCCHI, A. F. & BECKER, J. M. 2011. Truncated neurokinin-1 receptor is increased in colonic epithelial cells from patients with colitis-associated cancer. *Proc Natl Acad Sci U S A,* 108**,** 17420-5.

GONZALES, M. 2001. The 2000 World Health Organization classification of tumours of the nervous system. *J Clin Neurosci,* 8**,** 1-3.

HALBROOK, C. J., LYSSIOTIS, C. A., PASCA DI MAGLIANO, M. & MAITRA, A. 2023. Pancreatic cancer: Advances and challenges. *Cell,* 186**,** 1729-1754.

HOLLMANN, T. J. & HORNICK, J. L. 2011. INI1-Deficient Tumors: Diagnostic Features and Molecular Genetics. *The American Journal of Surgical Pathology,* 35**,** e47-e63.

ILIC, M. & ILIC, I. 2016. Epidemiology of pancreatic cancer. *World J Gastroenterol,* 22**,** 9694-9705.

ILMER, M., GARNIER, A., VYKOUKAL, J., ALT, E., VON SCHWEINITZ, D., KAPPLER, R. & BERGER, M. 2015. Targeting the Neurokinin-1 Receptor Compromises Canonical Wnt Signaling in Hepatoblastoma. *Mol Cancer Ther,* 14**,** 2712-21.

KOHASHI, K. & ODA, Y. 2017. Oncogenic roles of SMARCB1/INI1 and its deficient tumors. *Cancer Sci,* 108**,** 547-552.

KOLORZ, J., DEMIR, S., GOTTSCHLICH, A., BEIRITH, I., ILMER, M., LÜTHY, D., WALZ, C., DOROSTKAR, M. M., MAGG, T., HAUCK, F., VON SCHWEINITZ, D., KOBOLD, S., KAPPLER, R. & BERGER, M. 2021. The Neurokinin-1 Receptor Is a Target in Pediatric Rhabdoid Tumors. *Current Oncology,* 29**,** 94-110.

MERCANTI, L., SINDACO, M., MAZZONE, M., DI MARCANTONIO, M. C., PISCIONE, M., MURARO, R. & MINCIONE, G. 2023. PDAC, the Influencer Cancer: Cross-Talk with Tumor Microenvironment and Connected Potential Therapy Strategies. *Cancers (Basel),* 15.

MOLINOS-QUINTANA, A., TRUJILLO-HACHA, P., PIRUAT, J. I., BEJARANO-GARCIA, J. A., GARCIA-GUERRERO, E., PEREZ-SIMON, J. A. & MUNOZ, M. 2019. Human acute myeloid leukemia cells express Neurokinin-1 receptor, which is involved in the antileukemic effect of Neurokinin-1 receptor antagonists. *Invest New Drugs,* 37**,** 17-26.

MUNOZ, M., BERGER, M., ROSSO, M., GONZALEZ-ORTEGA, A., CARRANZA, A. & COVENAS, R. 2014. Antitumor activity of neurokinin-1 receptor antagonists in MG-63 human osteosarcoma xenografts. *Int J Oncol,* 44**,** 137-46.

MUNOZ, M. & COVENAS, R. 2013. Safety of neurokinin-1 receptor antagonists. *Expert Opin Drug Saf,* 12**,** 673-85.

MUNOZ, M. & COVENAS, R. 2014. Involvement of substance P and the NK-1 receptor in human pathology. *Amino Acids,* 46**,** 1727-50.

MUNOZ, M. & COVENAS, R. 2020. The Neurokinin-1 Receptor Antagonist Aprepitant: An Intelligent Bullet against Cancer? *Cancers (Basel),* 12.

MUÑOZ, M. & COVEÑAS, R. 2013. Involvement of substance P and the NK-1 receptor in cancer progression. *Peptides,* 48**,** 1-9.

MUNOZ, M., COVENAS, R., ESTEBAN, F. & REDONDO, M. 2015. The substance P/NK-1 receptor system: NK-1 receptor antagonists as anti-cancer drugs. *J Biosci,* 40**,** 441-63.

MUNOZ, M., CRESPO, J. C., CRESPO, J. P. & COVENAS, R. 2019a. Neurokinin-1 receptor antagonist aprepitant and radiotherapy, a successful combination therapy in a patient with lung cancer: A case report. *Mol Clin Oncol,* 11**,** 50-54.

MUNOZ, M., GONZALEZ-ORTEGA, A. & COVENAS, R. 2012. The NK-1 receptor is expressed in human leukemia and is involved in the antitumor action of aprepitant and other NK-1 receptor antagonists on acute lymphoblastic leukemia cell lines. *Invest New Drugs,* 30**,** 529-40.

MUNOZ, M. & ROSSO, M. 2010. The NK-1 receptor antagonist aprepitant as a broad spectrum antitumor drug. *Invest New Drugs,* 28**,** 187-93.

MUNOZ, M., ROSSO, M. & COVENAS, R. 2019b. Neurokinin-1 Receptor Antagonists against Hepatoblastoma. *Cancers (Basel),* 11.

MUNOZ, M., ROSSO, M., ROBLES-FRIAS, M. J., SALINAS-MARTIN, M. V., ROSSO, R., GONZALEZ-ORTEGA, A. & COVENAS, R. 2010. The NK-1 receptor is expressed in human melanoma and is involved in the antitumor action of the NK-1 receptor antagonist aprepitant on melanoma cell lines. *Lab Invest,* 90**,** 1259-69.

NEMES, K., BENS, S., KACHANOV, D., TELESHOVA, M., HAUSER, P., SIMON, T., TIPPELT, S., WOESSMANN, W., BECK, O., FLOTHO, C., GRIGULL, L., DRIEVER, P. H., SCHLEGEL, P. G., KHURANA, C., HERING, K., KOLB, R., LEIPOLD, A., ABBINK, F., GIL-DA-COSTA, M. J., BENESCH, M., KERL, K., LOWIS, S., MARQUES, C. H., GRAF, N., NYSOM, K., VOKUHL, C., MELCHIOR, P., KRONCKE, T., SCHNEPPENHEIM, R., KORDES, U., GERSS, J., SIEBERT, R., FURTWANGLER, R. & FRUHWALD, M. C. 2021. Clinical and genetic risk factors define two risk groups of extracranial malignant rhabdoid tumours (eMRT/RTK). *Eur J Cancer,* 142**,** 112-122.

NEMES, K., JOHANN, P. D., TUCHERT, S., MELCHIOR, P., VOKUHL, C., SIEBERT, R., FURTWANGLER, R. & FRUHWALD, M. C. 2022. Current and Emerging Therapeutic Approaches for Extracranial Malignant Rhabdoid Tumors. *Cancer Manag Res,* 14**,** 479-498.

OSTROM, Q. T., CHEN, Y., P, M. D. B., ONDRACEK, A., FARAH, P., GITTLEMAN, H., WOLINSKY, Y., KRUCHKO, C., COHEN, M. L., BRAT, D. J. & BARNHOLTZ-SLOAN, J. S. 2014. The descriptive epidemiology of atypical teratoid/rhabdoid tumors in the United States, 2001-2010. *Neuro Oncol,* 16**,** 1392-9.

QUANTE, A. S., MING, C., ROTTMANN, M., ENGEL, J., BOECK, S., HEINEMANN, V., WESTPHALEN, C. B. & STRAUCH, K. 2016. Projections of cancer incidence and cancer-related deaths in Germany by 2020 and 2030. *Cancer Med,* 5**,** 2649-56.

REDDY, A. T., STROTHER, D. R., JUDKINS, A. R., BURGER, P. C., POLLACK, I. F., KRAILO, M. D., BUXTON, A. B., WILLIAMS-HUGHES, C., FOULADI, M., MAHAJAN, A., MERCHANT, T. E., HO, B., MAZEWSKI, C. M., LEWIS, V. A., GAJJAR, A., VEZINA, L. G., BOOTH, T. N., PARSONS, K. W., POSS, V. L., ZHOU, T., BIEGEL, J. A. & HUANG, A. 2020. Efficacy of High-Dose Chemotherapy and Three-Dimensional Conformal Radiation for Atypical Teratoid/Rhabdoid Tumor: A Report From the Children's Oncology Group Trial ACNS0333. *J Clin Oncol,* 38**,** 1175-1185.

RICHARDSON, E. A., HO, B. & HUANG, A. 2018. Atypical Teratoid Rhabdoid Tumour : From Tumours to Therapies. *J Korean Neurosurg Soc,* 61**,** 302-311.

ROBINSON, P., ROSSO, M. & MUNOZ, M. 2023. Neurokinin-1 Receptor Antagonists as a Potential Novel Therapeutic Option for Osteosarcoma Patients. *J Clin Med,* 12.

RORKE, L. B., PACKER, R. J. & BIEGEL, J. A. 1996. Central nervous system atypical teratoid/rhabdoid tumors of infancy and childhood: definition of an entity. *J Neurosurg,* 85**,** 56-65.

SEUFFERLEIN, T. & ETTRICH, T. J. 2019. Treatment of pancreatic cancer-neoadjuvant treatment in resectable pancreatic cancer (PDAC). *Transl Gastroenterol Hepatol,* 4**,** 21.

SHINODA, S., NAKAMURA, N., ROACH, B., BERNLOHR, D. A., IKRAMUDDIN, S. & YAMAMOTO, M. 2022. Obesity and Pancreatic Cancer: Recent Progress in Epidemiology, Mechanisms and Bariatric Surgery. *Biomedicines,* 10.

SUNG, H., FERLAY, J., SIEGEL, R. L., LAVERSANNE, M., SOERJOMATARAM, I., JEMAL, A. & BRAY, F. 2021. Global Cancer Statistics 2020: GLOBOCAN Estimates of Incidence and Mortality Worldwide for 36 Cancers in 185 Countries. *CA Cancer J Clin,* 71**,** 209-249.

UN, H., UGAN, R. A., KOSE, D., BAYIR, Y., CADIRCI, E., SELLI, J. & HALICI, Z. 2020. A novel effect of Aprepitant: Protection for cisplatin-induced nephrotoxicity and hepatotoxicity. *Eur J Pharmacol,* 880**,** 173168.

VERSTEEGE, I., SÉVENET, N., LANGE, J., ROUSSEAU-MERCK, M.-F., AMBROS, P., HANDGRETINGER, R., AURIAS, A. & DELATTRE, O. 1998. Truncating mutations of hSNF5/INI1 in aggressive paediatric cancer. *Nature,* 394**,** 203-206.

XUE, Y., ZHU, X., MEEHAN, B., VENNETI, S., MARTINEZ, D., MORIN, G., MAIGA, R. I., CHEN, H., PAPADAKIS, A. I., JOHNSON, R. M., O'SULLIVAN, M. J., ERDREICH-EPSTEIN, A., GOTLIEB, W. H., PARK, M., JUDKINS, A. R., PELLETIER, J., FOULKES, W. D., RAK, J. & HUANG, S. 2020. SMARCB1 loss induces druggable cyclin D1 deficiency via upregulation of MIR17HG in atypical teratoid rhabdoid tumors. *J Pathol,* 252**,** 77-87.

YIN, J., CHAPMAN, K., CLARK, L. D., SHAO, Z., BOREK, D., XU, Q., WANG, J. & ROSENBAUM, D. M. 2018. Crystal structure of the human NK1 tachykinin receptor. *Proc Natl Acad Sci U S A,* 115**,** 13264-13269.

ZHOU, Y., ZHAO, L., XIONG, T., CHEN, X., ZHANG, Y., YU, M., YANG, J. & YAO, Z. 2013. Roles of full-length and truncated neurokinin-1 receptors on tumor progression and distant metastasis in human breast cancer. *Breast Cancer Res Treat,* 140**,** 49-61.

All figures were generated by using biorender.com.

Acknowledgement

I want to thank Prof. Dr. Michael Berger, Prof. Dr. Roland Kappler, Prof. Dr. Sebastian Kobold, Prof. Dr. Muensterer, Prof. Dr. Endres and Prof. Dr. von Schweinitz for allowing me to conduct my doctoral dissertation at the Research Laboratories of the Department of Pediatric Surgery and the Department of Clinical Pharmacology.

My deepest gratitude goes to Prof. Dr. Michael Berger, who took me under his wing and became a mentor for me, not only in the scientist world but also in the clinic as a pediatric surgeon. I look forward to the future.

Additionally, I want to thank Prof. Dr. Roland Kappler for guiding me and always lending an open ear when I needed it. I am very grateful for the many talks and advices.

Furthermore, I want to thank Dr. Salih Demir and Dr. Adrian Gottschlich for teaching me everything I needed to know in the laboratory. I learn so much from both of them and I believe they helped me become a decent scientist.

Additionally, I want to thank Alina Hotes, Tanja Schmidt, Daniel Lüthy and Ruth Grünmeier for helping and supporting me during my daily work in the laboratory.

And lastly, I want to thank my family, my parents, Stefanie and Christopher and my sisters, Anna and Paulina. Thank you for always being there for me and supporting my every move. I would not be where I am right now if it was not for your endless love and support.